

3-2016

Contact angle and IFT measurements of smart water at elevated temperatures and pressures for evaluating wettability in a selected carbonate reservoir in the UAE

Jassim Abubacker Ponnambathayil

Follow this and additional works at: https://scholarworks.uaeu.ac.ae/all_theses

Part of the [Petroleum Engineering Commons](#)

Recommended Citation

Ponnambathayil, Jassim Abubacker, "Contact angle and IFT measurements of smart water at elevated temperatures and pressures for evaluating wettability in a selected carbonate reservoir in the UAE" (2016). *Theses*. 363.
https://scholarworks.uaeu.ac.ae/all_theses/363

This Thesis is brought to you for free and open access by the Electronic Theses and Dissertations at Scholarworks@UAEU. It has been accepted for inclusion in Theses by an authorized administrator of Scholarworks@UAEU. For more information, please contact fadl.musa@uaeu.ac.ae.



United Arab Emirates University

College of Engineering

Department of Chemical and Petroleum Engineering

CONTACT ANGLE AND IFT MEASUREMENTS OF SMART
WATER AT ELEVATED TEMPERATURES AND PRESSURES
FOR EVALUATING WETTABILITY IN A SELECTED
CARBONATE RESERVOIR IN THE UAE

Jassim Abubacker Ponnambathayil

This thesis is submitted in partial fulfillment of the requirements for the degree of
Master of Science in Petroleum Engineering

Under the Supervision of Dr. Hazim Al-Attar

March 2016

Declaration of Original Work

I, Jassim Abubacker Ponnambathayil, the undersigned, a graduate student at the United Arab Emirates University (UAEU), and the author of this thesis entitled *“Contact angle and IFT measurements of Smart Water at elevated temperatures and pressures for evaluating wettability in a selected carbonate reservoir in the UAE”*, hereby, solemnly declare that this thesis is my own original research work that has been done and prepared by me under the supervision of Dr. Hazim Al Attar, in the College of Engineering at UAEU. This work has not previously been presented or published, or formed the basis for the award of any academic degree, diploma or a similar title at this or any other university. Any materials borrowed from other sources (whether published or unpublished) and relied upon or included in my thesis have been properly cited and acknowledged in accordance with appropriate academic conventions. I further declare that there is no potential conflict of interest with respect to the research, data collection, authorship, presentation and/or publication of this thesis.

Student's Signature _____

Date _____

Copyright © 2016 Jassim Abubacker Ponnambathayil
All Rights Reserved

Advisory Committee

1) Advisor: Dr. Hazim Al Attar

Title: Associate Professor

Department of Chemical and Petroleum Engineering

College of Engineering

2) Co-advisor: Dr. Abdulrazaq Zekri

Title: Professor

Department of Chemical and Petroleum Engineering

College of Engineering

Approval of the Master Thesis


This Master Thesis is approved by the following Examining Committee Members:

1) Advisor (Committee Chair): Dr. Hazim Al Attar

Title: Associate Professor

Department of Chemical and Petroleum Engineering

College of Engineering

Signature 

Date 17/05/2016

2) Member: Dr. Abdulrazaq Zekri

Title: Professor

Department of Chemical and Petroleum Engineering

College of Engineering

Signature 

Date 17/05/2016

3) Member: Dr. Gamal Abdalla Alusta

Title: Assistant Professor

Department of Chemical and Petroleum Engineering

College of Engineering

Signature 

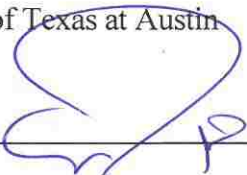
Date 16/5/2016

4) Member (External Examiner): Dr. Quoc Nguyen

Title: Associate Professor

Petroleum and Geosystems Engineering

The University of Texas at Austin

Signature 


Date 16/5/2016

This Master Thesis is accepted by:

Dean of the College of Engineering: Professor Sabah Alkass

Signature  Date 22/5/2016

Dean of the College of Graduate Studies: Professor Nagi Wakim

Signature  Date 26/5/2016

Copy 6 of 10

Abstract

Waterflooding has been regarded as a well-known secondary oil recovery method. In the recent years, extensive research on crude oil, brine, and rock systems has acknowledged that the composition of the injected water can change wetting properties of the reservoir during a waterflood in a promising way to improve oil recovery. Hence, injection of “smart water” with correct salinity and composition is considered as a tertiary recovery method. The mechanism behind wettability alteration that is promoted by smart water injection has been a topic of discussion in carbonate and sandstone formations. In this work, some key properties of sea water and its dilutions with natural and spiked sulphate concentrations have been thoroughly investigated in the laboratory. Interfacial tension (IFT) of crude oil/brine system was monitored at ambient and high pressure-high temperature conditions. The brine with the least IFT was then used as a non-wetting phase with aged samples of rock for the measurement of contact angle at high pressure-high temperature conditions. The rock samples are carbonates of a selected onshore oil field in UAE. The results of this work show that sea water of salinity 57,539 mg/l without sulphate spiking may be considered as the smart water for further core flooding investigation.

Keywords: Smart water, brine, Sulphate spiking, Interfacial Tension, Contact angle.

Title and Abstract (in Arabic)

تقييم خاصية التبلل في الصخور الكربوناتيّة لمكانن نفطيّة مختارة من الإمارات العربيّة المتحدّة عن طريق قياس زاوية التبلل و التوتر السطحي بين الصخور المكمّنية المشبعة بالنفط الخام و المياه الذكيّة عند ضغط و حرارة المكمّن النفطي

الملخص

تعتبر عملية ضخ المياه عملية ثانوية معروفة لاستخلاص النفط وفي السنوات الأخيرة جرت بحوث على النفط الخام والمياه المالحة والنظام الصخري وقد توصلت إلى أن تركيب مياه الضخ يمكنها تغيير خصائص التبلل للمكمن خلال عملية الضخ المائي بصورة واعدة وذلك لتحسين عملية استخلاص النفط وعليه فإن عملية ضخ "المياه الذكيّة" عند استخدام درجة ملوحة وتركيب مناسب تعتبر كطريقة استخلاص ثالثة وتعتبر آلية تغيير التبلل عبر ضخ المياه موضوع للمناقشة بالنسبة للمكانن الكربوناتيّة والتكوينات الرملية وفي هذا البحث تم استخدام بعض الخصائص الأساسية لمياه البحر والمياه المخففة مع الكبريت الطبيعي والمدبب في المختبر وقد تمت مراقبة التوتر السطحي بين النفط/ المياه المالحة وتم إجراء قياس التوتر السطحي في ظروف درجة الحرارة المحيطة ودرجات حرارة عالية وضغط مرتفع ومن ثم تم استخدام المياه المالحة مع قياسات التوتر السطحي الأخيرة كطور غير ميلل مع نماذج صخور قديمة لقياس زاوية التبلل تحت ظروف درجات حرارة عالية وضغط مرتفع وقد كانت نماذج الصخور عبارة عن صخور كاربونيتية من حقول برية في دولة الإمارات العربيّة المتحدّة حيث أظهرت نتائج هذا البحث أن مياه البحر ذات درجة الملوحة 57,539 ملجم/لتر بدون الكبريت المدبب يمكن اعتبارها هي المياه الذكيّة لإجراء مزيد من الاختبارات الأساسية على عمليات الضخ المائي.

مفاهيم البحث الرئيسية : المياه الذكيّة، المياه المالحة، الكبريت المدبب، التوتر السطحي، زاوية التبلل.

Acknowledgments

I would like to express my sincere thanks and appreciation to all those who were involved in this significant period of time. I owe my deepest gratitude and gratefulness to my thesis supervisors, Dr. Hazim Al Attar and Prof. Abdulrazaq Zekri, for their continuous encouragement, inestimable guidance, precious support and constructive assistance they offered me throughout the course of this study. It would have been next to impossible to complete this thesis without the time and effort they have allocated to it. I would like to thank them for the friendly environment they have created for me and invaluable piece of advice I received from them which played a major role in making some crucial decisions in my career and social life.

My appreciation also goes to the faculty and staff members in the department of chemical and petroleum engineering at UAE University for their precious support and encouragement. I would like to extend my special gratitude to my colleague Eng. Mohammed Jassem Khalifi for his valuable assistance he offered and the sweet memories he left through the experiment phase of the study. I would like to express my gratitude towards Eng. Essa Georges Lwisa and Eng. Abdul Salam Anvar from the Chemical and Petroleum Engineering laboratories at UAEU for their great efforts and help during experimental work.

Finally, I would like to thank my parents, for their invaluable encouragement and unlimited support that I have received from them in all aspects which helped me to overcome the obstacles I have faced during my graduate life and motivated me to achieve any success in my life.

Dedication

To my beloved parents and family

Table of Contents

Title	i
Declaration of Original Work	ii
Copyright	iii
Advisory Committee	iv
Approval of the Master Thesis	v
Abstract	vii
Title and Abstract (in Arabic)	viii
Acknowledgments	ix
Dedication	x
Table of Contents	xi
List of Tables	xiii
List of Figures	xiv
List of Abbreviations/Nomenclatures/Symbols	xv
Chapter 1: Introduction	1
Chapter 2: Literature Review	3
2.1 Oil Recovery Mechanisms	3
2.1.1 Primary Recovery	3
2.1.2 Secondary Recovery	4
2.1.2 Enhanced Oil Recovery	4
2.2 Wettability	5
2.2.1 Wettability Alteration Mechanism	8
2.2.2 Interfacial Tension	9
2.2.3 Contact Angle	10
Chapter 3: Methodology	14
3.1 Asab Oil Field	14
3.2 Crude Oil	14
3.3 Brines	14
3.3.1 Brine Composition	15
3.4 Core Samples	18
3.5 Core Preparation	19

3.6 Density and Viscosity Measurements	19
3.7 Interfacial Tension measurements	20
3.7.1 IFT measurement at 20°C.....	21
3.7.2 IFT measurement at high pressure high temperature (HPHT)	22
3.8 Contact Angle Measurements	24
Chapter 4: Results and Discussion.....	26
4.1 Results of Brine Density and Viscosity	26
4.2 IFT Measurements	30
4.2.1 IFT results of different Brines at 20°C.....	30
4.2.2 IFT of Brines at HPHT	35
4.2.3 IFT measurements with temperature	40
4.3 Contact Angle Measurements at single temperature and pressure	43
Chapter 5: Conclusion and Recommendation.....	49
5.1 Conclusion	49
5.2 Recommendations.....	50
Bibliography	51
Appendix I: Brine Preparation Procedure	56
Appendix II: Sulphate Spiking Calculations.....	58
Appendix III: Density and viscosity categories at 20°C.....	59
Appendix IV: IFT categories at 20°C	65
Appendix V: IFT categories at high Pressure and high temperature	71
Appendix VI: IFT Images at high Pressure and high temperature	75
Appendix VII: Contact Angle categories at HPHT	79
Appendix VIII: Contact Angle Images at HPHT.....	82

List of Tables

Table 3.1: Composition of the prepared brine	16
Table 3.2 Properties of selected core samples	18
Table 4.1: Density and Viscosity of Brines	27
Table 4.2: Brine Categorization based on Density, Viscosity and IFT at 20°C	28
Table 4.3: Summary of IFT measurements at 20°C	31
Table 4.4: IFT measurements at HPHT	36
Table 4.5: Brine Categorization of IFT at High Pressure High Temperature.....	37
Table 4.6: IFT measurements of brine with temperature.....	41
Table 4.7: Contact angle measurements of different brines at HPHT	44
Table 4.8: Brine Categorization of Contact Angle at High Pressure High Temperature.....	44

List of Figures

Figure 2.1: a) Dalmatian wetting and b) Mixed Wetting	7
Figure 3.1: Core sample 22-3.....	18
Figure 3.2: Trim End.....	19
Figure 3.3: a) Pycnometer b) Canon-Fenske	20
Figure 3.4: Teclis Tracker.....	20
Figure 3.5: Beaker of Teclis Tracker	21
Figure 3.6: Teclis Tracker HPHT cell and Stand.....	23
Figure 3.7: Contact Angle measurement	24
Figure 4.1: Density and Viscosity of all the categories	29
Figure 4.2: IFT measurements at 20°C of all categories	32
Figure 4.3: IFT at HPHT of all categories	38
Figure 4.4: Variation of IFT measurements of the different brines with temperature	42
Figure 4.5: Percentage reduction of IFT between 20°C and HPHT	42
Figure 4.6: Contact angle measurements at HPHT of all categories together	45
Figure 4.7: Change in contact angle at high pressure high temperature conditions ..	45
Figure 4.8: Contact Angle measurements with time.....	48

List of Abbreviations/Nomenclatures/Symbols

CA	Contact Angle
Cat.	Category
FW	Formation Water
HPHT	High Pressure High Temperature
IFT	Interfacial Tension
IW	Injection Water
SW	Sea Water
SW/y	Sea water/y times diluted
SW/y xZ SO ₄	Sea water/y times diluted and it's spiked by Z times the sulphate of formation water (885 mg/L)
TDS	Total Dissolved Solids

Chapter 1: Introduction

Half of the world's hydrocarbon reserves is occupied by carbonate rocks. The mechanism that governs the recovery should be known for a successful oil production. An important factor that controls the fluid distribution in a reservoir is formation wettability. Most carbonate reservoirs are preferentially oil wet and they do have a negative capillary pressure. These reservoirs exhibit reduced oil recovery compared to sandstones because of their fractured nature. The permeability of the matrix block is in the range of 1 – 10 mD which makes carbonate reservoirs good candidates for Enhanced Oil Recovery. Most of the petrophysical parameters like capillary pressure, relative permeability, electrical properties and waterflood behavior are dependent on wettability (Alotaibi et al., 2010; Hognesen et al., 2005). Consequently, any wettability alteration would affect the above parameters and eventually the whole flooding process.

If the wettability is between water-wet and intermediate-wet, injected water will be spontaneously imbibed by the matrix block (Torsaeter, 1984). In an oil-wet rock, negative capillary pressure will make the spontaneous imbibition impossible. Whereas in a fractured oil-wet reservoir, the injected water moves through the high permeable fractures and results in early water breakthrough (Al-Hadhrami & Blunt, 2000).

Wettability alteration studies between sea water and rock gained momentum after the successful injection of sea water into the highly fractured Ekofisk field in the North Sea (Torsaeter, 1984; Zhang et al., 2007). Calcium and Sulphate have been found to exhibit strong potential towards the calcite surfaces (Pierre, 1990). Also low salinity flooding has proven to be effective in some carbonate reservoirs (Al-Attar et

al., 2013; Zahid et al., 2012). No extensive work was done to find the effect on increased sulphate ion concentration in sea water on possible wettability change. It is the objective of this thesis to carry out an extensive laboratory work on the measurement of key properties under high pressure high temperature conditions which are believed to have direct impact on wettability alteration of crude oil/water/rock systems. Contact angle and IFT measurements of different brines were obtained to have a better understanding of the effect of dilution, sulphate spiking and temperature in wettability alteration.

Chapter 2: Literature Review

The literature reviewed in this work includes the conventional recovery mechanisms, smart waterflooding in carbonate reservoirs, interfacial tension (IFT), contact angle, capillary pressure and wettability alteration mechanisms.

2.1 Oil Recovery Mechanisms

The oil recovery of reservoirs has been traditionally classified into three stages: primary, secondary and tertiary recovery.

2.1.1 Primary Recovery

Natural energy present in a reservoir is the driving force in the primary recovery phase that helps in displacing oil towards producing wells. To have a clear picture about the reservoir behavior and to predict future performance, the driving mechanism should be identified. There are six driving mechanisms that provide the natural energy for the oil recovery. These natural driving mechanisms include pore compaction and connate water expansion, depletion drive, gas cap drive, water drive, gravity drainage drive and combination drive (Ahmed, 2006).

In pore compaction and connate water expansion, a decline in reservoir pressure causes the pore size reduction and connate water expansion because of their individual compressibility factors and squeezes the crude oil out of the pore space to wellbore. The depletion drive mechanism in under-saturated oil reservoirs occurs when there is a decline in pressure from initial reservoir pressure to bubble point, this forces the oil to expand with all the dissolved gas in it. Below the bubble point, gas liberates in the form of dispersed gas bubbles within the microscopic pore spaces. These gas bubbles will expand and forces the oil to come out of the pore spaces,

provided that free gas saturation is less than or equal to critical gas saturation. In a gas cap drive, gas cap present in the saturated oil reservoir helps to produce oil by the expansion of gas cap (frontal displacement) present. In a water drive, the presence of an aquifer will force water to move into the pore spaces originally occupied by oil and displace the oil into producing wells (frontal displacement process). The mechanism behind the gravity drainage drive is the difference in the densities of the fluids in a reservoir. Whereas in a combination drive two or more driving mechanisms can be active (Ahmed, 2006).

2.1.2 Secondary Recovery

Natural energy of the reservoir is supported by injection of gas or water to displace oil towards the producing wells and/or to maintain reservoir pressure. In gas injection, gas is either injected into gas cap for pressure maintenance and gas cap expansion or into the oil layer to displace oil immiscibly to the producers. Immiscible gas injection is less efficient compared to waterflooding and thus waterflooding is commonly considered as a secondary recovery process (Green & Willhite, 2008). In onshore fields, the highly saline water from an aquifer is injected into the reservoir whereas in offshore operations, sea water is injected to recover more oil.

2.1.2 Enhanced Oil Recovery

Original oil in place is left behind after secondary recovery because of capillary and viscous forces (Moeini et al., 2014). Thus the Enhanced Oil recovery (EOR) process has become crucial in the recovery of this remaining oil. The EOR is a process which involves injection of some type of fluid into a reservoir to provide the necessary mechanism to displace the remaining oil. The fluid for an EOR process is selected on the basis of physical/chemical requirements, availability and cost of the fluid (Dake,

2010). The favorable condition for the recovery of the remaining oil is created by the interaction of fluid with reservoir oil/rock system i.e., like lowering interfacial tension (IFT), oil swelling, oil viscosity reduction, wettability modification or favorable change of phase behavior. These interactions take place by physical or chemical mechanisms. Injection of gases or liquid chemicals or thermal energy is also considered as an EOR method. Commonly used gases includes hydrocarbon gases, carbon dioxide, nitrogen and flue gases. Only miscible gas injection falls into the category of EOR whereas immiscible gas injection is a secondary recovery process. Polymer, surfactant and hydrocarbon solvent are categorized under liquid chemicals. The thermal energy from steam or hot water is used an EOR process to recover heavy crude oil (Green & Willhite, 2008).

Injection of more than one fluid is also considered as an EOR process. A primary slug which is an expensive chemical is injected to mobilize the oil. The primary slug is displaced by a large volume of secondary slug, which is an inexpensive chemical. If needed, the secondary slug is followed by an injection of another inexpensive fluid to reduce the cost. So the multiple fluid injection is also considered an EOR process. Normally water or gas will be the last candidate for multiple fluid injection, their prime duty is to volumetrically displace the earlier injected fluids (Green & Willhite, 2008).

2.2 Wettability

Wettability is defined as the relative adhesion of two fluids to a solid surface. In a porous medium, it is a measure of preferential tendency of one of the fluids to wet the surface. A porous medium usually contains two or more fluids (Tiab & Donaldson, 2010).

Depending on the brine-oil interaction, the wettability of a system ranges from strongly water-wet to strongly oil-wet. Brine-oil-rock system will exhibit neutral wettability, if rock doesn't show any preference to either brines. Or in other words, neutral wettability is defined as a condition when both fluids equally wet the rock surface (Tiab & Donaldson, 2010).

Fractional wettability is a type of wettability where scattered areas of the rock are strongly oil wet, the remaining area is strongly water-wet. Fractional wettability is also known as "Dalmatian wetting" as shown in Figure 2.1 a) (Brown et al., 1956; Willhite, 1986). It occurs when surface of the rocks are composed of many minerals having different surface chemical properties, which leads to a change in wettability throughout the internal surface of the pores. The core exhibiting fractional wettability will imbibe small amount of oil when water saturation is high like at residual oil saturation (S_{or}) and will imbibe a small quantity of water when oil saturation is high like at irreducible water saturation (S_{wi}).

Mixed wettability is defined as condition where larger pores are oil wet and a continuous filament of oil exists throughout the core in larger pores whereas the small pores are occupied by water as shown in Figure 2.1 b) (Anderson, 1986; Salathiel, 1973, Willhite, 1986). Residual oil saturation of mixed wettability is low because oil is located in the large pores of the rock in continuous path that makes the oil displaced from the cores even at very low oil saturation. Mixed wettability can occur when oil containing interfacial active polar organic compounds invades a water-wet rock saturated with brine. After displacing brine from the larger pores, the interfacial active compounds react with the rock's surface, displacing the remaining aqueous film and, thus, producing an oil-wet lining in the large pores. The water film

between the rock and the oil in the pore is stabilized by a double layer of electrostatic forces. As the thickness of the film is diminished by the invading oil, the electrostatic force balance is destroyed and the film ruptures, allowing the polar organic compounds to displace the remaining water and react directly with the rock surface.

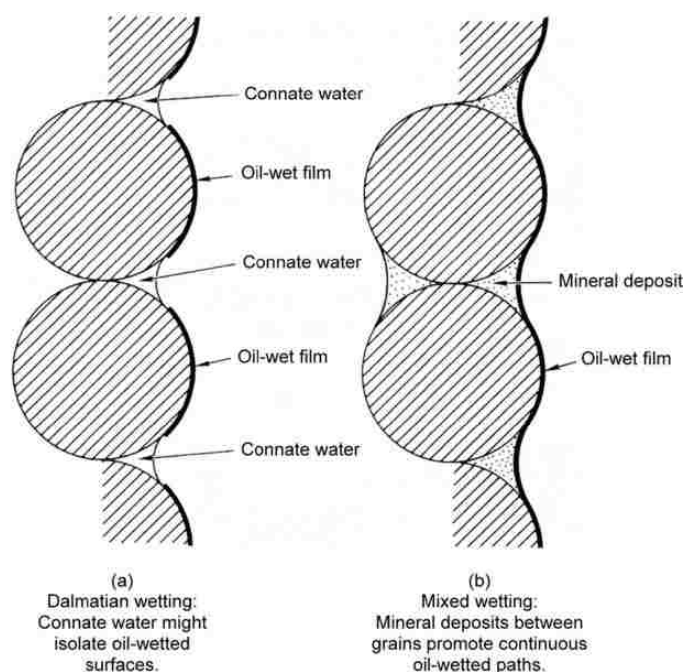


Figure 2.1: a) Dalmatian wetting and b) Mixed Wetting (Willhite, 1986)

So the overall average characteristic of a heterogeneous system with microscopic relative wetting throughout the porous medium is the wettability of a rock-fluid system (Iwankow, 1958). The preferential wetting tendencies of water or oil towards the rock pore surfaces leads to various states of overall wettability. This overall wettability has an effect on the fluid flow and electrical properties of the water-hydrocarbon-rock system. It is capable of controlling the capillary pressure and relative permeability behavior that leads to the hydrocarbon displacement and ultimate recovery (Donaldson & Thomas, 1971; Emery, Mungan, & Nicholson, 1970; Kyte, Naumann, & Mattax, 1961; Masalmeh, 2002).

2.2.1 Wettability Alteration Mechanism

In carbonate reservoirs, wettability alteration is the main challenge in displacing more oil and enhancing the oil recovery (Alotaibi et al., 2010). Strand (2008) has shown the effect of calcium, magnesium and sulphate ions on oil recovery. For any wettability improvement, activation energy for the chemical reaction is required. Bonding energy between the polar components in oil and carbonates is high compared to sandstones. Also the carbonate rock is capable of absorbing the carboxylic component in the crude oil onto carbonate surface and because of this reason, wettability always remains between neutral and preferential oil wet. Sulphate ion is capable of acting as a wettability modifier without any addition of surfactants. Sulphate is an ion that showed up good potential towards the limestone (Pierre et al., 1990; Strand et al., 2008; Strand et al., 2003).

In an imbibition test using seawater, the effect of ions (sulphate and calcium) with temperatures seems to have a crucial role in wettability alteration. An increase in the concentration of calcium in sea water increases the adsorption of sulphate, this is because of the co-adsorption of calcium ion towards the carbonate surface. The positive charge of the rock surface decreases with adsorption of sulphate onto the carbonate rocks, because of reduced electrostatic repulsion it increases the calcium ions at the surface (Austad et al., 2007; Strand et al., 2006; Strand et al., 2008).

Adsorption of sulphate onto chalk surface leads to the desorption of negatively charged carboxylic material by changing the surface charge of the chalk surface (Strand et al., 2003). Temperature increase leads to a strong adsorption of sulphate and calcium onto the chalk surface, which enhances the imbibition rate and oil recovery. At low temperature, adsorption of magnesium ions is less compared to calcium ions

onto the chalk surface (Zhang & Austad, 2006; Zhang et al., 2007). The increase in temperature replaces calcium on the chalk surface by magnesium. Magnesium becomes more reactive because of dehydration and gets replaced instead of calcium from the surface lattice of the chalk. The presence of sulphate, calcium and magnesium is necessary to change the wettability of rock. Limestone also showed similar interactions with sea water (Alotaibi et al., 2010).

The wettability of carbonate rocks was studied by Lichaa et al. (1992) for preserved and cleaned core samples. Rock/fluid interaction can be evaluated by Contact angle, Amott and USBM. In a brine/crude oil/rock system, the surface charges on the rock surface and fluid interfaces are strongly affected by the salinity and pH of the brine, which in turn effects the wettability. The presence of cations like calcium, magnesium and strontium in the formation water of injection water and the weak base characteristic of reservoir rock, suggests a preferential oil wet system should prevail in the presence of polar components in the crude oil. pH of the brine has an effect on the wetting nature, when the zeta potential crosses the zero point of charge.

2.2.2 Interfacial Tension

When two immiscible fluids (gas-liquid or liquid-liquid) are in contact, the fluids are separated by a well-defined interface, which is only a few molecular diameters in thickness. Within the fluid and away from the interface and the walls of the container, the molecules attract each other in all directions. At the surface between two immiscible fluids, there are no similar molecules beyond the interface and, therefore, there is an inward-directed force that attempts to minimize the surface by pulling it into the shape of a sphere. This surface activity creates a film-like layer of molecules that are in tension, which is a function of the specific free energy of the

interface. The interfacial tension (IFT) has the dimensions of force per unit length (newtons/meter), which is the modern standard expression of the units. In the earlier literature, however, it is expressed as dynes/centimeter, which is numerically equal to millinewtons per meter $[(N \times 10^{-3})/m \text{ or } mN/m]$ (Tiab and Donaldson, 2010).

During the development phase and to implement an optimal reservoir management strategy for a reservoir, the knowledge about the reservoir fluid properties is very important (Amyx et al., 1988). IFT along with contact angle are important parameters for any reservoir engineering studies. They can be used in the estimation of fluid saturation in gas-oil transition zone (Tiab and Donaldson, 2010). No general methods are available for estimating IFT, so it has to be measured in the lab for reservoir samples at reservoir conditions (Okasha and Al-Shiwaish, 2010).

The study of oil/brine IFT is closely related to wettability. So IFT and film formation can help to explain the change in contact angle and wettability. Pressure was found to have less effect on IFT compared to temperature. So temperature is considered as a major factor affecting IFT (Hjelmeland & Larrondo, 1986).

2.2.3 Contact Angle

Contact angle is a function between solid/liquid and liquid/liquid interfaces. Wettability of the reservoir rocks shows a thermodynamical equilibrium between the mineral surface of the pore walls and fluid within the pores. The main factors of wettability are pressure, temperature and fluid characteristics. Contact angle is affected by the heterogeneity and roughness of solid wall and affects the hysteresis. The contact angle hysteresis is the difference between advancing (maximal) contact angle and receding (minimal) contact angle. Where advancing contact angle to receding contact angle is a range of contact angles, when a drop is placed on the surface of rock. Contact

angle of 0° and 180° means completely water wet and completely oil wet, respectively. Anderson (1986) classified the wettability in terms of contact angle as water wet ($0-75^\circ$), intermediate wet ($75-115^\circ$) and oil wet ($115-180^\circ$). Weakly water wet and weakly oil wet conditions are represented as ($55-75^\circ$) and ($115-135^\circ$).

Hjelmeland & Larrondo (1986) studied the effect of temperature, pressure and oil composition on the wettability of the calcium carbonate rocks. They concluded that the temperature had an influence on the wettability. At low temperature (72°F), the rock surface was oil wet and at high temperature ($>140^\circ\text{F}$), rock surface showed water wet behavior. An intermediate state of wettability was observed at 104°F . There was no effect of pressure on wettability. Light fraction of oil had no effect on the wettability of calcium carbonate.

Saner (1991) studied a carbonate reservoir using contact angle, Amott and USBM. Synthetic brines with salinity ranging from 20 to 200,000 ppm was used with crude oil under elevated temperature and pressure conditions. He concluded that an increase of temperature from ambient to 158°F , changed the wettability from neutral wet to moderately water wet conditions. Also an increase in salinity from 20 – 200,000 ppm, decreased the contact angle from 61° to 42° . Low salinity brines didn't show up any significant change in contact angle between ambient (32°) and elevated temperature (28°) conditions. Pressure was found to have no influence on the contact angle, as the pressure was increased from 20 to 2800 psia at constant temperature (158°F). Salinity effect was almost negligible at similar temperature conditions.

Lichaa et al. (1992) studied the wettability of Saudi Arabian carbonate reservoirs using the contact angle, Amott and USBM technique. The receding contact angle measurement of the calcite, marble and formation rock was made using the

synthetic formation water, sea water and dead oil. The experiment was conducted at different pressures (ambient to 50 psia) and different temperatures (77 -194°F). They found that at high temperature, calcite surface became preferential water wet. The contact angle of brine/Marble/oil shows oil wet to intermediate wet, and at high temperatures wettability changed to weakly water wet. Formation rocks showed oil wet at room temperature and weakly oil at high temperature.

Effect of pressure and temperature on reservoir rock wettability was investigated by Wang & Gupta (1995). Stock tank oil and reservoir brine from a carbonate reservoir was used. Pressure had no major effect on the contact angle of the calcite rock, increase in contact angle was only 5% when there was an increase of 3000 psig pressure. An increase of temperature from 72.5 to 175°F, changed the wettability of the system towards weakly water wet. A change in the fluid chemistry at the interface with increase in temperature, leads to the change in wettability.

Almehaideb et al. (2004) investigated the effect of salinity on the carbonate rock. Limestone rock, crude oil and NaCl solution were used in the study. Distilled water, 1,000, 10,000 and 50,000ppm of brines were used. All the experiments were conducted at room temperature. 10,000 ppm brine showed a significant reduction in contact angle compared to other brines.

Yu et al. (2007) studied the effect of the brine containing sulphate on the chalk rock. They measured the contact angle on calcite and chalk rocks at high temperatures (up to 266°F). A temperature of 194°F helped to change the wettability of calcite towards water wet. Accelerated desorption of the stearic acid from the calcite helped to change the wettability of the all fluid systems investigated towards water wet. Replacing distilled water by sulphate containing water, resulted in a decrease of

contact angle. Also a decrease in contact angle was observed when sulphate containing was used at high temperatures around 266°F.

The wettability of the crude oil/ reservoir brine/ reservoir rock system was evaluated at elevated temperatures using axisymmetric drop shape analysis (ADSA) technique by Yang et al. (2008). Vuggy limestone of intermediate wettability was used in the study. An increase in contact angle was observed with increase in pressure. At 29 psia pressure and 80.6°F temperature, a slight fluctuation of contact angle was observed. This slight fluctuation might be because of the strong electrostatic interaction between crude oil and reservoir brine. A decrease of contact angle was observed with an increase of temperature.

The advancing and receding contact angles were measured as a function of temperature by Hamouda and Karoussi (2008). All the contact angle measurements were made on modified calcite surfaces with .005 M stearic acid dissolved in decane. A maximum temperature of 194°F was used in the experiments. An increase in temperature reduced the contact angle indicating system is becoming more water wet with temperature increase. This happens because of the total interaction potential, which consists of Van der waals attractive, short range born repulsive and double layer electrostatic forces.

Chapter 3: Methodology

3.1 Asab Oil Field

The crude oil and core samples were taken from the Asab onshore oil field in UAE, operated by Abu Dhabi Company for onshore Petroleum Operation Ltd (ADCO). The field was discovered in 1965 and is located approximately 185 km South of Abu Dhabi, in rolling sand dunes some 30 km north of the Liwa oasis. The reservoir rock is carbonates with total proven reserves of 3.6 billion barrels of oil and current production rate is about 450,000 barrels per day. The current average reservoir pressure is around 3100 psia with a temperature of 255°F.

3.2 Crude Oil

Reservoir crude oil from the Asab field was used in all experiments. The dead oil density and viscosity at 20°C are 0.8276 g/cc and 2.93 cp, respectively. The oil is a sweet oil that has no H₂S gas. The oil was filtered through a 5µm filter paper in the presence of vacuum to remove any solid particles.

3.3 Brines

In this study, a total of 26 brines were used including the formation water (FW) and injection water (IW) of Asab field. All the brines were prepared using the standard procedure as mentioned in appendix I. From the literature, sea water has shown good recovery in carbonate reservoirs (RezaeiDoust et al., 2009; Zhang et al., 2007). Also the effect of sulphate ions in water has shown some additional oil recovery. Sea water was collected from the Arabian Gulf, the water body close to Asab field and ionic analysis was performed. Sea water of Total Dissolved Solids (TDS) 57,539 mg/l was selected as base brine and was synthetically prepared in the lab. Different brines were

prepared by diluting the sea water and by spiking the sea water by sulphate. Spiking was based on the 885 mg/l of sulphate in formation water. Brines were spiked by 1,770 mg/l (x2 SO₄) and 5,310 mg/l (x6 SO₄). As stated in the literature review, the x3 SO₄ and x4 SO₄ spiking have been found to increase oil recovery (P. Zhang & Austad, 2005) . Therefore, a sulphate spiking of x6 SO₄ was attempted in this work to see how it could alter the IFT and contact angle measurements. Sulphate spiking calculation is presented in appendix II. Formation water and injection water samples were collected from the field and subjected to ionic analysis. Asab oil field has a Formation water of TDS 157,488 mg/l with a density of 1.1034 g/ml and viscosity of 1.3483 cp at ambient conditions. The Injection water of the field has a TDS of 258,250 mg/l with a density of 1.1639 mg/l and viscosity of 1.75 cp at ambient conditions.

3.3.1 Brine Composition

Table 3.1, shows the composition of all brines used in the work. Ionic analysis was performed to find the composition of formation water, injection water and sea water. The brine composition of sea water dilutions and sulphate spiking (Appendix II) was thus calculated.

Table 3.1: Composition of the prepared brine

<i>Ion</i>	<i>SW</i> <i>mg/L</i>	<i>SW/10</i> <i>mg/L</i>	<i>SW/50</i> <i>mg/L</i>	<i>SW/100</i> <i>mg/L</i>	<i>SW/200</i> <i>mg/L</i>	<i>SW/300</i> <i>mg/L</i>	<i>FW</i> <i>mg/L</i>
Sodium	19054	1905.4	381.08	190.54	95.27	63.51	44261
Calcium	690	69	13.8	6.9	3.45	2.30	13840
Magnesium	2132	213.2	42.64	21.32	10.66	7.11	1604
Bromide	<0.1	<0.1	<0.1	<0.1	<0.1	<0.1	0
Potassium	672	67.2	13.44	6.72	3.36	2.24	0
Zinc	<0.1	<0.1	<0.1	<0.1	<0.1	<0.1	0
Phosphate	<0.1	<0.1	<0.1	<0.1	<0.1	<0.1	0
Chloride	30924	3092.4	618.48	309.24	154.62	103.08	96566
Bicarbonate	123	12.3	2.46	1.23	0.615	0.41	332
Sulphate	3944	394.4	78.88	39.44	19.72	13.15	885
Carbonate	0	0	0	0	0	0	0
TDS (mg/L)	57539	5754	1151	575	288	192	157488

<i>Ion</i>	<i>SW/400</i> <i>mg/L</i>	<i>SW/500</i> <i>mg/L</i>	<i>SW x2 SO₄</i> <i>mg/L</i>	<i>SW x6 SO₄</i> <i>mg/L</i>	<i>SW/10 x2 SO₄</i> <i>mg/L</i>	<i>SW/10 x6 SO₄</i> <i>mg/L</i>	<i>SW/50 x2 SO₄</i> <i>mg/L</i>
Sodium	47.64	38.11	19054	19054	1905.4	4449.65	1229.81
Calcium	1.73	1.38	690	690	69	69	13.8
Magnesium	5.33	4.26	2132	2132	213.2	213.2	42.64
Bromide	<0.1	<0.1	<0.1	<0.1	<0.1	<0.1	<0.1
Potassium	1.68	1.34	672	672	67.2	67.2	13.44
Zinc	<0.1	<0.1	<0.1	<0.1	<0.1	<0.1	<0.1
Phosphate	<0.1	<0.1	<0.1	<0.1	<0.1	<0.1	<0.1
Chloride	77.31	61.85	30924	30924	3092.4	3092.4	618.48
Bicarbonate	0.31	0.25	123	123	12.3	12.3	2.46
Sulphate	9.86	7.89	5714	9254	2164.4	5704.4	1848.88
Carbonate	0	0	0	0	0	0	0
TDS (mg/L)	144	115	59309	62849	7524	13608	3770

Table 3.1: Composition of the prepared brines - Continued

<i>Ion</i>	<i>SW/50 x6 SO₄</i> <i>mg/L</i>	<i>SW/100 x2 SO₄</i> <i>mg/L</i>	<i>SW/100 x6 SO₄</i> <i>mg/L</i>	<i>SW/200 x2 SO₄</i> <i>mg/L</i>	<i>SW/200 x6 SO₄</i> <i>mg/L</i>	<i>SW/300 x2 SO₄</i> <i>mg/L</i>	<i>SW/300 x6 SO₄</i> <i>mg/L</i>
Sodium	2925.33	1039.27	2734.79	944.00	2639.52	912.25	2607.77
Calcium	13.8	6.9	6.9	3.45	3.45	2.3	2.3
Magnesium	42.64	21.32	21.32	10.66	10.66	7.11	7.11
Bromide	<0.1	<0.1	<0.1	<0.1	<0.1	<0.1	<0.1
Potassium	13.44	6.72	6.72	3.36	3.36	2.24	2.24
Zinc	<0.1	<0.1	<0.1	<0.1	<0.1	<0.1	<0.1
Phosphate	<0.1	<0.1	<0.1	<0.1	<0.1	<0.1	<0.1
Chloride	618.48	309.24	309.24	154.62	154.62	103.08	103.08
Bicarbonate	2.46	1.23	1.23	0.615	0.615	0.41	0.41
Sulphate	5388.88	1809.44	5349.44	1789.72	5329.72	1783.15	5323.15
Carbonate	0	0	0	0	0	0	0
TDS (mg/L)	9005	3194	8430	2906	8142	2811	8046

<i>Ion</i>	<i>SW/400 x2 SO₄</i> <i>mg/L</i>	<i>SW/400 x6 SO₄</i> <i>mg/L</i>	<i>SW/500 x2 SO₄</i> <i>mg/L</i>	<i>SW/500 x6 SO₄</i> <i>mg/L</i>	<i>IW</i> <i>mg/L</i>
Sodium	896.37	2591.89	886.84	2582.36	72237
Calcium	1.725	1.725	1.38	1.38	19763
Magnesium	5.33	5.33	4.264	4.264	3569
Bromide	<0.1	<0.1	<0.1	<0.1	1039.3
Potassium	1.68	1.68	1.344	1.344	1859.3
Zinc	<0.1	<0.1	<0.1	<0.1	0
Phosphate	<0.1	<0.1	<0.1	<0.1	5
Chloride	77.31	77.31	61.85	61.85	158518.34
Bicarbonate	0.31	0.31	0.246	0.246	43.33
Sulphate	1779.86	5319.86	1777.89	5317.89	268.3
Strontium	0	0	0	0	943.7
Nitrate	0	0	0	0	4
Carbonate	0	0	0	0	0
TDS (mg/L)	2763	7998	2734	7969	258250

3.4 Core Samples

Four core samples were selected from well number 567 in Asab field. The properties of the core samples are listed in the Table 3.2, indicating all the core samples are limestone. Also all core samples are horizontal sections, mentioned as “H” in the column of sample number. Each core sample was cut into 3 pieces horizontally because trim ends are required for contact angle measurements and named as sample no-1, 2, and 3. A core sample is shown in Figure 3.1. A piece of trim end as shown in Figure 3.2 was obtained by cutting the shortened core sample and used for contact angle measurements.

Table 3.2 Properties of selected core samples

Sample No.	Depth (ft)	at Ambient Conditions	Grain Density gm/cc	Description
		$\text{O}(\text{He})$ (Hz) %		
1H	7743.42	9.7	2.70	Limestone
2H	7744.09	11.6	2.70	Limestone
21H	7753.40	18.9	2.73	Limestone
22H	7753.60	18.4	2.72	Limestone



Figure 3.1: Core sample 22-3



Figure 3.2: Trim End

3.5 Core Preparation

Standard core lab procedures were implemented in cutting, trimming and cleaning the core samples. Core samples are provided by the Abu Dhabi National Operating Company (ADNOC) and are cylindrical in shape, 4" in length and 1.5" in diameter. The core samples were cut into three horizontal pieces using the core trimming machine. For cleaning, Soxhlet extraction apparatus was used. The core samples were placed in medium of Toulene and then in the medium of methanol. Toulene was used to extract hydrocarbon and methanol to remove salts. Then all the cleaned core samples were placed in oven for drying.

3.6 Density and Viscosity Measurements

Density measurements of all brine were conducted by pycnometer as shown in figure 3.3 a). Canon - Fenske viscometer as shown in Figure 3.3 b) was used to measure the dynamic viscosity.



Figure 3.3: a) Pycnometer b) Canon-Fenske

3.7 Interfacial Tension measurements

All Interfacial Tension (IFT) measurements of oil/brine were carried out using Teclis Tracker as shown in Figure 3.4 by pendant drop technique. It is a technique by which a drop of liquid is suspended from the end of a tube by surface tension. Teclis tracker is capable of running IFT measurements at ambient and high pressure high temperature conditions.



Figure 3.4: Teclis Tracker

3.7.1 IFT measurement at 20°C

Interfacial tension was measured at a temperature of 20°C and ambient pressure. The following are steps followed for the measurement of IFT at 20°C and ambient pressure.

1. Beaker was filled with 25ml of brine as shown in Figure 3.5.

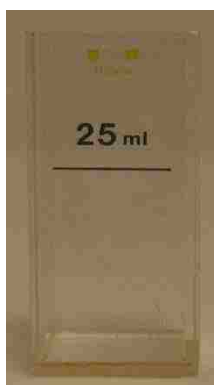


Figure 3.5: Beaker of Teclis Tracker

2. Filled the Hamilton syringe with filtered crude oil and fixed the U-type needle to luer lock of the syringe.
3. Fixed the Hamilton syringe to the pump in the tracker and placed the needle of the syringe immersed in the medium of brine in the beaker. Adjust the position of the beaker in a way to see the tip of the needle through the camera
4. Manually operated the pump to throw off 2-3 drop of oil from the tip of the syringe, this will eliminate the possibility of the tip of the needle having some air bubbles.
5. Opened the Teclis tracker software, mention the density of the crude oil and brine, Volume of the drop and run the experiment. Tracker makes use of the axisymmetric drop shape analysis (ADSA) technique to find the interfacial tension by fitting Laplace equation.

6. Ran the measurement until a stabilized IFT value is obtained.

3.7.2 IFT measurement at high pressure high temperature (HPHT)

A cell capable of withstanding high pressure high temperature is used. The cell was pressurized to prevent evaporation of brine. A maximum pressure of 248 psia and maximum temperature of 90°C was used. This HPHT conditions will closely resemble the reservoir conditions and there comes the significance of HPHT experiments.

1. Beaker is filled with 25ml of brine as shown in Figure 3.5.
2. Filled the Hamilton syringe with filtered crude oil and fixed the U-type needle to luer lock of the syringe.
3. Placed the beaker in the stand as shown in the Figure 3.6 and fixed the syringe with sealing to the top of the stand. Placed the stand inside the cell as shown in Figure 3.6. Fixed the cell to the tracker with the piston of syringe connected to pump. Adjusted the position of the cell in a way to see the tip of the needle through the camera.
4. Connected the cell to the heating jackets, nitrogen cylinder and teperature probe.
5. Opened the camera via the software, manually operated the pump to throw off 2-3 drop of oil from the tip of the syringe, this will eliminate the possibility of having some air bubbles at the tip of the needle.



Figure 3.6: Teclis Tracker HPHT cell and Stand

6. Opened the Teclis tracker software, mentioned the density of the crude oil and brine, Volume of the drop and run the experiment. Tracker makes use of the axisymmetric drop shape analysis (ADSA) technique to find the interfacial tension by fitting Laplace equation. Volume of the oil drop should be set at a volume slightly less than the final volume. This gives enough time for the drop to stabilize at HPHT conditions. Then stop the equipment.
7. Increased the pressure to 200 psia and increased the temperature step by step up to 90°C. Ran the measurement until a stabilized IFT is obtained.

3.8 Contact Angle Measurements

The following are the procedure for contact angle measurement

1. The cleaned trim end was aged in the filtered crude oil at 90°C for three weeks.
2. The aged sample was placed in the beaker as shown in Figure 3.5 containing a medium of brine. While filling the brine care should be taken not to have air bubbles on the surface of the trim ends.
3. Placed the beaker in the stand as shown in the Figure 3.6 and fixed the empty syringe with sealing to the top of the stand. Place the stand inside the cell as shown in Figure 3.6. Fixed the cell to the tracker with the piston of syringe connected to pump. Adjusted the cell in a way to see the upper surface of the trim end through the camera.
4. Connected the cell to the heating jackets, nitrogen cylinder and teperature probe
5. Opened the Teclis tracker software, changed the setting to take a picture of the system at routine intervals (we took pictures every 20 minutes)
6. Increased the pressure to 200 psia and then increase the temperatures step by step up to 90°C.
7. Monitored the contact angle for 72 hours.
8. Contact angle was measured manually from the water (denser phase) as shown in Figure 3.7.

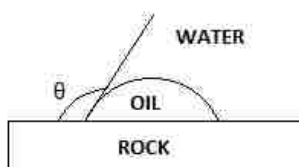


Figure 3.7: Contact Angle measurement

The advantage of this contact angle measurement is that the drainage process is natural. The measurement will generate the real contact angle in reservoir because of continuous change in saturation.

Chapter 4: Results and Discussion

4.1 Results of Brine Density and Viscosity

The density of the brine samples was measured using the pycnometer (typical technique for measuring density). Viscosity measurement was conducted using Canon-Fenske Viscometer at ambient conditions. A summary of the results is presented in Table 4.1. Categorization of the different brines based on their densities, viscosities and IFT are listed in Table 4.2. A summary of results of density and viscosity measurements at 20°C for the twelve categories are plotted in Figure 4.1. The results of the density and viscosity measurements with proposed trendlines of the individual categories are shown in Appendix III.

Figure 4.1 compares the results of one category with another. Category 1, shows an increasing trend in density and viscosity from SW to IW, due to increasing amount of total dissolved solids in the latter. Categories 2 to 9 except category 8, show an increasing viscosity and density with increased sulphate of the brine from natural sulphate to six times sulphate spiked. The addition of sulphate, increases the mass of the brine and lead to increase of density and viscosity. In category 8, density and viscosity was decreasing, this might be due to observational error. In categories 5 to 9, the variation of density and viscosity is slight because the mass of the added salts was not enough to change the total mass. Categories 10 to 12 follow a decreasing trend of density and viscosity, indicating that dilution of brines has reduced their mass significantly and thus reduced the density and viscosity.

Table 4.1: Density and Viscosity of Brines

Sl. No	Brine	Density g/ml	Viscosity cp
1	FW	1.1034	1.3483
2	IW	1.1639	1.7500
3	SW	1.0409	1.1901
4	SW x2 SO4	1.0439	1.2049
5	SW x6 SO4	1.0518	1.2566
6	SW/10	1.0071	1.0024
7	SW/10 x2 SO4	1.0111	1.0836
8	SW/10 x6 SO4	1.0101	1.0987
9	SW/50	1.0002	1.0315
10	SW/50 x2 SO4	1.0101	1.0702
11	SW/50 x6 SO4	1.0141	1.0894
12	SW/100	1.0081	1.0367
13	SW/100 x2 SO4	1.0081	1.0419
14	SW/100 x6 SO4	1.0081	1.0581
15	SW/200	1.0071	1.0339
16	SW/200 x2 SO4	1.0071	1.0380
17	SW/200 x6 SO4	1.0081	1.0466
18	SW/300	1.0062	1.0353
19	SW/300 x2 SO4	1.0062	1.0442
20	SW/300 x6 SO4	1.0062	1.0555
21	SW/400	1.0062	1.0981
22	SW/400 x2 SO4	1.0052	1.0721
23	SW/400 x6 SO4	1.0052	1.0654
24	SW/500	1.0012	1.0515
25	SW/500 x2 SO4	1.0012	1.0494
26	SW/500 x6 SO4	1.0052	1.0523

Table 4.2: Brine Categorization based on Density, Viscosity and IFT at 20°C

<i>Category 1</i>	<i>Category 2</i>	<i>Category 3</i>	<i>Category 4</i>	<i>Category 5</i>	<i>Category 6</i>	<i>Category 7</i>	<i>Category 8</i>	<i>Category 9</i>
SW2	SW2	SW2/10	SW2/50	SW2/100	SW2/200	SW2/300	SW2/400	SW2/500
FW	SW2 x2 SO ₄	SW2/10 x2 SO ₄	SW2/50 x2 SO ₄	SW2/100 x2 SO ₄	SW2/200 x2 SO ₄	SW2/300 x2 SO ₄	SW2/400 x2 SO ₄	SW2/500 x2 SO ₄
IW	SW2 x6 SO ₄	SW2/10 x6 SO ₄	SW2/50 x6 SO ₄	SW2/100 x6 SO ₄	SW2/200 x6 SO ₄	SW2/300 x6 SO ₄	SW2/400 x6 SO ₄	SW2/500 x6 SO ₄

<i>Category 10</i>	<i>Category 11</i>	<i>Category 12</i>
SW2	SW2 x2 SO ₄	SW2 x6 SO ₄
SW2/10	SW2/10 x2 SO ₄	SW2/10 x6 SO ₄
SW2/50	SW2/50 x2 SO ₄	SW2/50 x6 SO ₄
SW2/100	SW2/100 x2 SO ₄	SW2/100 x6 SO ₄
SW2/200	SW2/200 x2 SO ₄	SW2/200 x6 SO ₄
SW2/300	SW2/300 x2 SO ₄	SW2/300 x6 SO ₄
SW2/400	SW2/400 x2 SO ₄	SW2/400 x6 SO ₄
SW2/500	SW2/500 x2 SO ₄	SW2/500 x6 SO ₄

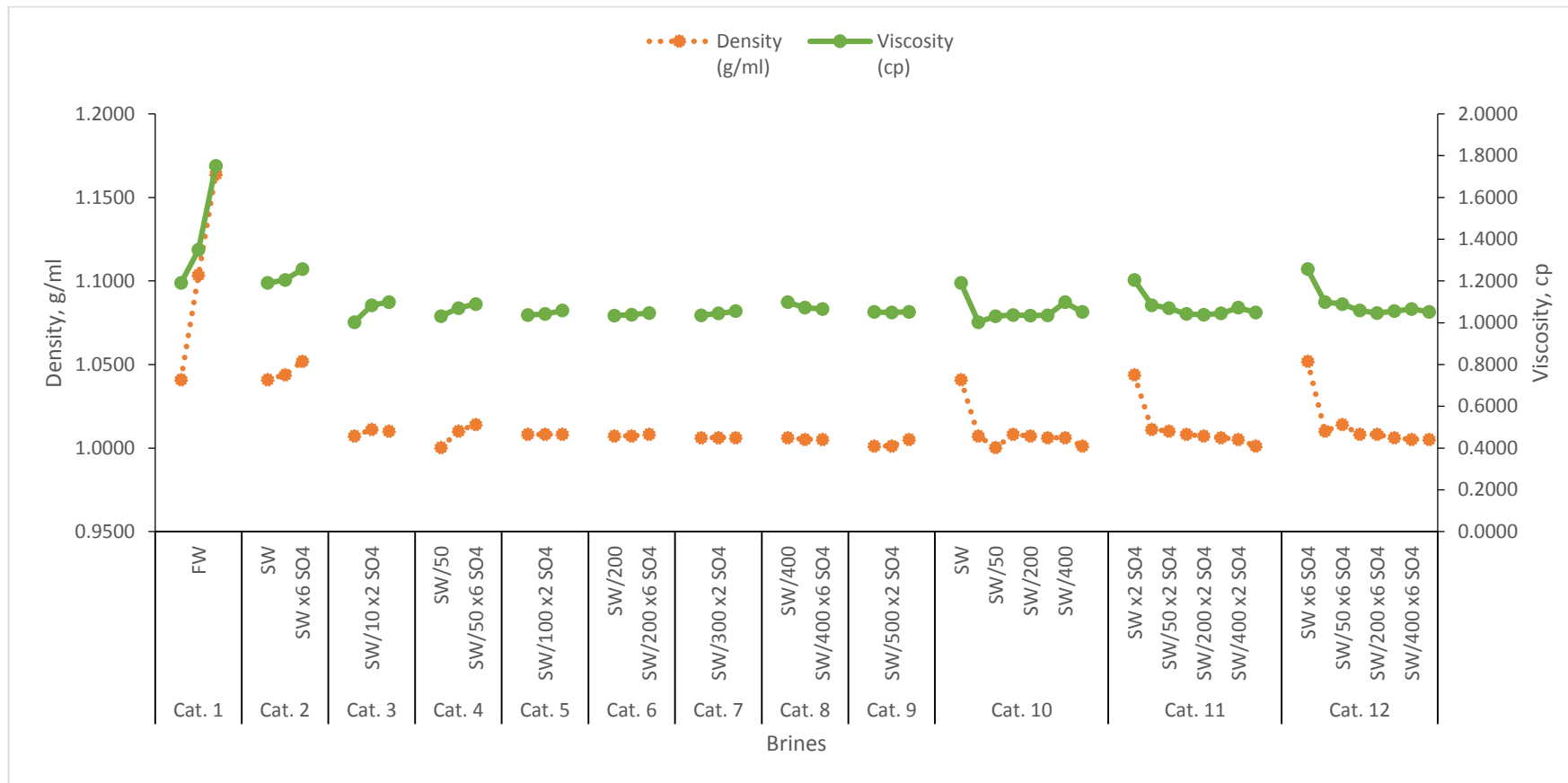


Figure 4.1: Density and Viscosity of all the categories

4.2 IFT Measurements

IFT measurements were made using Teclis Tracker. Initially, the IFT values of all the prepared brines were measured at 20°C and ambient pressure. Then the brines showing the least IFT and some high IFT were selected. Then the measurements were made at high pressure high temperature (HPHT). Still some high IFT brines at 20°C were selected for HPHT to show how much the IFT can be reduced at elevated temperature. All the IFT measurements were done using pendant drop method.

4.2.1 IFT results of different Brines at 20°C

IFT of all the brines were measured at 20°C and ambient pressure. All runs were carried out at a constant volume until stabilized IFT was obtained. The stabilized value of the Interfacial tension in dyne/cm at the end of each IFT test has been recorded and tabulated as presented in Table 4.3. Figure 4.2 is prepared on the basis of data from Table 4.3 and the categories listed in Table 4.2. A trendline was drawn for each category to generalize the behavior of brines in that category. The results of IFT measurements with proposed trendlines of the individual groups are shown in Appendix IV.

Table 4.3: Summary of IFT measurements at 20°C

Sl. No	Brine	IFT at 20°C dyne/cm
1	FW	15.07
2	SW	13.48
3	SW x2 SO4	11.9
4	SW x6 SO4	14.21
5	SW/10	17.99
6	SW/10 x2 SO4	20.85
7	SW/10 x6 SO4	16.01
8	SW/50	21.93
9	SW/50 x2 SO4	23.5
10	SW/50 x6 SO4	20.214
11	SW/100	24.81
12	SW/100 x2 SO4	22.91
13	SW/100 x6 SO4	23.07
14	SW/200	25.82
15	SW/200 x2 SO4	26.38
16	SW/200 x6 SO4	24.6
17	SW/300	24.8
18	SW/300 x2 SO4	23.78
19	SW/300 x6 SO4	21.92
20	SW/400	23.63
21	SW/400 x2 SO4	25.34
22	SW/400 x6 SO4	25.05
23	SW/500	18.76
24	SW/500 x2 SO4	24.189
25	SW/500 x6 SO4	22.48

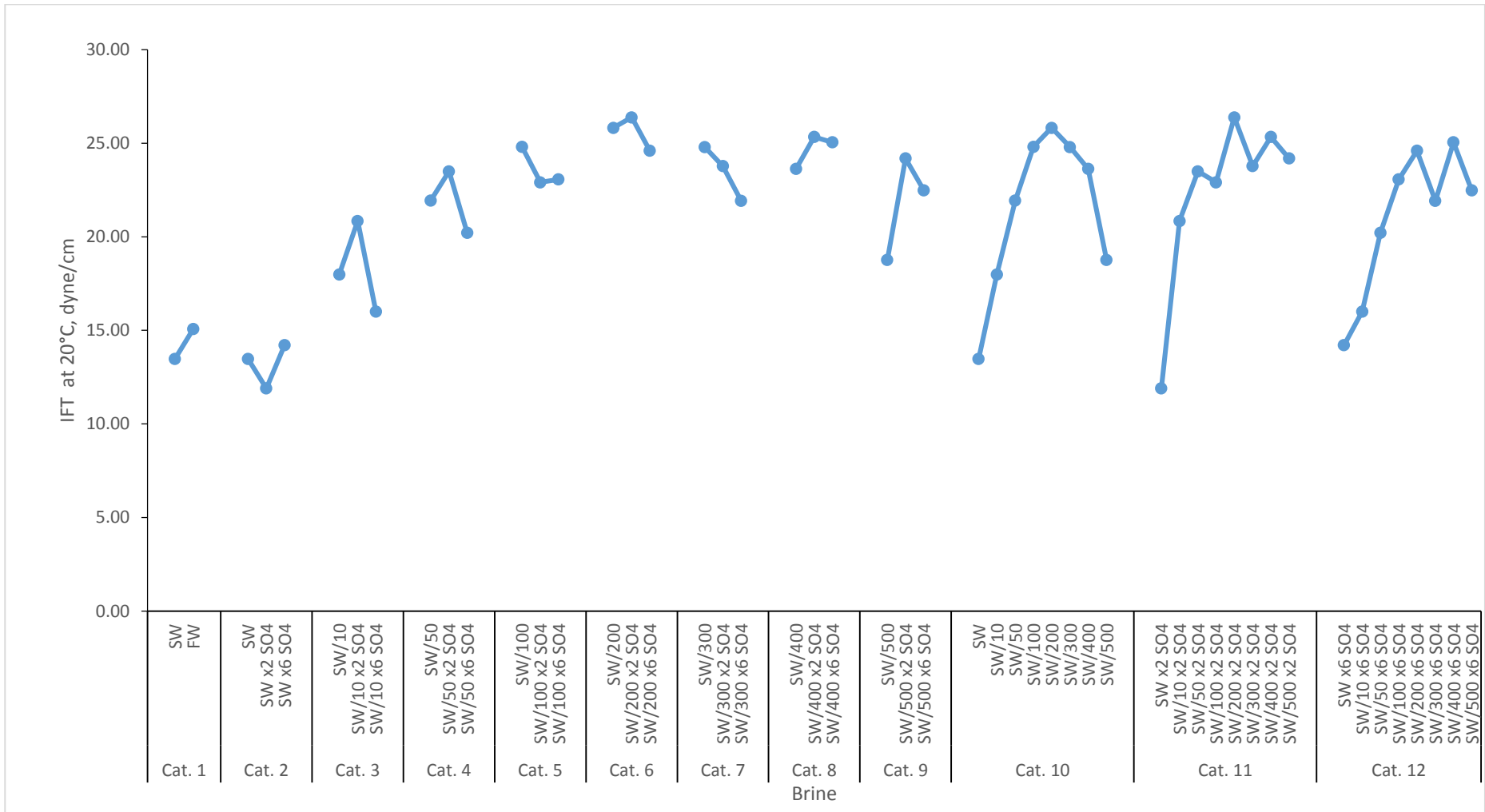


Figure 4.2: IFT measurements at 20°C of all categories

Category 1 shows a decreasing trend of IFT, similar to that observed by Taha and Alshiwaish (2009). These authors studied the effect of salinity on IFT and concluded that the decrease of salt concentration from 200,000 mg/l to 50,000 mg/l did reduce the IFT. They named the 50,000 mg/l Brine as low Salinity brine. The reduction of IFT results in the weakening of the intermolecular forces between oil and brine which assisted by the gravity effects promotes oil detachment from the brine. Category 1 also includes three different natural brines (SW, FW and IW) without dilution or sulphate spiking. The SW shows the least IFT compared to FW and IW, which is due to least amount of TDS in the SW.

Category 2 shows an increase in IFT with the effect of sulphate spiking. The IFT of six times sulphate spiked brine of SW is 5.41% greater than that of SW with natural sulphate. This increase of IFT in category 2, is due to the increased amount of sulphate by 5,310 mg/L in the spiked brine.

Categories 3 to 9, shows the combined effect of dilution and sulphate spiking. Categories 3 to 7 show a declining trend of IFT with increased concentration of sulphate. In category 3, the IFT of six times sulphate spiked brine of SW/10 is 11% less than that of SW/10 without sulphate spiking. In category 4, the IFT of six times sulphate spiked brine of SW/50 is 7.8 % less than that of SW/50 without sulphate spiking. In category 5, the IFT of six times sulphate spiked brine of SW/100 is 7.8 % less than that of SW/100 without sulphate spiking. In category 6, the IFT of six times sulphate spiked brine of SW/200 is 4.7 % less than that of SW/200 without sulphate spiking. In category 7, the IFT of six times sulphate spiked brine of SW/300 is 11.6 % less than that of SW/300 without sulphate spiking. This reduction of IFT in category

3 to 7, is due to the increased amount of sulphate by 5,310 mg/L in the spiked brine. So in categories 3 to 7, effect of sulphate spiking is more dominant than the effect of dilution. Observational error in Category 8 and 9 lead to an increasing trend of IFT. The same to be confirmed from the IFT at high pressure high temperature conditions because the sulphate has more effect at higher temperatures. In category 8, the IFT of six times sulphate spiked brine of SW/400 is 6% greater than that of SW/400 without sulphate spiking. In category 9, the IFT of six times sulphate spiked brine of SW/500 is 19.8% greater than that of SW/500 without sulphate spiking. This increase of IFT in category 8 and 9, is due to the increased amount of sulphate by 5,310 mg/L in the spiked brine. So effect of dilution is more than the effect of sulphate spiking in categories 8 and 9.

Category 10 shows the effect of dilution. Categories 11 and 12 show the combined effect of dilution and spiking. The categories 10 to 12 have large number of brines compared to the brines in the categories 2 to 9. An increase in IFT was observed for categories 10 to 12, because of reduction of ions with dilutions. Six times sulphate spiked brine of SW/500 has more amount of sulphate ion compared to other ions in the same brine, but still no promising IFT was observed.

The SW (Categories 1,2 and 10), SW x2 SO₄ (Categories 2 and 11) and SW x6 SO₄ (Categories 2 and 12) are the three brines that show the least IFT in Table 4.3 with SW x2 SO₄ shows the least IFT. Any further dilution from SW and the sulphate spiking of diluted SW would not be sufficient to reduce the IFT.

4.2.2 IFT of Brines at HPHT

Nine brines with the least IFT at 20°C were selected as candidates for IFT measurement at High pressure and high temperature (HPHT). Six more brines with high IFT at 20°C were also selected for the same purpose, to have an idea how HPHT conditions can affect the IFT measurements of these two sets of brines. Also IFT of formation water and Injection water were measured at HPHT. All IFT measurements were obtained at 90°C and 248 psi, namely, HPHT condition. Pressure has been found to have a little effect on IFT (Hjelmeland & Larrondo, 1986). In this work, pressure was applied to prevent evaporation of brine at the elevated temperature. Table 4.4 shows the IFT's of different brines at HPHT. All runs were continued until a stabilized IFT was obtained. Brines that show the least IFT with Asab crude oil were considered for further contact angle measurements. The reduced IFT promotes oil detachment from the brine surface and more oil will be recovered. Figure 4.3 is prepared on the basis of data from Table 4.4 and categories defined in Table 4.5. A trendline was drawn for each category to generalize the behavior of brines in that category. The results of IFT measurements at HPHT conditions with proposed trendlines of the individual groups are shown in appendix V and the IFT images at high pressure high temperature are shown in appendix VI. The discussion that follows is based on Figure 4.3.

Table 4.4: IFT measurements at HPHT

Brine	IFT at HPHT dyne/cm
FW	13.037
IW	19.608
SW	9.503
SW x2 SO4	9.572
SW x6 SO4	8.343
SW/10	11.741
SW/10 x2 SO4	11.145
SW/10 x6 SO4	10.351
SW/50	13.86
SW/50 x2 SO4	13.645
SW/50 x6 SO4	12.992
SW/200	17.281
SW/200 x6 SO4	17.217
SW/300	17.312
SW/400	18.519
SW/400 x2 SO4	15.302
SW/400 x6 SO4	15.731

Table 4.5: Brine Categorization of IFT at High Pressure High Temperature

Category IFT 1	Category IFT 2	Category IFT 3	Category IFT 4	Category IFT 5	Category IFT 6	Category IFT 7	Category IFT 8
SW	SW	SW/10	SW/50	SW/400	SW	SW2 x2 SO ₄	SW2 x6 SO ₄
FW	SW x2 SO ₄	SW/10 x2 SO ₄	SW/50 x2 SO ₄	SW/400 x2 SO ₄	SW/10	SW2/10 x2 SO ₄	SW2/10 x6 SO ₄
	SW x6 SO ₄	SW/10 x6 SO ₄	SW/50 x6 SO ₄	SW/400 x6 SO ₄	SW/50	SW2/50 x2 SO ₄	SW2/50 x6 SO ₄
					SW/200	SW2/400 x2 SO ₄	SW2/200 x6 SO ₄
					SW/300		SW2/400 x6 SO ₄
				SW/400			

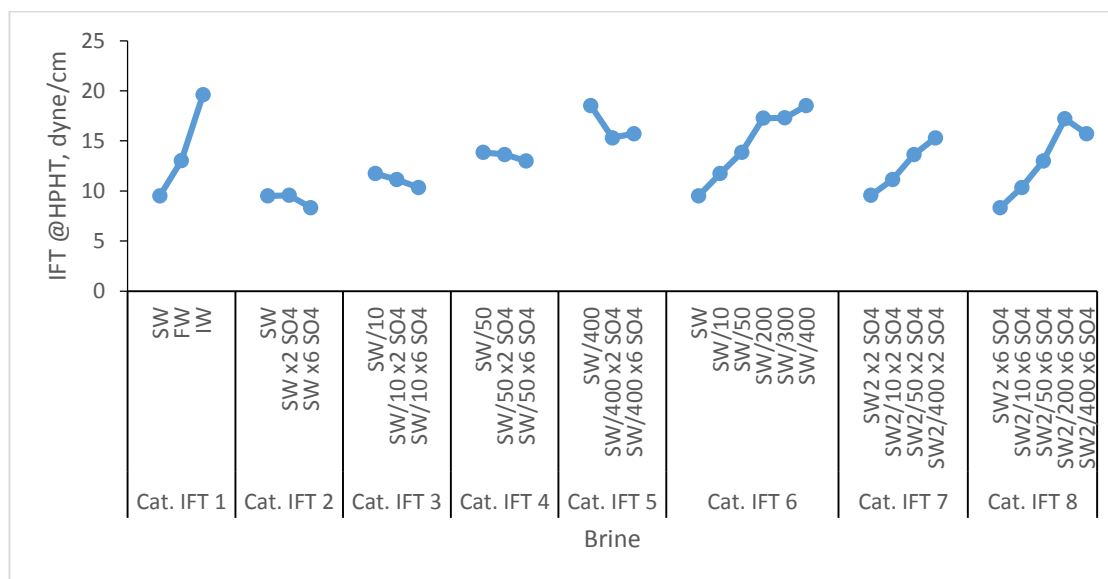


Figure 4.3: IFT at HPHT of all categories

HPHT conditions reduce the IFT values of category IFT 1 significantly compared to IFT at 20°C. Among the three brines in this category, SW corresponds to the least value of TDS and results in the least IFT. The formation and injection water, however, show high values of IFT even at HPHT conditions. There is an increasing trend in IFT for the category IFT 1.

Wang & Gupta (1995) concluded that the increase or decrease of IFT values depends on the composition of the brine. From categories IFT 2 to 5, there is a decreasing trend of IFT. Category 2 shows the effect of sulphate spiking. Combined effect of dilution and sulphate spiking is observed in categories 3 to 5. The three brines in categories 2 to 5, mainly differ in the concentration of sulphate ion and an overall reduction of IFT with sulphate spiking at HPHT can be observed. Combined effect of increasing temperature and sulphate concentration would result in a reduction of IFT. In category IFT 2, as the sulphate concentration is increased from 3,944 mg/L to 9,254 mg/L, the IFT decreased by 12.2%. The IFT of SW decreased by 29.5% at HPHT conditions comparing to 20°C and ambient pressure conditions. In category IFT 3, as

the sulphate concentration is increased from 394 mg/L to 5,704 mg/L, the IFT decreased by 11.83%. In category IFT 4, as the sulphate concentration is increased from 79 mg/L to 5,389 mg/L, the IFT decreased by 6.26%. In category IFT 5, as the sulphate concentration is increased from 10 mg/L to 5,320 mg/L, the IFT decreased by 15%.

From categories IFT 6 to 8, there is an increasing trend of IFT. Categories 6 to 8 show the effect of dilution. So dilution seems to have a negative effect on the IFT at HPHT conditions for categories IFT 6, 7 and 8. In category IFT 6, there is 94.8% increase in IFT compared to SW/400 with SW, which is quite significant. During dilution of brines the concentration of potential ions like calcium, magnesium and sulphate were reduced, which lead to an increase in IFT with dilution. In category IFT 7, there is 60% increase in IFT by going from SW x2 SO₄ to SW/400 x2 SO₄. Even though all the brines were twice spiked and had more sulphate compared to category IFT 6, IFT was slightly reduced. In category IFT 8, there is 88.5% increase in IFT by going from SW x6 SO₄ to SW/400 x6 SO₄ with. During the dilution of six times sulphate brines, concentration of potential ions like calcium, magnesium and sulphate were reduced, diluted brines had higher sulphate compared to other ions in the brine. These higher sulphate ions were not able to reduce the IFT.

The SW, SW x2 SO₄ and SW x6 SO₄ are the three brines that show the least IFT in Table 4.4 with SW x6 SO₄ showed the least IFT. Any further dilution from SW and the sulphate spiking of diluted SW would not be sufficient to reduce the IFT. So IFT results at HPHT conditions are in good agreement with IFT measurements at 20°C.

4.2.3 IFT measurements with temperature

The IFT was measured with temperature to see the effect of temperature on IFT. Nine best brine that showed the least IFT at HPHT conditions were selected as the candidates for IFT measurement with temperature. IFT values were recorded with temperature varying from 20°C to 90°C and pressure varying from 200 psi to 248 psi. Pressure has been found to have a little effect on IFT (Hjelmeland & Larrondo, 1986). The system was pressurized to avoid evaporation of the brine. The IFT values versus temperature are listed in Table 4.6.

In Figure 4.4, the IFT of all brines show a declining trend with temperature. The percentage reduction of IFT between 20°C and HPHT is shown in Figure 4.5. So the temperature plays a key role in lowering the IFT. From Figure 5, the highest percentage reduction of IFT was for SW/10 x2 SO₄ (-46.55%) and the lowest percentage reduction of IFT was for SW x2 SO₄ (-19.56%). Flock et al. (1986) and Karnanda et al. (2012) observed similar trend in IFT with increased temperature. As explained by Wang and Gupta (1995) and in the present work, the composition of oil seems to be an important factor in reducing IFT with temperature.

Table 4.6: IFT measurements of brine with temperature

SW2		SW2 x2 SO4		SW2 x6 SO4	
Temp °C	IFT dyne/cm	Temp °C	IFT dyne/cm	Temp °C	IFT dyne/cm
20	13.48	20	11.9	20	14.21
32.3	11.211	40	11.437	51	10.137
40.5	10.343	49.6	10.519	60	9.547
49.1	10.258	61.7	10.18	71	8.814
67.8	9.95	78.5	9.779	81	8.539
77.9	9.762	89.4	9.572	89.5	8.343
82.6	9.689				
89.6	9.503				

SW2/10		SW2/10 x2 SO4		SW2/10 x6 SO4	
Temp °C	IFT dyne/cm	Temp °C	IFT dyne/cm	Temp °C	IFT dyne/cm
20	17.99	20	20.85	20	16.01
41.4	17.476	41.4	19.979	42.2	14.295
58.4	13.845	49.6	15.809	57.6	11.639
67.8	13.776	55.1	15.806	62.8	11.046
89.2	11.741	63.4	13.337	89.4	10.351
		74.4	12.56		
		81.5	11.806		
		89.6	11.145		

SW2/50		SW2/50 x2 SO4		SW2/50 x6 SO4	
Temp °C	IFT dyne/cm	Temp °C	IFT dyne/cm	Temp °C	IFT dyne/cm
20	21.93	20	23.495	20	20.214
44.9	21.883	41.4	21.392	55.4	16.962
63.4	17.67	51.3	18.916	63.6	14.771
72.2	15.32	63.4	17.86	79.9	13.283
89.7	13.86	68.9	16.68	89.3	12.992
		78.2	15.157		
		81.8	14.37		
		89.5	13.406		

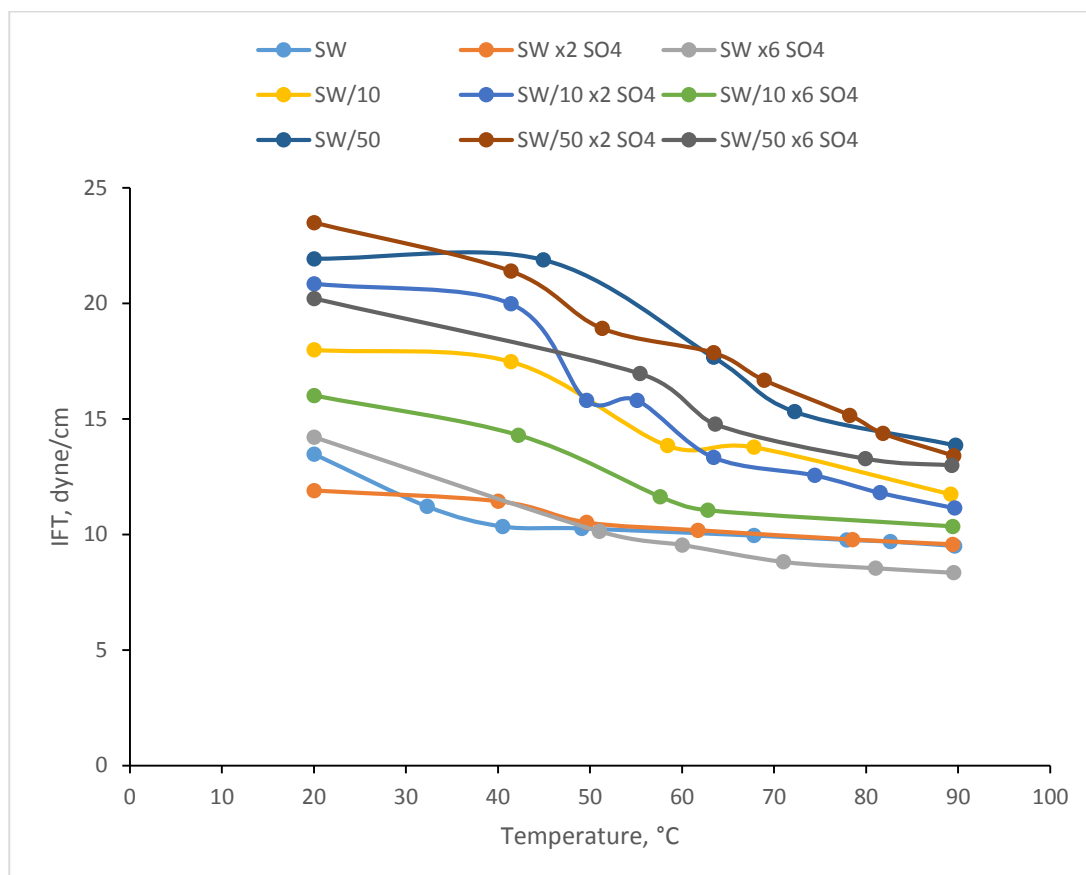


Figure 4.4: Variation of IFT measurements of the different brines with temperature

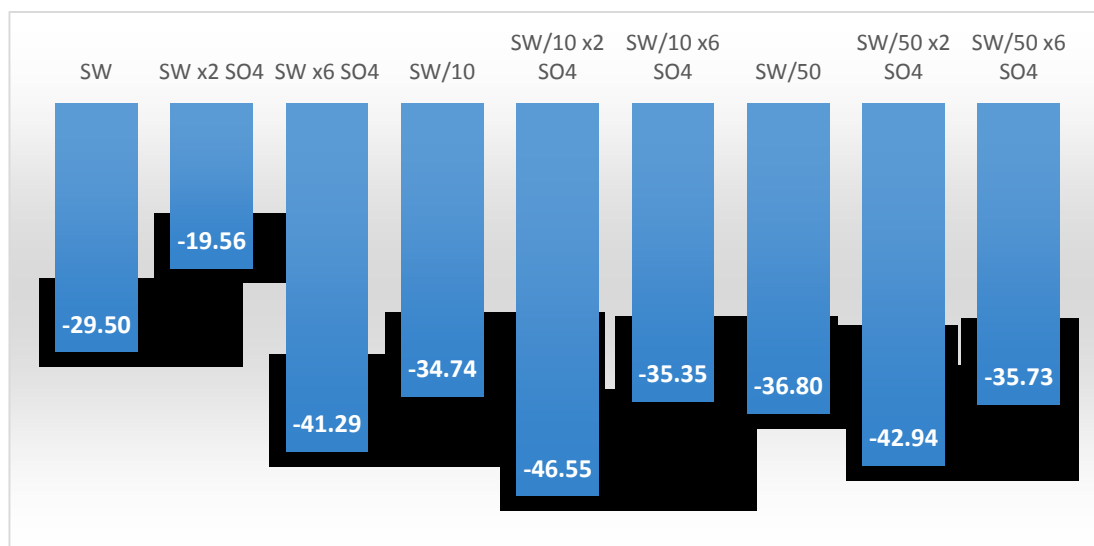


Figure 4.5: Percentage reduction of IFT between 20°C and HPHT

4.3 Contact Angle Measurements at single temperature and pressure

Contact angle measurements are crucial for identifying wettability and wettability alterations in a liquid/solid system. Contact angle is a function of IFT at solid/liquid and liquid/liquid interfaces. Wettability of a reservoir rock is a manifestation of the thermodynamic equilibrium between fluid in the pores and the mineral surfaces of the pore walls. Temperature, pressure and fluid characteristics are strongly believed to have an effect on wettability (Alotaibi et al., 2010). In this work, all contact angle measurements were performed on aged rock samples in oil, making the rock surface oil-wet with contact angle of 180° . A zero contact angle represents the condition of a fully water-wet system. Neutral wettability is considered at 90° . The brines that exhibited least IFT's were selected as candidate for contact angle. All contact angle measurements were carried out at 90°C and 248 psi. The aim is to verify how far the brine is capable of changing the wettability. Alotaibi et al. (2010) and Anderson (1986) classified wettability in terms of contact angle as being water-wet ($0-75^\circ$), intermediate-wet ($75-115^\circ$) and oil-wet ($115-180^\circ$). Weakly water-wet and oil-wet conditions are represented by ($55-75^\circ$) and ($115-135^\circ$), respectively. Some contact angle measurements were also carried out for brines of high IFT values even at HPHT conditions. All the measurements were monitored for 72 hours. Stabilized contact angle measurements after elapsed time of 72 hours are given in Table 4.7. Figure 4.6 is based on data from Table 4.7 and Table 4.8. The graph of each contact angle category with trendline is shown in appendix VII. Contact angle images of all brines can be found in the Appendix VIII. All the discussions are based on Figure 4.6 and trendline of each category in appendix VII. Figure 4.7 shows the change in contact angle at high pressure high temperature condition.

Table 4.7: Contact angle measurements of different brines at HPHT

<i>Brine</i>	<i>Contact Angle after 72 hrs Degree</i>	<i>Wettability Mode</i>
SW	113	Intermediate Wet
SW/10	131	Oil Wet
SW/50	114	Intermediate Wet
SW/500	135	Oil Wet
SW x2 SO4	138	Oil Wet
SW/10 x2 SO4	123	Oil Wet
SW/50 x2 SO4	147	Oil Wet
SW/200 x2 SO4	158	Oil Wet
SW/400 x2 SO4	150	Oil Wet
SW x6 SO4	162	Oil Wet
SW/10 x6 SO4	142	Oil Wet
SW/50 x6 SO4	148	Oil Wet

Table 4.8: Brine Categorization of Contact Angle at High Pressure High Temperature

<i>Category CA 1</i>	<i>Category CA 2</i>	<i>Category CA 3</i>	<i>Category CA 4</i>	<i>Category CA 5</i>	<i>Category CA 6</i>
SW	SW/10	SW/50	SW	SW x2 SO4	SW x6 SO4
SW x2 SO4	SW/10 x2 SO4	SW/50 x2 SO4	SW/10	SW/10 x2 SO4	SW/10 x6 SO4
SW x6 SO4	SW/10 x6 SO4	SW/50 x6 SO4	SW/50	SW/50 x2 SO4	SW/50 x6 SO4
			SW/500	SW/200 x2 SO4	
				SW/400 x2 SO4	

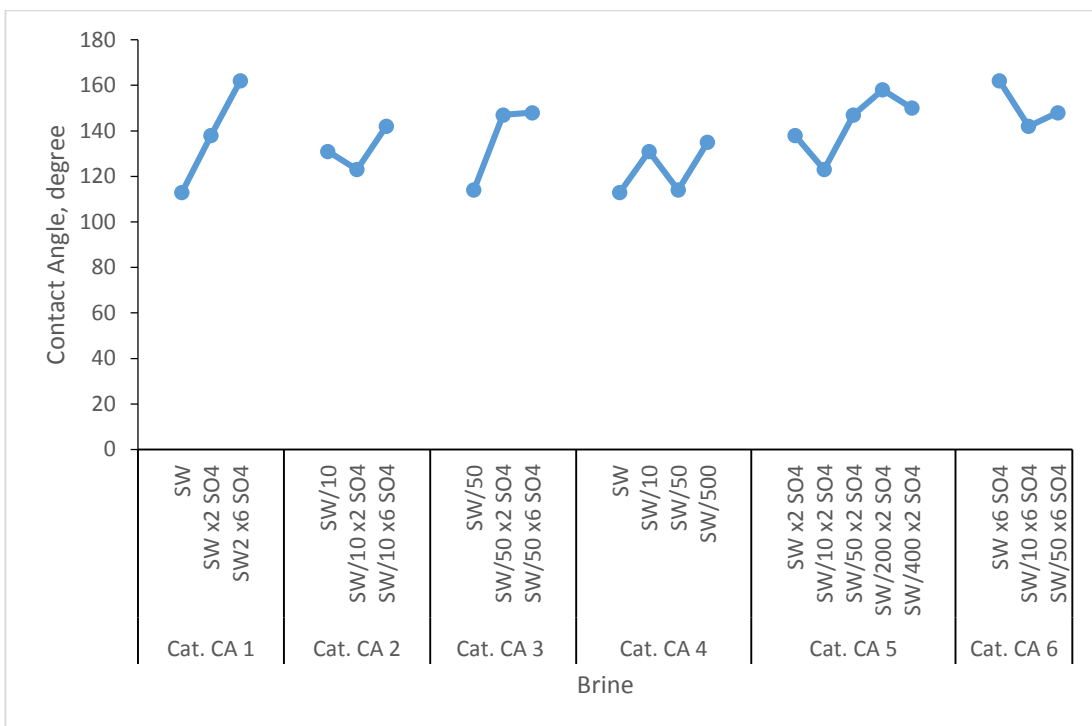


Figure 4.6: Contact angle measurements at HPHT of all categories together

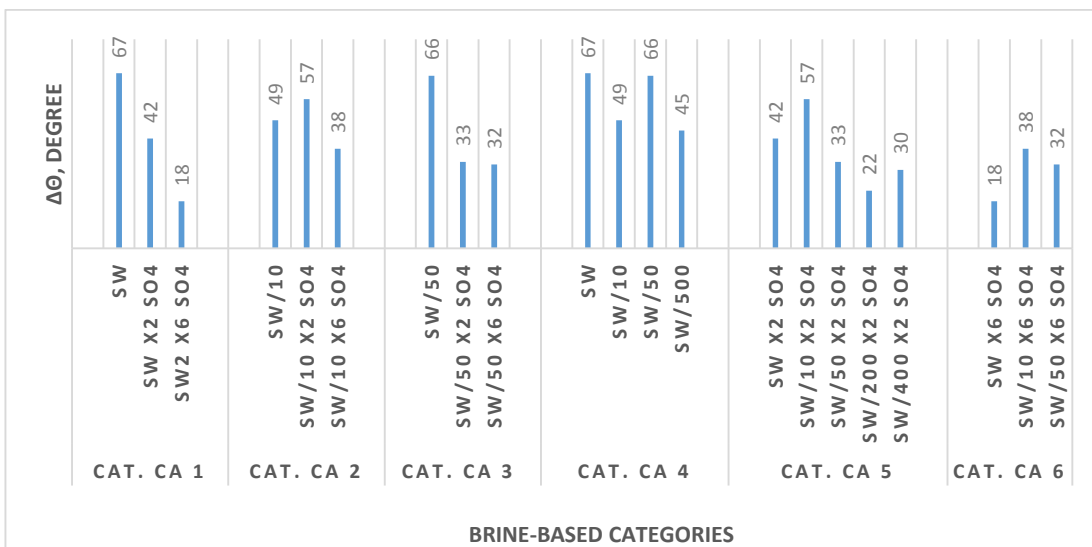


Figure 4.7: Change in contact angle at high pressure high temperature conditions

In category CA 1, Sulphate spiking of the SW makes the rock surface more oil-wet. Also SW ($\Delta\theta = 67^\circ$) was capable of changing the wettability from oil-wet to the border line of intermediate-wet system. In category CA 2, SW/10 ($\Delta\theta = 49^\circ$) changed the wettability from oil wet to weakly oil wet. In category CA 3, SW/50 ($\Delta\theta = 66^\circ$) changed the wettability from oil-wet to border line of intermediate wettability. The category CA 1 to 3 shows that sulphate spiking increased the contact angle. Hognesen et al. (2005) reported that the ratio of Calcium to sulphate ion is a key factor in altering the wettability. It seems like sulphate spiking was not enough to achieve that optimum calcium-sulphate ratio. Although this observation contradicts the results of Pierre et al. (1990); Strand et al. (2008); Strand et al. (2003) who concluded that sulphate is the ion that shows good potential towards limestone. Contact angle is dependent on temperature and independent of pressure (Wang & Gupta, 1995). All measurements were done at high temperature to incorporate that effect.

Categories CA 4 and 5 shows an increasing contact angle with dilution. It seems that calcium-sulphate ratio wasn't good enough to alter the wettability. In category CA 6, although the contact angle has decreased but didn't change the wettability from oil wet to intermediate wet.

SW was thus selected as the most likely smart brine from the observations of this work because it had the least contact angle and changed the wettability from oil-wet to the border line of intermediate-wet conditions. Also the IFT of SW is among the least. So contact angle results are in agreement with IFT. Also the SW/50 changed the wettability from oil-wet to border line of intermediate-wet conditions, but it doesn't cater for dilution cost with deionised water. It seems like sea water does have the optimum ratio of sulphate to calcium ions because sea water changed the wettability

from oil-wet to the border line of intermediate wet. Ratio of sulphate and calcium ions of SW, SW x2 SO₄ and SW x6 SO₄ are 5.72, 8.28 and 13.41, respectively. So, a ratio of 5.72 may be considered as the optimum ratio of sulphate to calcium in this work. All the six times sulphate spiked brine stood strongly in oil wet nature.

Figure 4.8 shows the contact angle measurement versus time. All the measurements were started from 180° (strongly oil-wet). The contact angle of all the brines stabilized after some point in time, indicating no further reduction in wettability.

SW and SW/50 are the brines that changed the wettability from oil-wet to the border line of intermediate-wet conditions under high temperature and high pressure conditions.

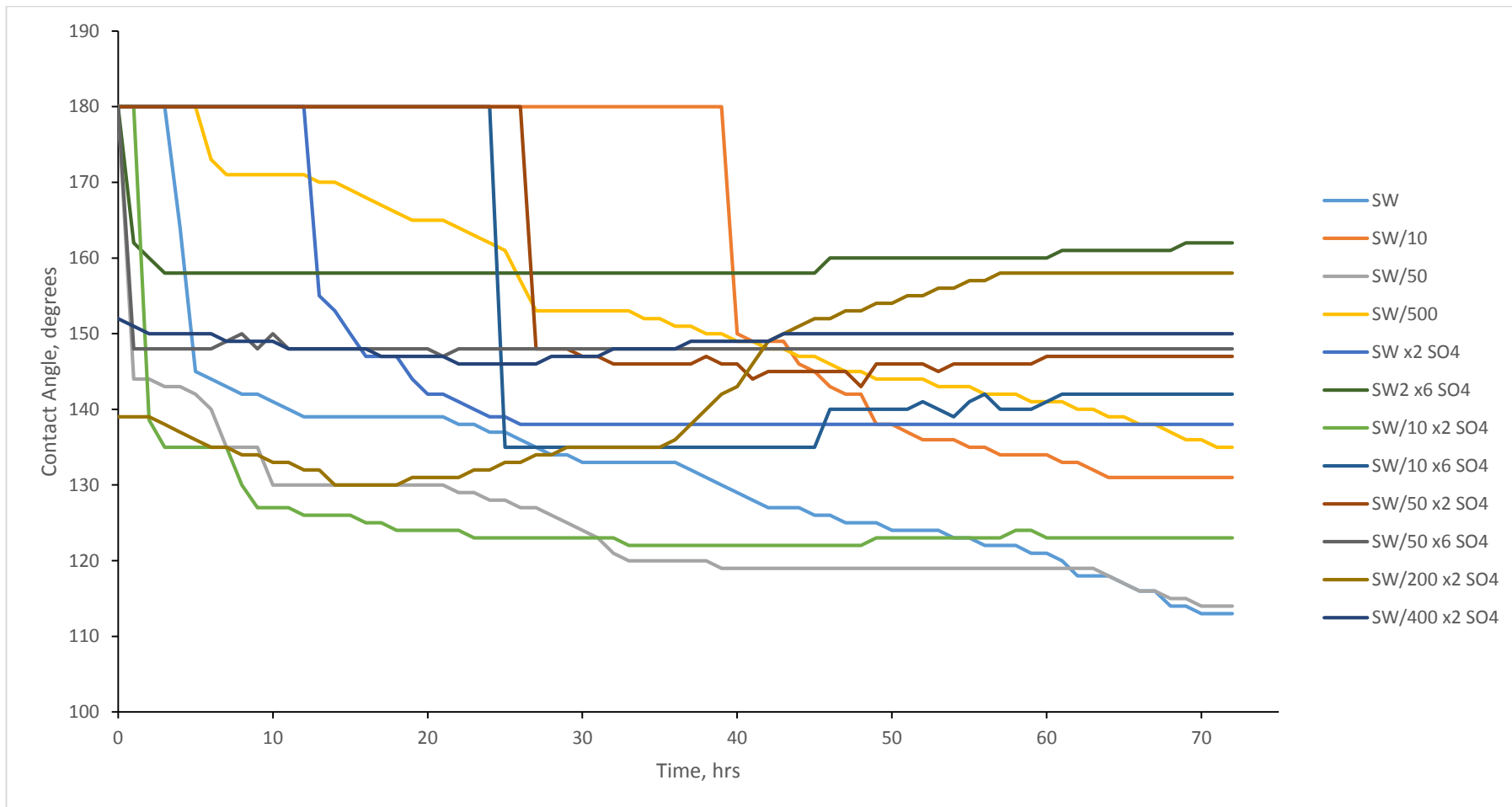


Figure 4.8: Contact Angle measurements with time

Chapter 5: Conclusion and Recommendation

5.1 Conclusion

1. Based on the results of IFT measurements at 20°C, SW and its twice and six times sulphate spiked may be considered as the three best brines that have shown the least IFT. Among these three brines the SW x2 SO₄ brine has shown the least IFT.
2. The results of IFT measurements at HPHT conditions have shown that SW, its twice and six times sulphate spiked seem to be the three best brines of least IFT. Increasing the test temperature has been found to reduce the IFT. Among these three brines the SW x6 SO₄ brine has shown the least IFT, because the sulphate ion was capable of interacting more at 90°C.
3. From Appendix VI, as the IFT value decreases, the shape of the drop becomes elongated at its base which indicates the tendency of the drop to leave the brine medium, when the IFT image of SW is compared with its diluted brines.
4. From the contact angle results at high pressure high temperature, the best brines that showed the least contact angle are SW and SW/50. These brines changed the wettability of rock from oil-wet to border line of intermediate-wet.
5. Sulphate spiking at HPHT conditions has shown a good impact on IFT and a negative impact on contact angle.
6. Brine dilution at HPHT conditions has shown a negative impact on IFT and contact angle.
7. From above results and economic point of view, SW is the most likely smart water which has an IFT of 9.503 dyne /cm at HPHT conditions and a contact angle of 113 degrees ($\Delta\theta = 67^\circ$).

5.2 Recommendations

1. Amott, USBM and Flooding test should be conducted under similar conditions on the SW to confirm the results of this work.
2. Further investigation is needed to identify any optimum sulphate – calcium ratio below 5.72 and/or any optimum combination of sulphate – calcium - magnesium which could significantly promote wettability alteration.

Bibliography

- Ahmed, T. (2006). *Reservoir engineering handbook* (3rd ed). Amsterdam: Elsevier, GPP.
- Al-Attar, H. H., Mahmoud, M. Y., Zekri, A. Y., Almehaideb, R. A., & Ghannam, M. T. (2013). Low Salinity Flooding in a Selected Carbonate Reservoir: Experimental Approach. Society of Petroleum Engineers. <http://doi.org/10.2118/164788-MS>
- Al-Hadhrami, H. S., & Blunt, M. J. (2000). Thermally Induced Wettability Alteration to Improve Oil Recovery in Fractured Reservoirs. Society of Petroleum Engineers. <http://doi.org/10.2118/59289-MS>
- Almehaideb, R. A., Ghannam, M. T., & Zekri, A. Y. (2004). Experimental Investigation of Contact Angles Under Oil-Microbial Solution on Carbonate Rocks. *Petroleum Science and Technology*, 22(3-4), 423–438. <http://doi.org/10.1081/LFT-120024568>
- Alotaibi, M. B., Azmy, R., & Nasr-El-Din, H. A. (2010). Wettability Challenges in Carbonate Reservoirs. Society of Petroleum Engineers. <http://doi.org/10.2118/129972-MS>
- Amyx, J. W., Bass, D. M., & Whiting, R. L. (1988). *Petroleum reservoir engineering: physical properties*. New York: McGraw-Hill.
- Anderson, W. G. (1986). Wettability Literature Survey- Part 1: Rock/Oil/Brine Interactions and the Effects of Core Handling on Wettability. *Journal of Petroleum Technology*, 38(10), 1125–1144. <http://doi.org/10.2118/13932-PA>
- Austad, T., Strand, S., Madland, M. V., Puntervold, T., & Korsnes, R. I. (2007). Seawater in Chalk: An EOR and Compaction Fluid. International Petroleum Technology Conference. <http://doi.org/10.2523/11370-MS>
- Brown, R. J. S., & Fatt, I. (1956). Measurements Of Fractional Wettability Of Oil Fields' Rocks By The Nuclear Magnetic Relaxation Method. Society of Petroleum Engineers. <http://doi.org/10.2118/743-G>
- Dake, L. P. (2010). *The practice of reservoir engineering* (Rev. ed., reprint. Transferred to digital printing). Amsterdam: Elsevier.
- Donaldson, E. C., & Thomas, R. D. (1971). Microscopic Observations of Oil Displacement in Water-Wet and Oil-Wet Systems. Society of Petroleum Engineers. <http://doi.org/10.2118/3555-MS>

- Emery, L. W., Mungan, N., & Nicholson, R. W. (1970). Caustic Slug Injection in the Singleton Field. *Journal of Petroleum Technology*, 22(12), 1569–1576. <http://doi.org/10.2118/2425-PA>
- Flock, D. L., Le, T. H., & Gibeau, J. P. (1986). The Effect Of Temperature On The Interfacial Tension Of Heavy Crude Oils Using The Pendant Drop Apparatus. *Journal of Canadian Petroleum Technology*, 25(02). <http://doi.org/10.2118/86-02-06>
- Green, D. W., & Willhite, G. P. (2008). *Enhanced oil recovery* (4. Nachdr.). Richardson, Tex: Henry L. Doherty Memorial Fund of AIME, Society of Petroleum Engineers.
- Hamouda, A. A., & Karoussi, O. (2008). Effect of Temperature, Wettability and Relative Permeability on Oil Recovery from Oil-wet Chalk. *Energies*, 1(1), 19–34. <http://doi.org/10.3390/en1010019>
- Hjelmeland, O. S., & Larrondo, L. E. (1986). Experimental Investigation of the Effects of Temperature, Pressure, and Crude Oil Composition on Interfacial Properties. *SPE Reservoir Engineering*, 1(04), 321–328. <http://doi.org/10.2118/12124-PA>
- Hognesen, E. J., Strand, S., & Austad, T. (2005). Waterflooding of preferential oil-wet carbonates: Oil recovery related to reservoir temperature and brine composition. Society of Petroleum Engineers. <http://doi.org/10.2118/94166-MS>
- Iwankow, E. N. (1958). *A Correlation of Interstitial Water Saturation and Heterogeneous Wettability*.
- Karnanda, W., Benzagouta, M. S., AlQuraishi, A., & Amro, M. M. (2012). Effect of temperature, pressure, salinity, and surfactant concentration on IFT for surfactant flooding optimization. *Arabian Journal of Geosciences*, 6(9), 3535–3544. <http://doi.org/10.1007/s12517-012-0605-7>
- Kyte, J. R., Naumann, V. O., & Mattax, C. C. (1961). Effect of Reservoir Environment on Water-Oil Displacements. *Journal of Petroleum Technology*, 13(06), 579–582. <http://doi.org/10.2118/55-PA>
- Lichaa P et al. (1992). Wettability Evaluation of a Carbonate Reservoir Rock. *Advances in Core Evaluation III Reservoir Management*.

- Masalmeh, S. K. (2002). Studying the effect of wettability heterogeneity on the capillary pressure curves using the centrifuge technique. *Journal of Petroleum Science and Engineering*, 33(1–3), 29–38. [http://doi.org/10.1016/S0920-4105\(01\)00173-5](http://doi.org/10.1016/S0920-4105(01)00173-5)
- Moeini, F., Hemmati-Sarapardeh, A., Ghazanfari, M.-H., Masihi, M., & Ayatollahi, S. (2014). Toward mechanistic understanding of heavy crude oil/brine interfacial tension: The roles of salinity, temperature and pressure. *Fluid Phase Equilibria*, 375, 191–200. <http://doi.org/10.1016/j.fluid.2014.04.017>
- Okasha, T. M., & Alshiwaish, A. (2009). Effect of Brine Salinity on Interfacial Tension in Arab-D Carbonate Reservoir, Saudi Arabia. Society of Petroleum Engineers. <http://doi.org/10.2118/119600-MS>
- Okasha, T. M., & Al-Shiwaish, A.-J. A. (2010). Effect of Temperature and Pressure on Interfacial Tension and Contact Angle of Khuff Gas Reservoir, Saudi Arabia. Society of Petroleum Engineers. <http://doi.org/10.2118/136934-MS>
- Pierre, A., Lamarche, J. M., Mercier, R., Foissy, A., & Persello, J. (1990). Calcium as Potential Determining Ion in Aqueous Calcite Suspensions. *Journal of Dispersion Science and Technology*, 11(6), 611–635. <http://doi.org/10.1080/01932699008943286>
- RezaeiDoust, A., Puntervold, T., Strand, S., & Austad, T. (2009). Smart Water as Wettability Modifier in Carbonate and Sandstone: A Discussion of Similarities/Differences in the Chemical Mechanisms. *Energy & Fuels*, 23(9), 4479–4485. <http://doi.org/10.1021/ef900185q>
- Salathiel, R. A. (1973). Oil Recovery by Surface Film Drainage In Mixed-Wettability Rocks. *Journal of Petroleum Technology*, 25(10), 1216–1224. <http://doi.org/10.2118/4104-PA>
- Saner. (1991). Wettability study of saudi arabian reservoir core sample. *Arabian Journal of Science and Technology*.
- Strand, S., Høgnesen, E. J., & Austad, T. (2006). Wettability alteration of carbonates—Effects of potential determining ions (Ca²⁺ and SO₄²⁻) and temperature. *Colloids and Surfaces A: Physicochemical and Engineering Aspects*, 275(1–3), 1–10. <http://doi.org/10.1016/j.colsurfa.2005.10.061>
- Strand, S., Puntervold, T., & Austad, T. (2008). Effect of Temperature on Enhanced Oil Recovery from Mixed-Wet Chalk Cores by Spontaneous Imbibition and Forced Displacement Using Seawater. *Energy & Fuels*, 22(5), 3222–3225. <http://doi.org/10.1021/ef800244v>

- Strand, S., Standnes, D. C., & Austad, T. (2003). Spontaneous Imbibition of Aqueous Surfactant Solutions into Neutral to Oil-Wet Carbonate Cores: Effects of Brine Salinity and Composition. *Energy & Fuels*, 17(5), 1133–1144. <http://doi.org/10.1021/ef030051s>
- Tiab, D., & Donaldson, E. C. (2010). *Petrophysics: theory and practice of measuring reservoir rock and fluid transport properties* (2. ed. with new and updated materials, [reprint.]). Amsterdam: Elsevier [u.a.].
- Torsaeter, O. (1984). An Experimental Study of Water Imbibition in Chalk From the Ekofisk Field. Society of Petroleum Engineers. <http://doi.org/10.2118/12688-MS>
- Wang, W., & Gupta, A. (1995). Investigation of the Effect of Temperature and Pressure on Wettability Using Modified Pendant Drop Method. Society of Petroleum Engineers. <http://doi.org/10.2118/30544-MS>
- Willhite, G. P. (1986). *Waterflooding* (3. printing). Richardson, Tex: Society of Petroleum Engineers.
- Yang, D., Gu, Y., & Tontiwachwuthikul, P. (2008). Wettability Determination of the Crude Oil–Reservoir Brine–Reservoir Rock System with Dissolution of CO₂ at High Pressures and Elevated Temperatures. *Energy & Fuels*, 22(4), 2362–2371. <http://doi.org/10.1021/ef800012w>
- Yu, L., Standnes, D. C., & Skjæveland, S. M. (2007). Wettability Alteration of Chalk by Sulphate Containing Water, Monitored by Contact Angle Measurement. Presented at the International Symposium of the Society of Core Analysts, Calgary, Canada.
- Zahid, A., Shapiro, A. A., & Skauge, A. (2012). Experimental Studies of Low Salinity Water Flooding Carbonate: A New Promising Approach. Society of Petroleum Engineers. <http://doi.org/10.2118/155625-MS>
- Zhang, P., & Austad, T. (2005). The Relative Effects of Acid Number and Temperature on Chalk Wettability. Society of Petroleum Engineers. <http://doi.org/10.2118/92999-MS>
- Zhang, P., & Austad, T. (2006). Wettability and oil recovery from carbonates: Effects of temperature and potential determining ions. *Colloids and Surfaces A: Physicochemical and Engineering Aspects*, 279(1–3), 179–187. <http://doi.org/10.1016/j.colsurfa.2006.01.009>

Zhang, P., Tweheyo, M. T., & Austad, T. (2007). Wettability alteration and improved oil recovery by spontaneous imbibition of seawater into chalk: Impact of the potential determining ions Ca^{2+} , Mg^{2+} , and SO_4^{2-} . *Colloids and Surfaces A: Physicochemical and Engineering Aspects*, 301(1–3), 199–208. <http://doi.org/10.1016/j.colsurfa.2006.12.058>

Appendix I: Brine Preparation Procedure

The following procedure has been used for preparation of brine:

1. Obtained a 1L volumetric flask, and checked whether it is clean. If not, flask is washed by deionized water
2. Half of the volumetric flask is filled with deionized water and placed a clean magnetic stirrer carefully into the flask.
3. Flask is placed on the stirrer pad and switched on.
4. Salts are carefully weighed and placed in the flask.
5. Flask is filled up to the mark with deionized water, ensuring any salts clinging to the neck are washed down.
6. Stir until all the salts have dissolved.
7. Took a clean side-arm flask, vacuuming equipment, filter equipment and magnetic stirrer.
8. Check the flask is clean as described in step 1.
9. Placed the three pieces of filter paper into the filter funnel and poured a small amount of brine on top, enough to dampen and flatten down the filter paper. Filter paper was smoothed manually to ensure the filter paper is thoroughly flattened.
10. Vacuum was switched on and slowly poured brine into the funnel.
11. When brine was completely transferred, switched off the vacuum and checked whether the brine is properly filtered or not, by ensuring that it is transparent and has no particles noticeable in it. If it is not filtered properly repeat steps 9, 10 using one 'medium' and one 'slow' filter paper.
12. Removed the funnel, switched on the magnetic stirrer in the brine and placed a rubber bung on top of the flask.

13. Switched the vacuum on, and degassed for 5 minutes only. Vacuuming more than this time may affect the brine concentration because of evaporation, and hence the electrical properties of the brine.
14. When the brine has been degassed, transferred it to a clean plastic brine container. Ensured that no gas is introduced into the brine. Label the container with brine name.
15. Thoroughly cleaned all the equipment used.
16. Measured the density and viscosity of brine. Checked it with Schlumberger type chart, if it is within ± 0.002 ohm-m at 77°F resistivity, then the brine is ready for use.

Appendix II: Sulphate Spiking Calculations

Sulphate spiking was accomplished by using Sodium Sulphate (Na_2SO_4) Salt. An increase in sulphate concentration will lead to an increase in sodium as well. In the literature review, the sodium has been found to have no significant effect on the oil recovery (Alotaibi et. al, 2010). Molar mass of Sodium and Sulphate are 23 g/mol and 96 g/mol, respectively. So 1 mole of Na_2SO_4 contains 142 g/mol. Or in other words, 1 mole of Na_2SO_4 contains 46 g (46,000 mg) of sodium and 96 g (96,000 mg) of sulphate, respectively.

Twice SO_4 Spiking

To have the brine twice spiked, an addition of 1,770 mg/L of SO_4 is necessary. One mole of Na_2SO_4 contains 96,000 mg of SO_4 . So an additional 2.62 g of $\text{Na}_2\text{SO}_4/\text{L}$ is needed to increase the sulphate ion concentration by 1,770 mg/L, making the brine twice sulphate spiked. An equivalent increase of sodium concentration takes place. Also one mole of Na_2SO_4 contains 46,000 mg of Na. There will be an increase of 848.73 mg of Na/L due to the addition of 2.62 g of $\text{Na}_2\text{SO}_4/\text{L}$.

Six times SO_4 Spiking

To have the brine six times sulphate spiked, an addition of 5,310 mg/L of SO_4 is necessary. One mole of Na_2SO_4 contains 96,000 mg of SO_4 . So an additional 7.854 g of $\text{Na}_2\text{SO}_4/\text{L}$ is needed to increase the sulphate ion concentration by 5,310 mg/L, making the brine six times sulphate spiked. An equivalent increase of sodium concentration takes place. Also one mole of Na_2SO_4 contains 46,000 mg of Na. There will be an increase of 2,544.25 mg of Na/L due to the addition of 7.854 g of $\text{Na}_2\text{SO}_4/\text{L}$.

Appendix III: Density and viscosity categories at 20°C

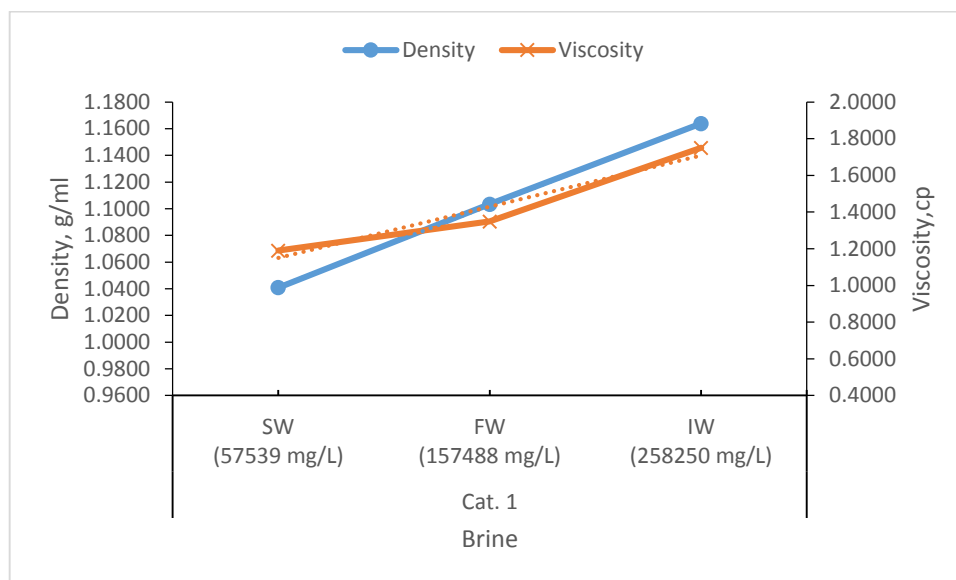


Figure III.1: Density and Viscosity of Category 1

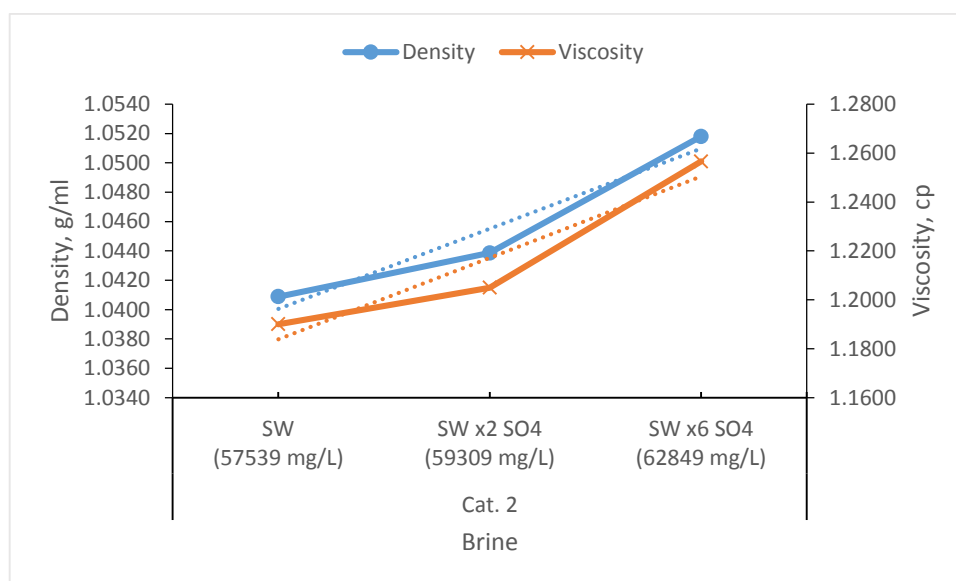


Figure III.2: Density and Viscosity of Category 2

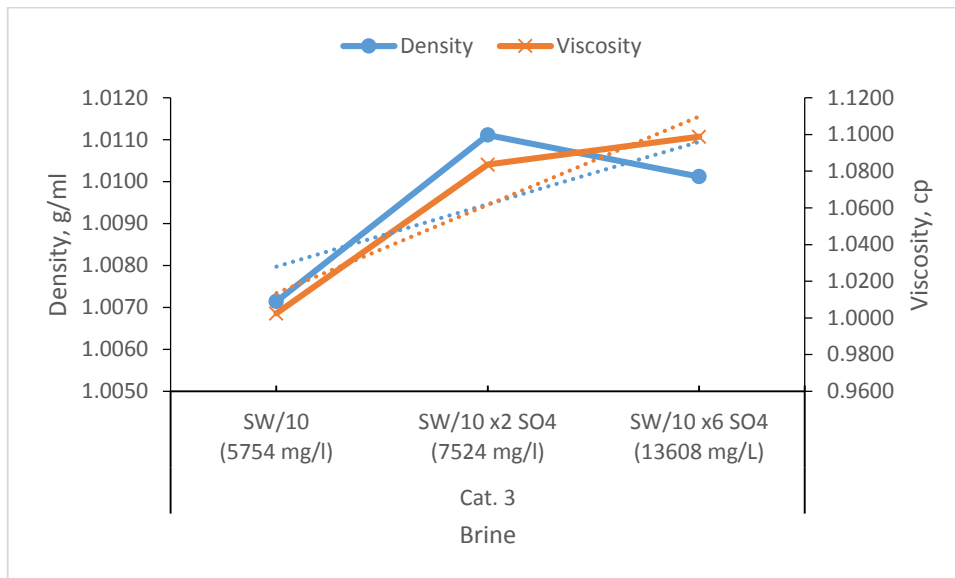


Figure III.3: Density and Viscosity of Category 3

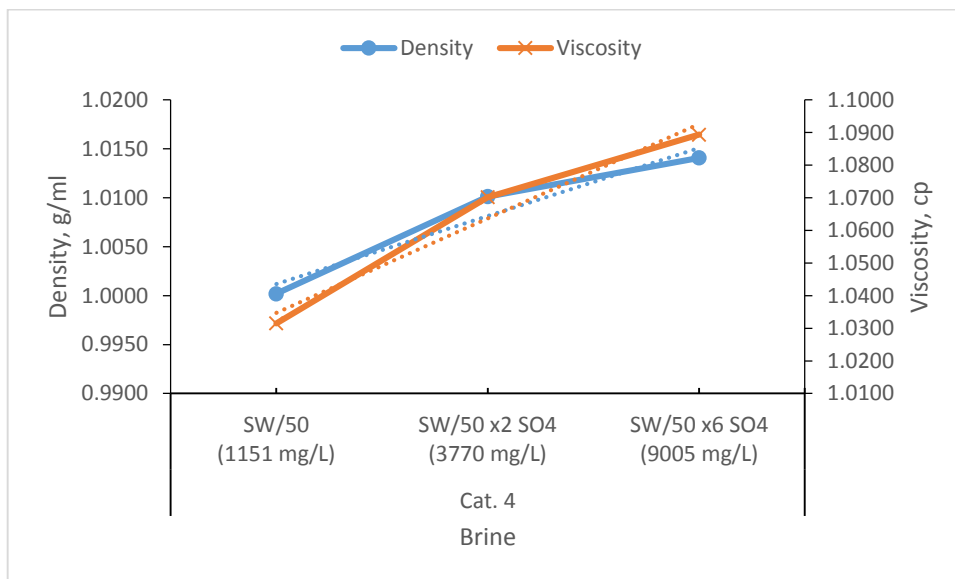


Figure III.4: Density and Viscosity of Category 4

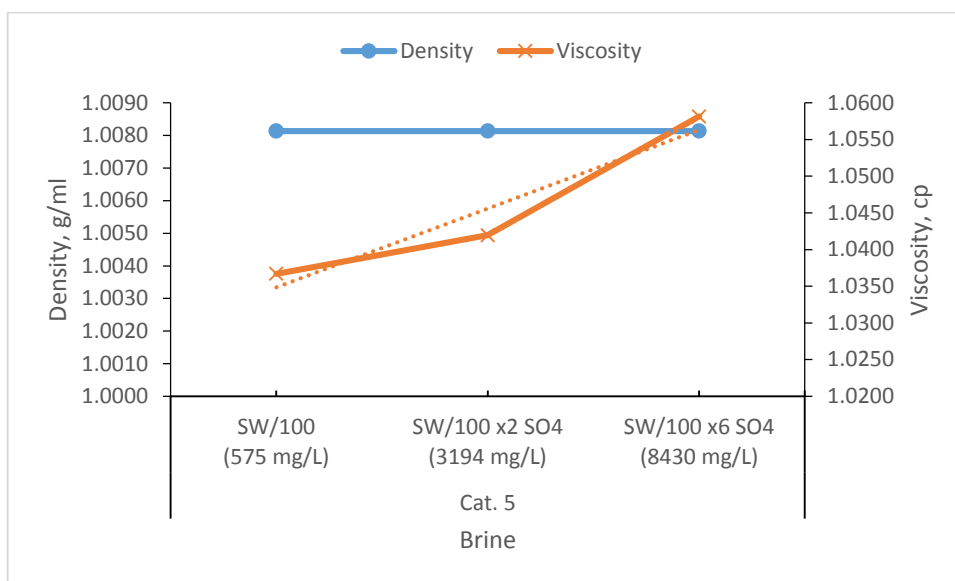


Figure III.5: Density and Viscosity of Category 5

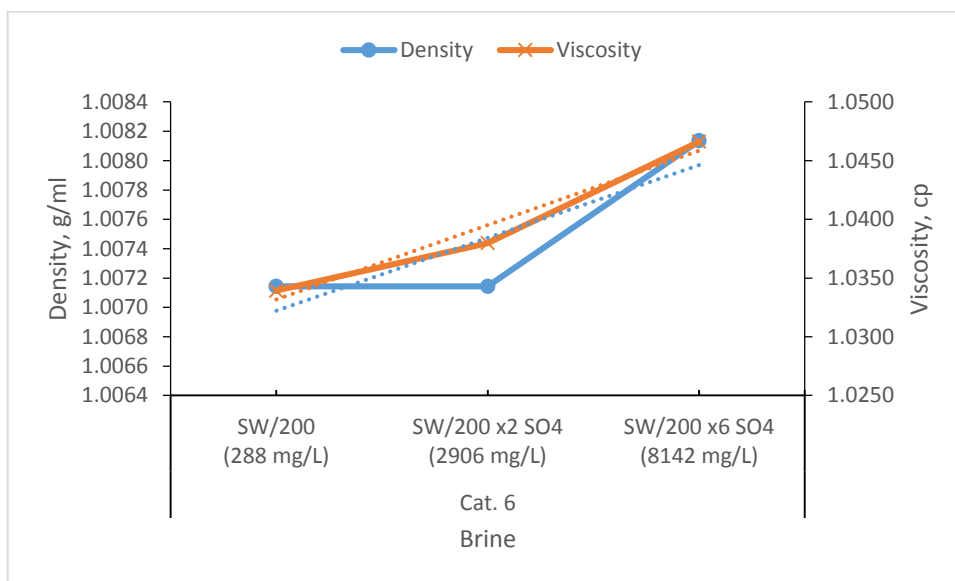


Figure III.6: Density and Viscosity of Category 6

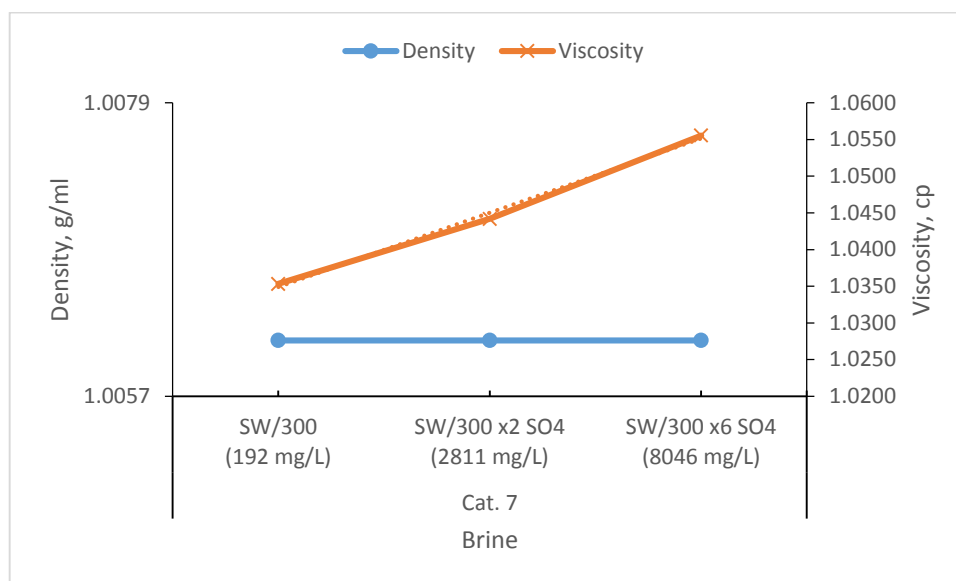


Figure III.7: Density and Viscosity of Category 7

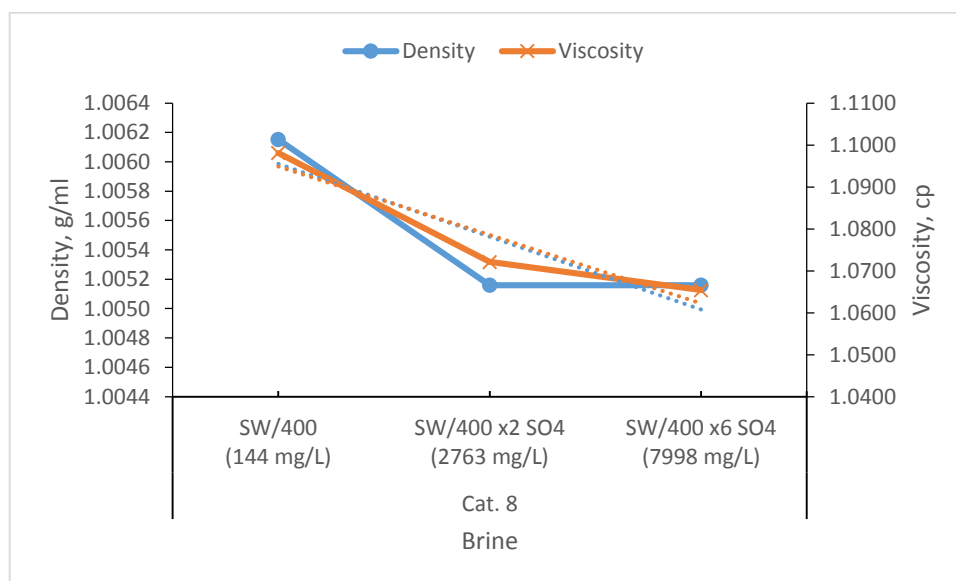


Figure III.8: Density and change in density Viscosity of Category 8

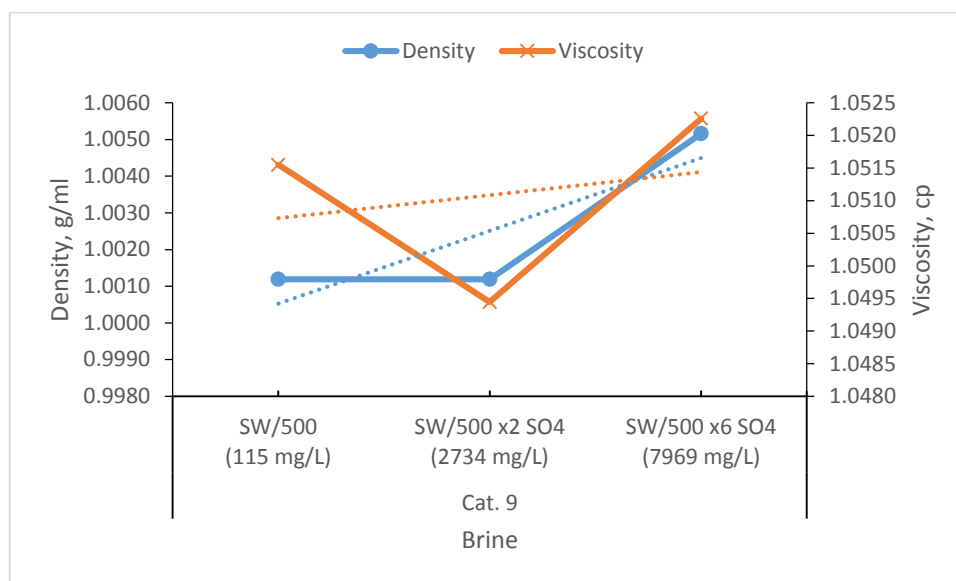


Figure III.9: Density and Viscosity of Category 9

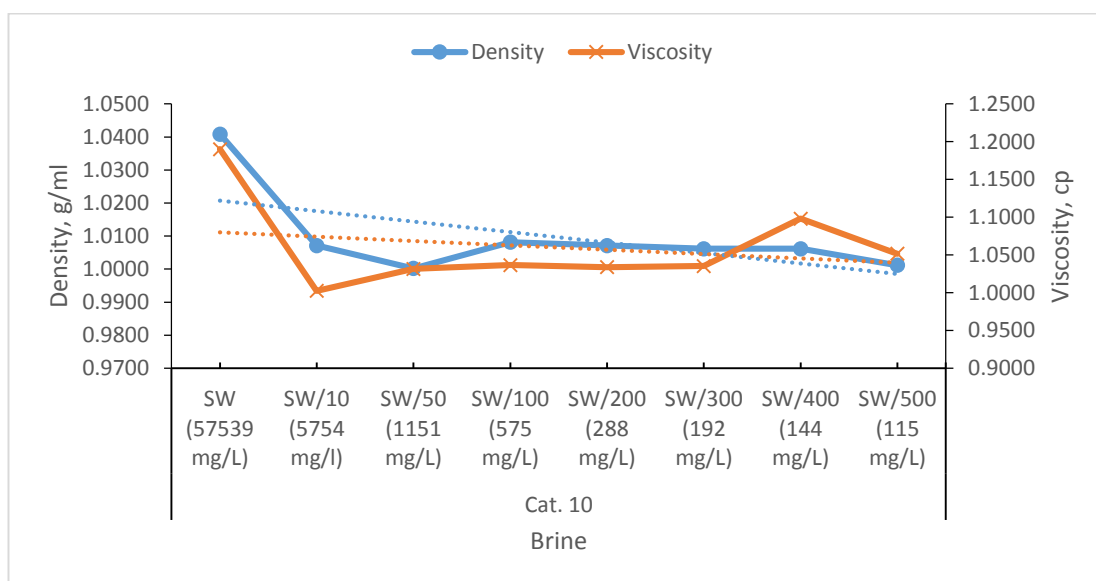


Figure III.10: Density and Viscosity of Category 10

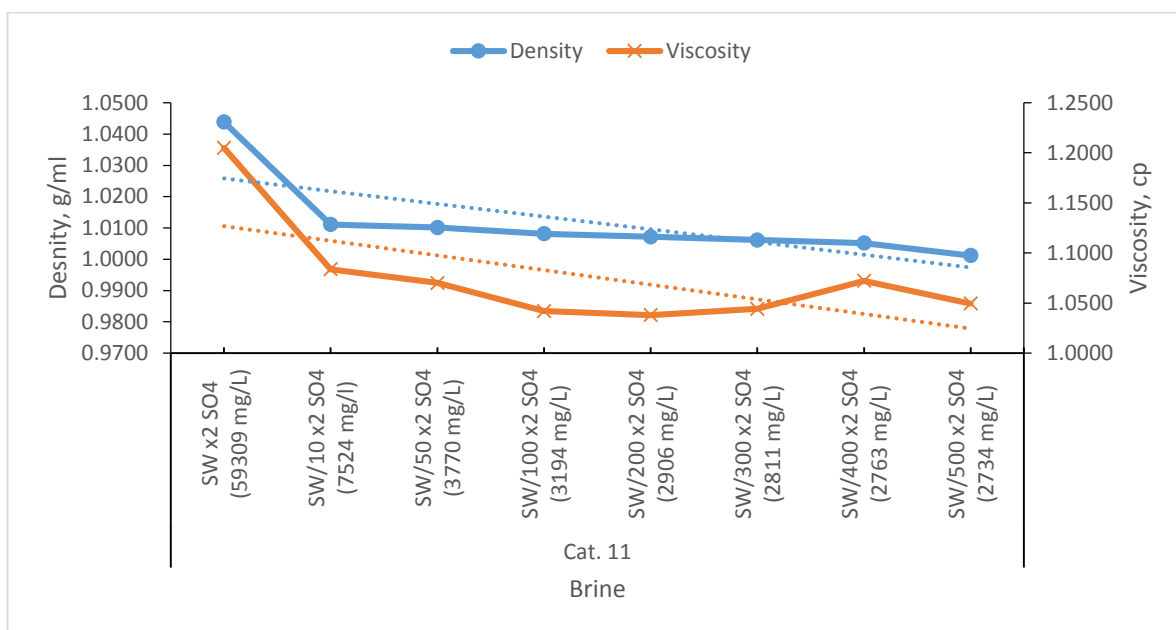


Figure III.11: Density and Viscosity of Category 11

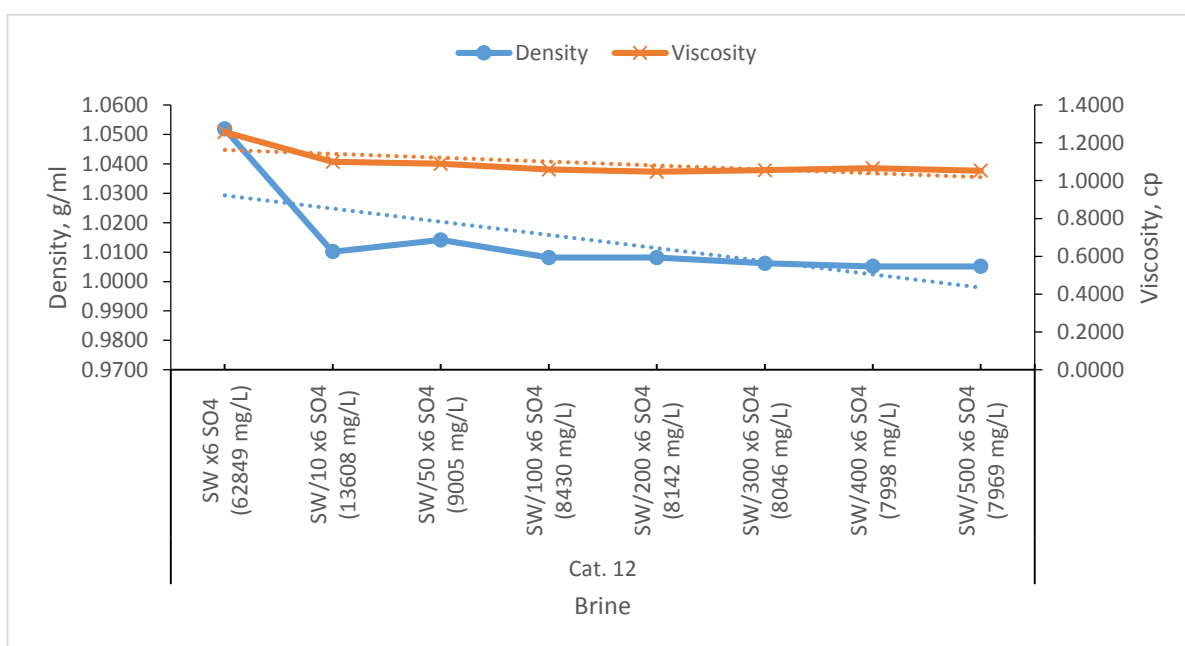


Figure III.12: Density and Viscosity of Category 12

Appendix IV: IFT categories at 20°C

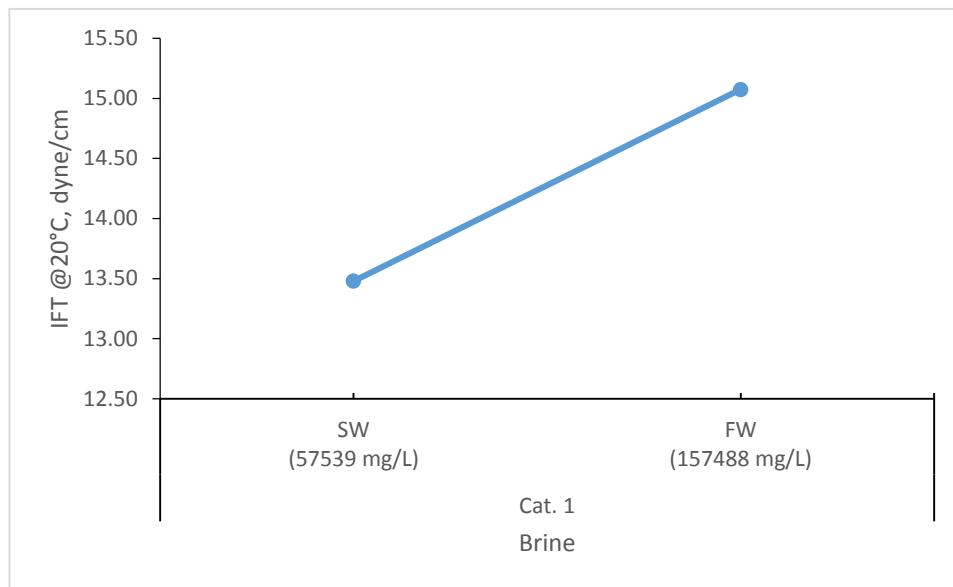


Figure IV.1: IFT Measurements of Category 1

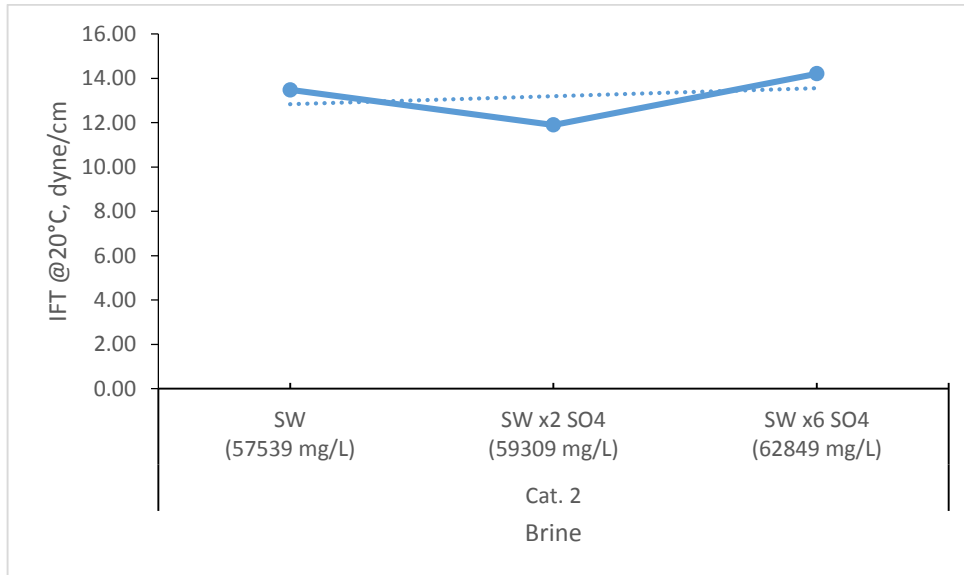


Figure IV.2: IFT measurements of Category 2

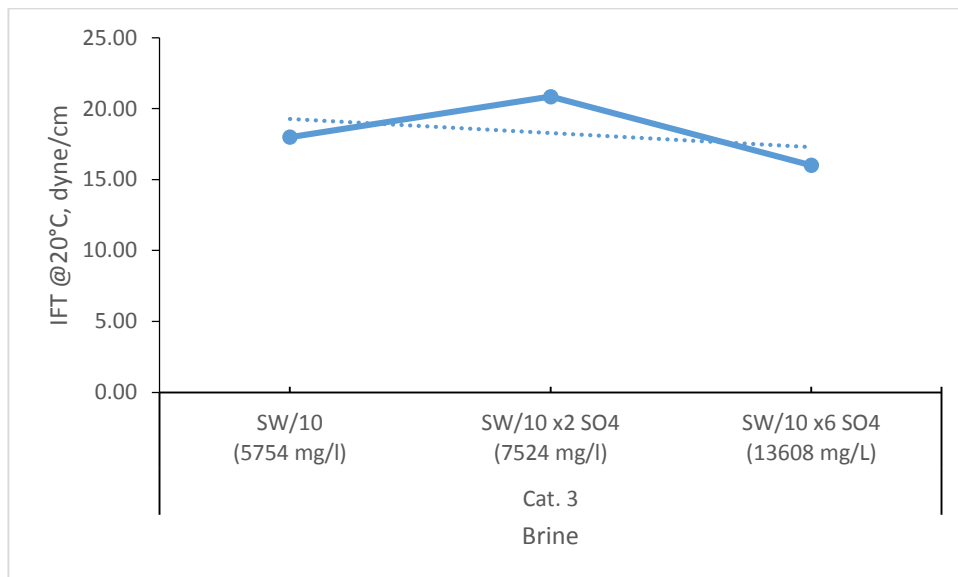


Figure IV.3: IFT measurements of Category 3

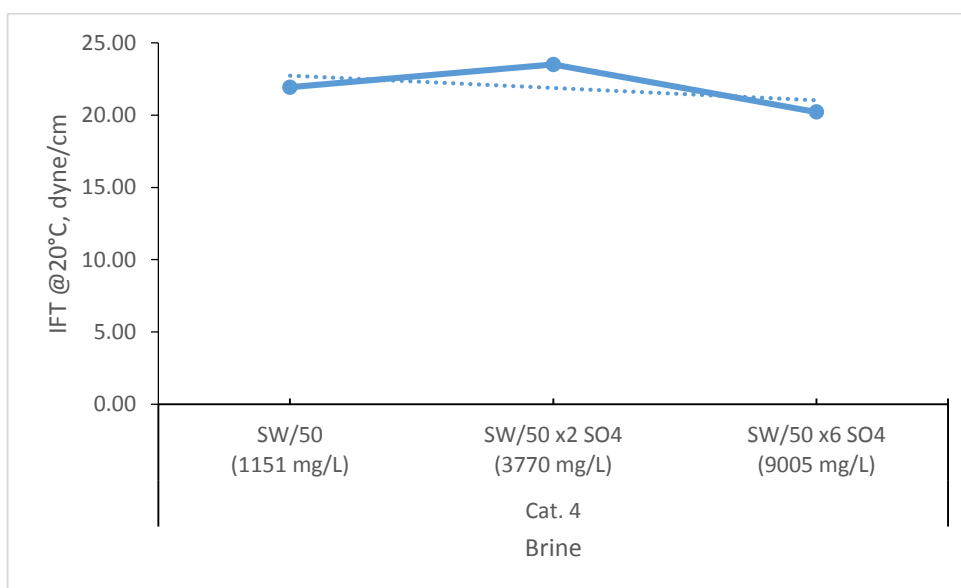


Figure IV.4: IFT Measurements of Category 4

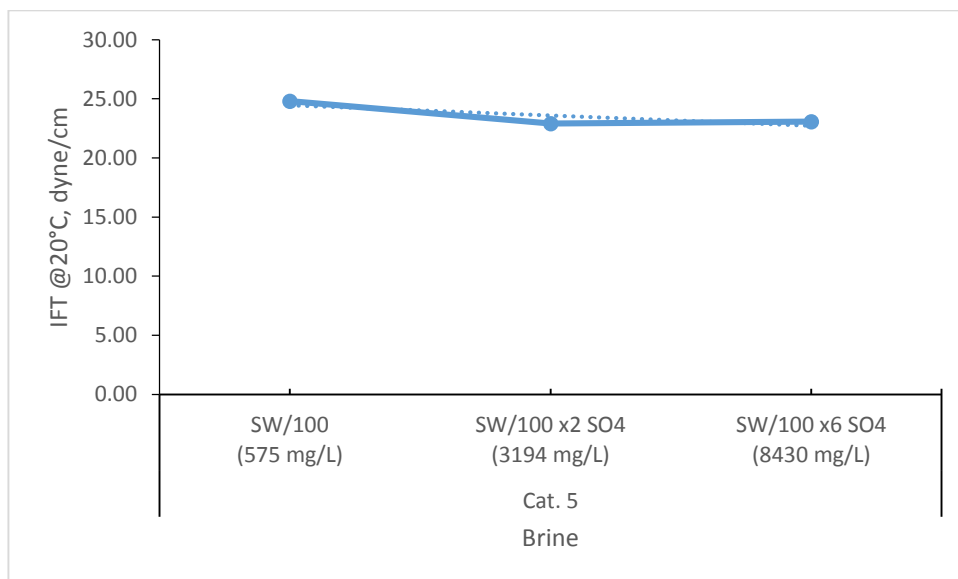


Figure IV.5: IFT Measurements of Category 5

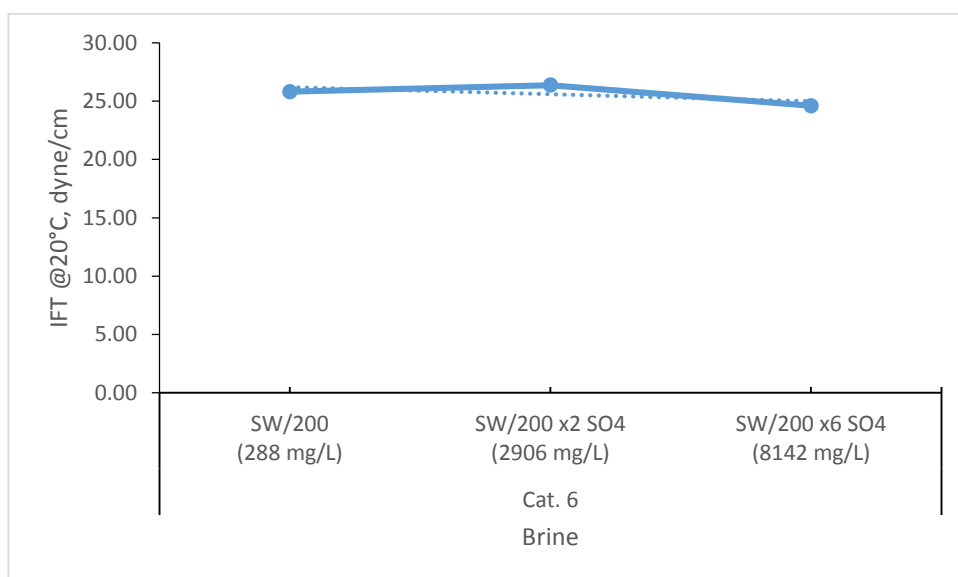


Figure IV.6: IFT Measurements of Category 6

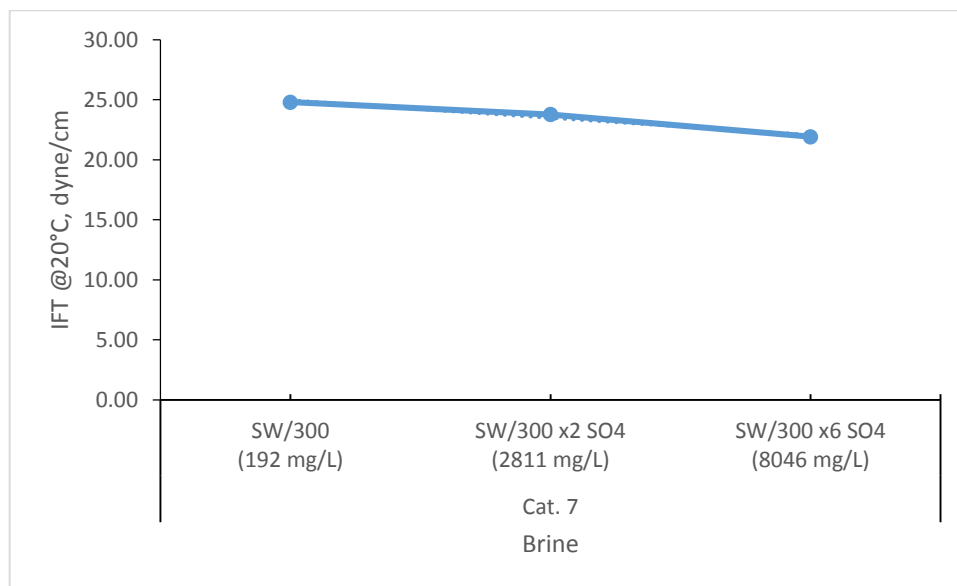


Figure IV.7: IFT Measurements of Category 7

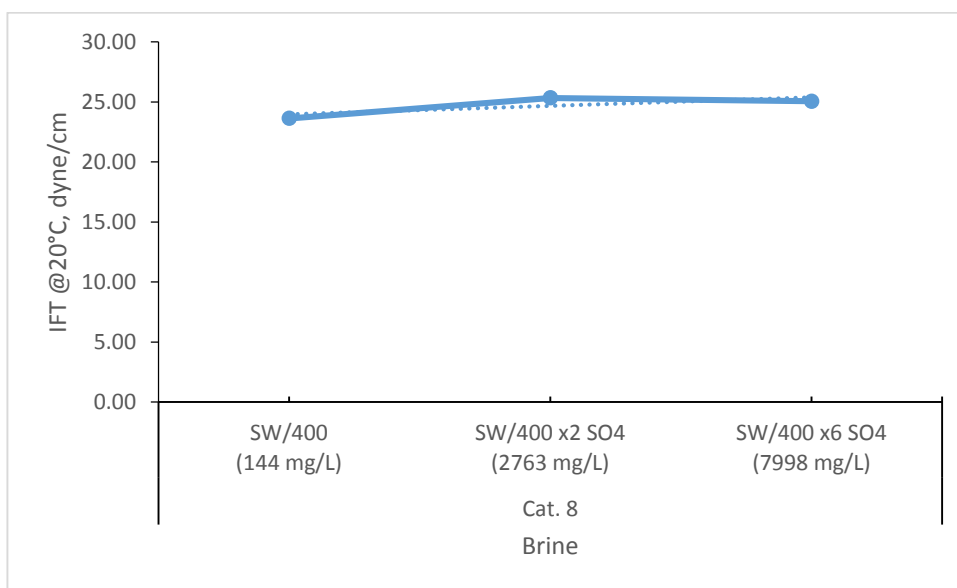


Figure IV.8: IFT Measurements of Category 8

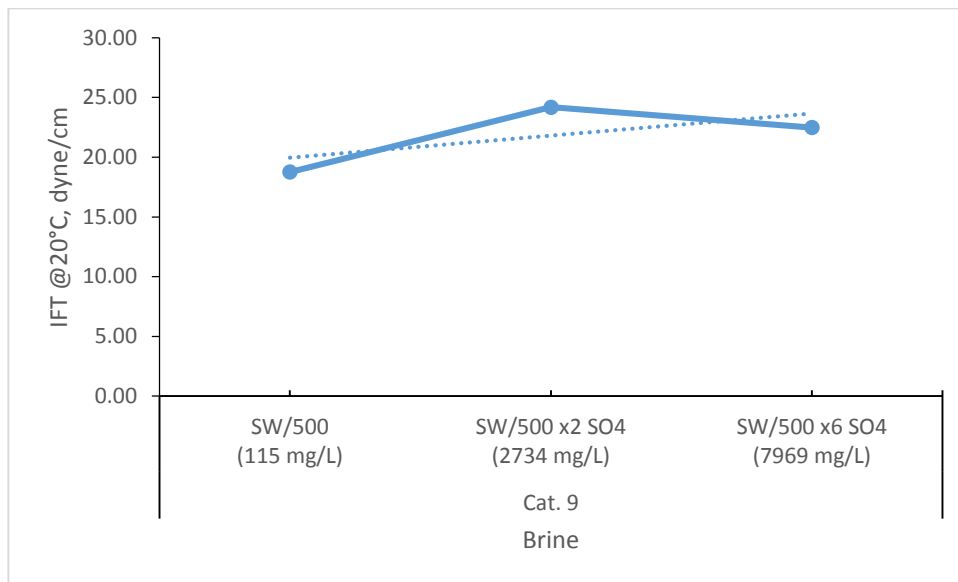


Figure IV.9: IFT measurements of Category 9

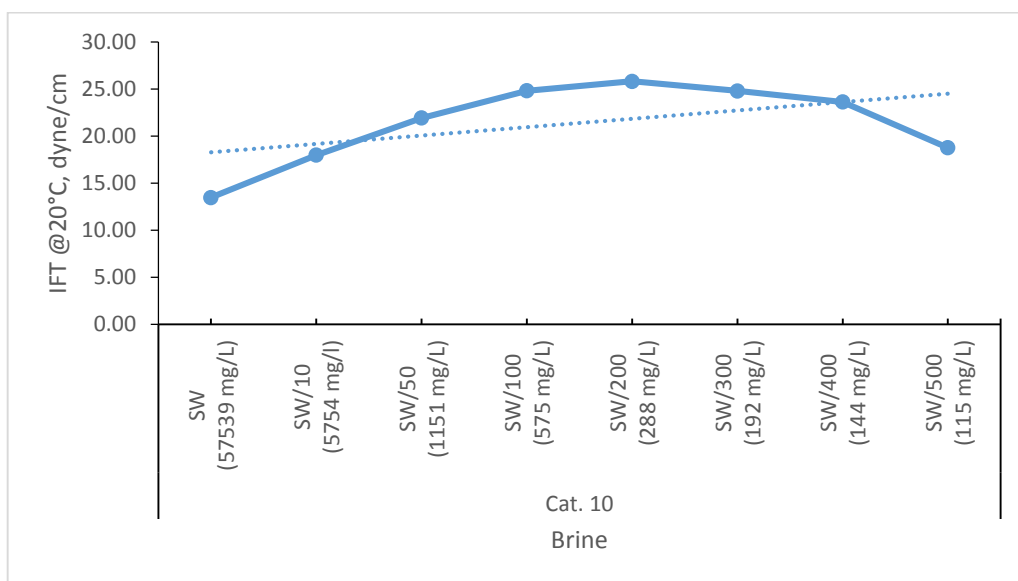


Figure IV.10: IFT Measurements of Category 10

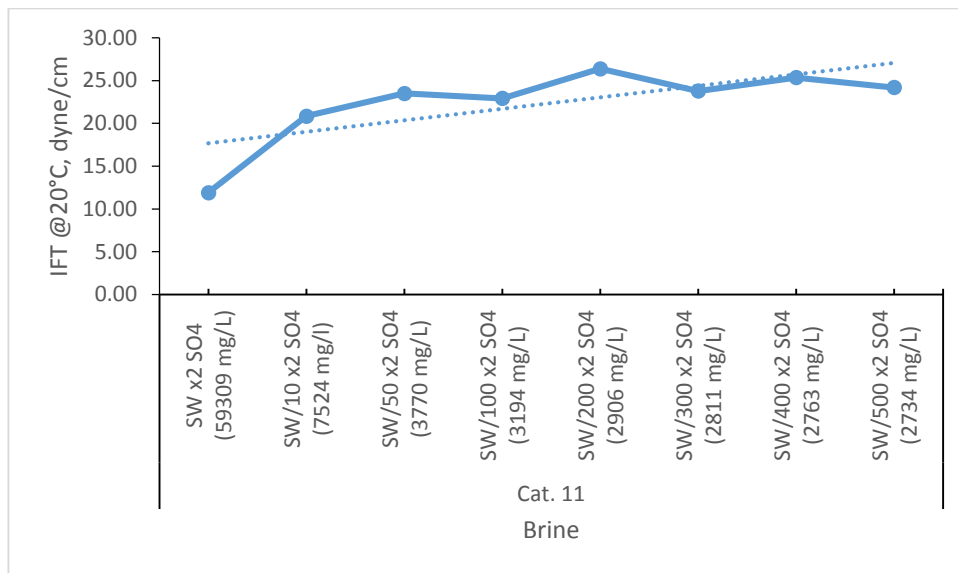


Figure IV.11: IFT Measurements of category 11

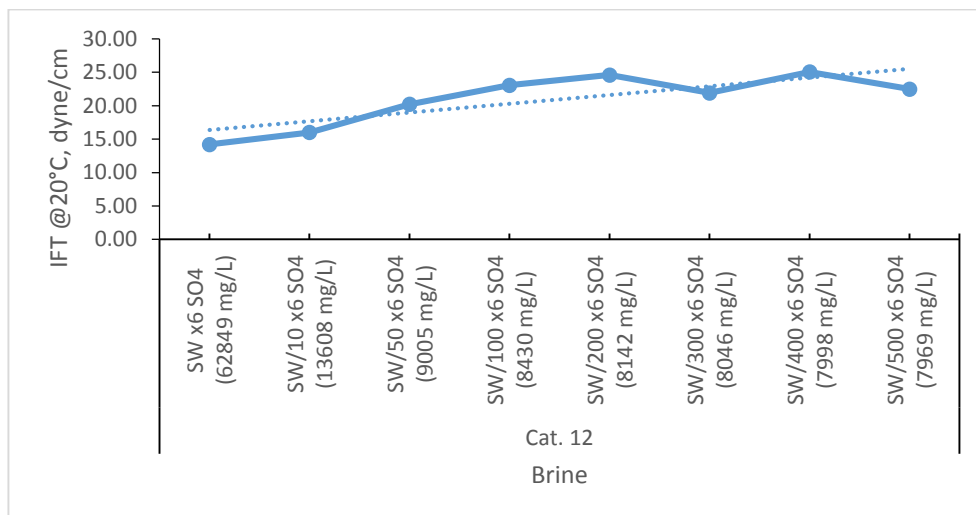


Figure IV.12: IFT Measurements of category 12

Appendix V: IFT categories at high Pressure and high temperature

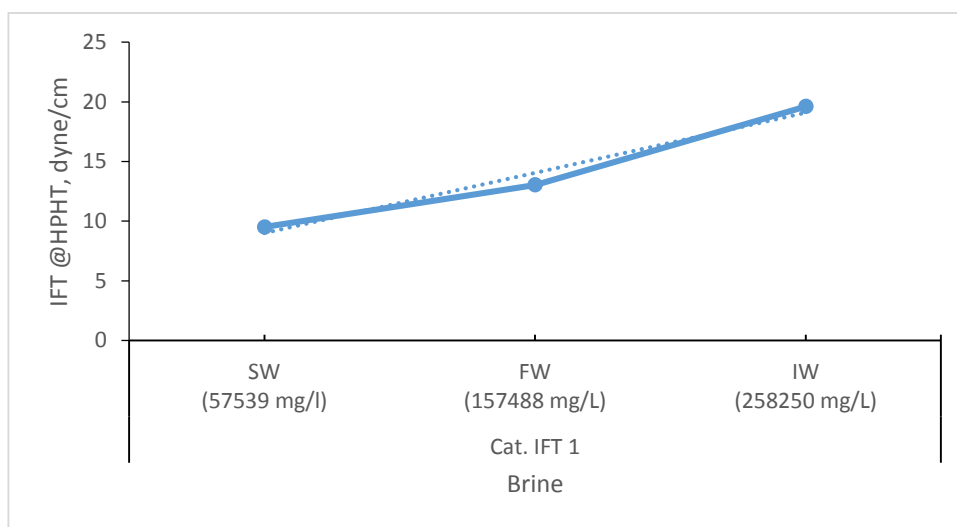


Figure V.1: IFT measurements of Category IFT 1

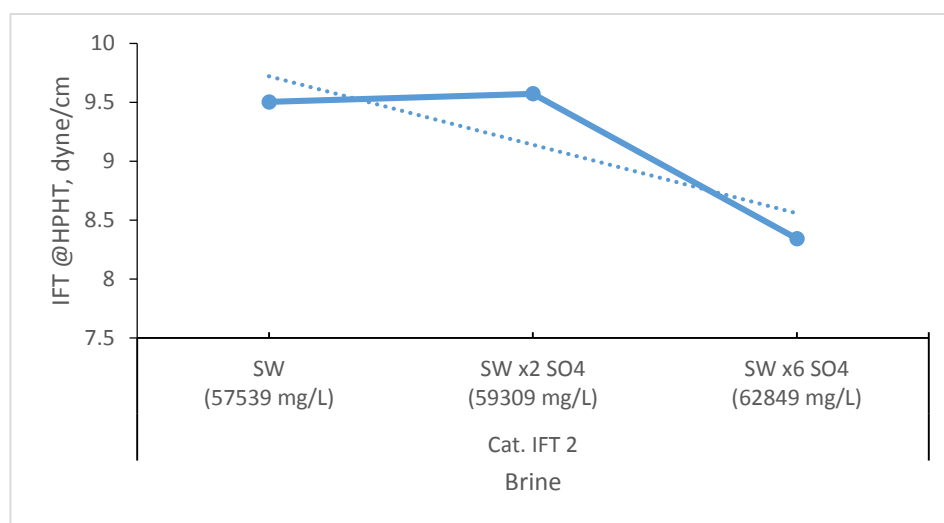


Figure V.2: IFT measurements of category IFT 2

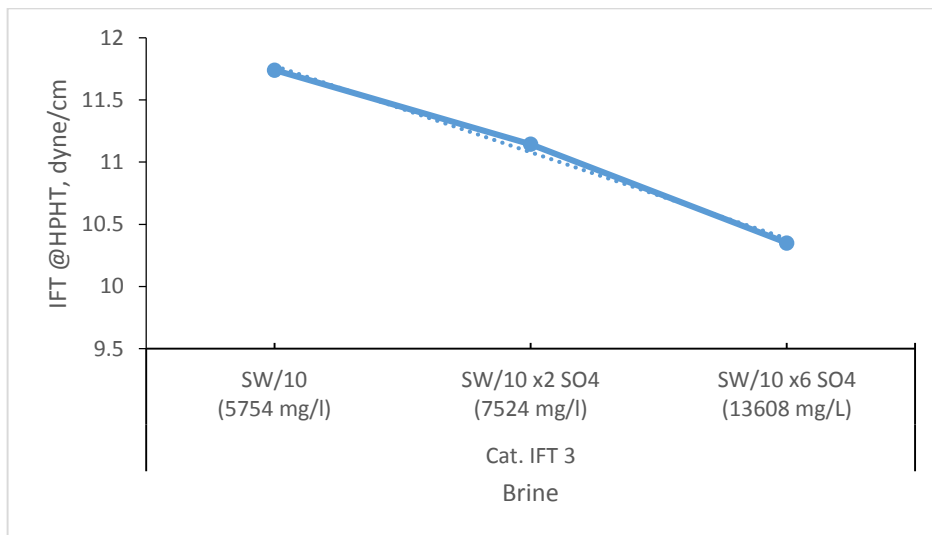


Figure V.3: IFT measurement of category IFT 3

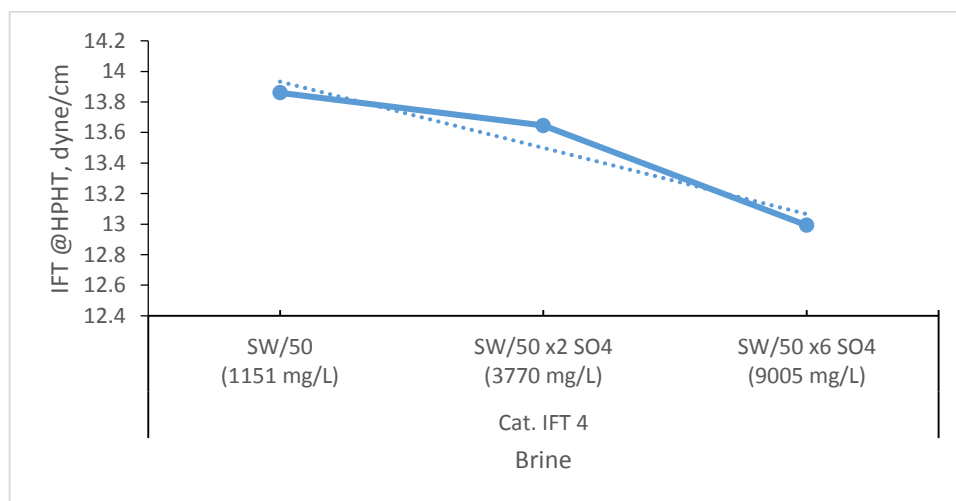


Figure V.4: IFT measurement of category IFT 4

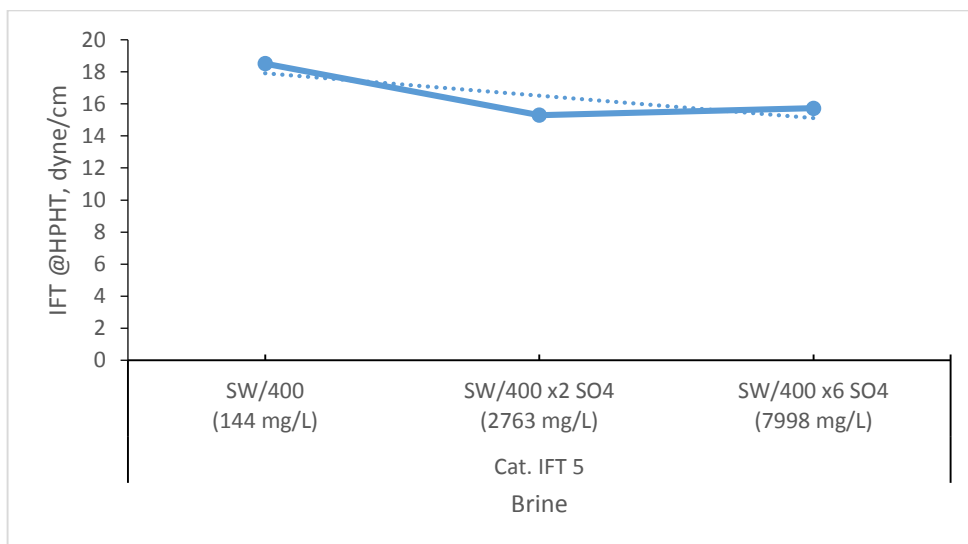


Figure V.5: IFT measurement of category IFT 5

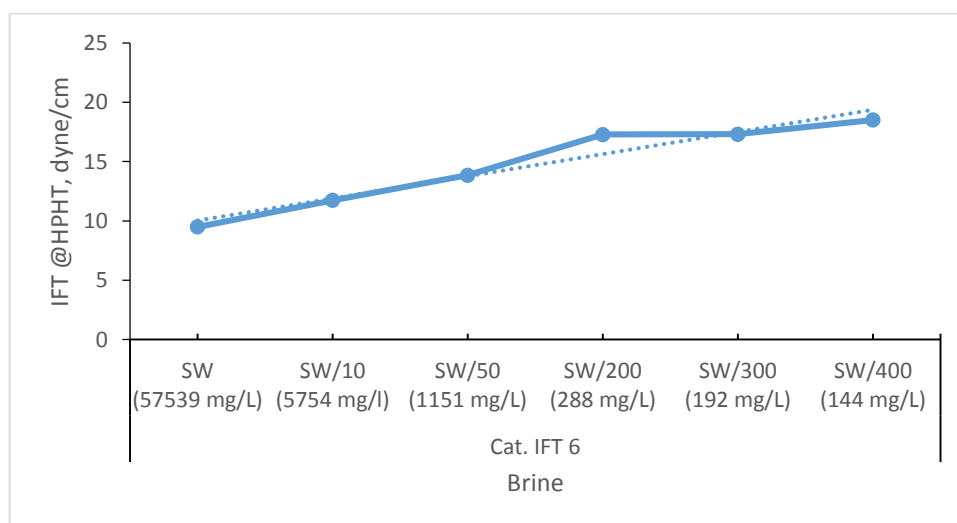


Figure V.6: IFT measurement of category IFT 6

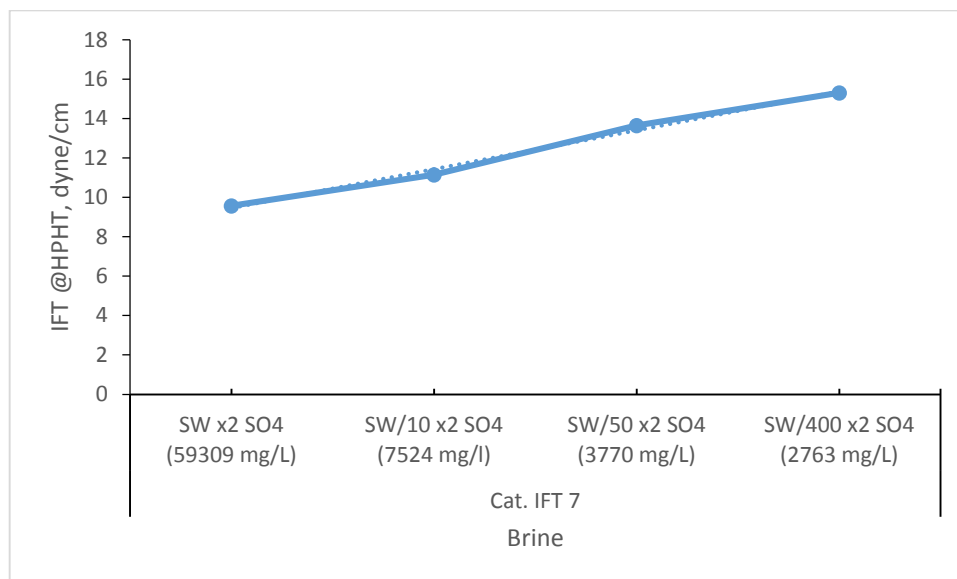


Figure V.7: IFT measurement of category IFT 7

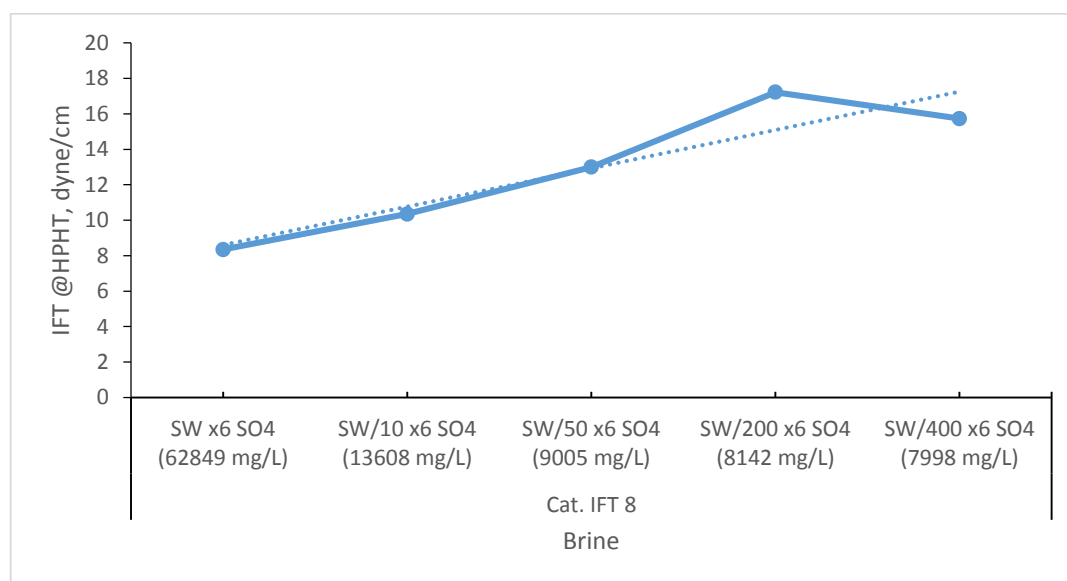
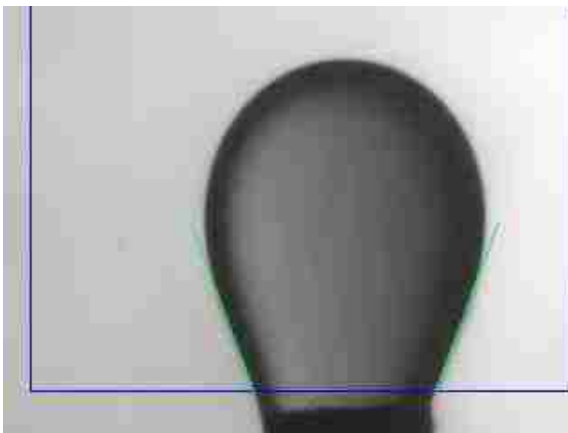
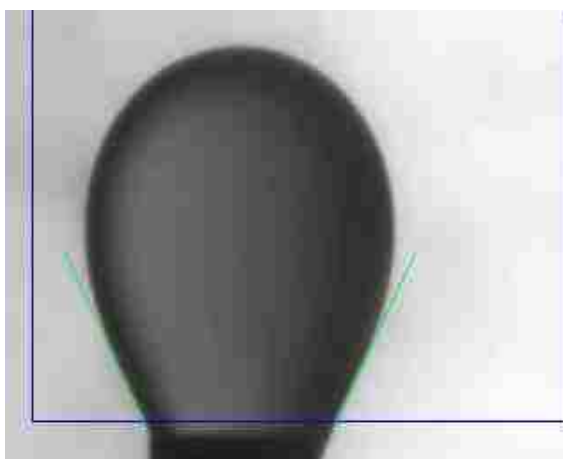


Figure V.8: IFT measurement of category IFT 8

Appendix VI: IFT Images at high Pressure and high temperature



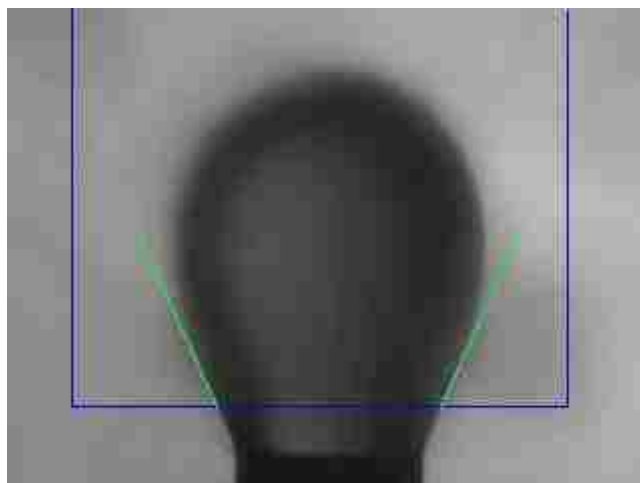
Oil drop in the medium of Injection Water



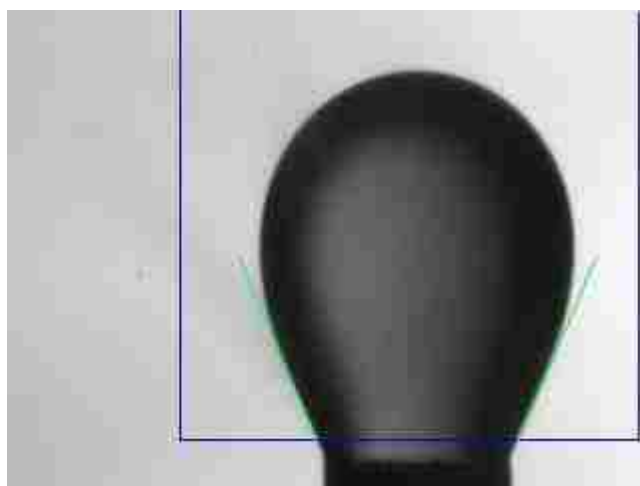
Oil drop in the medium of Formation Water



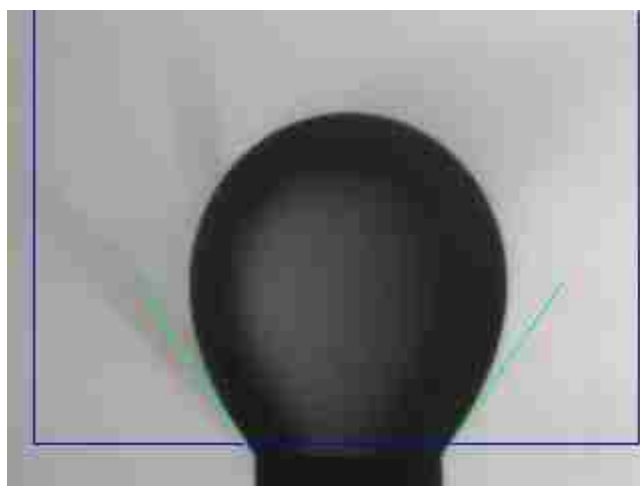
Oil drop in the medium of Sea Water



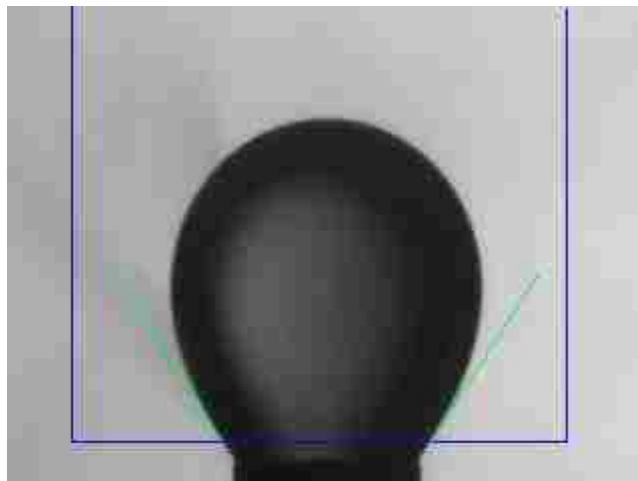
Oil drop in the medium of SW x2 SO₄



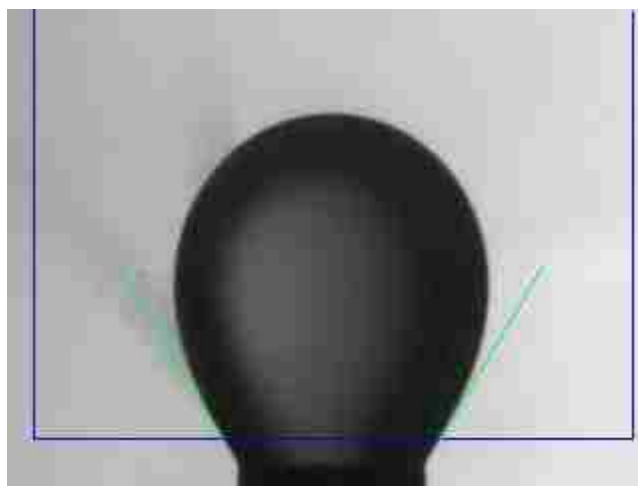
Oil drop in the medium of SW x6 SO₄



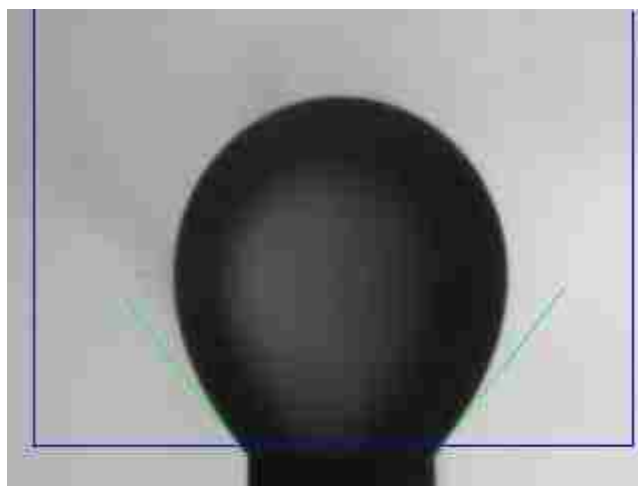
Oil drop in the medium of SW/10



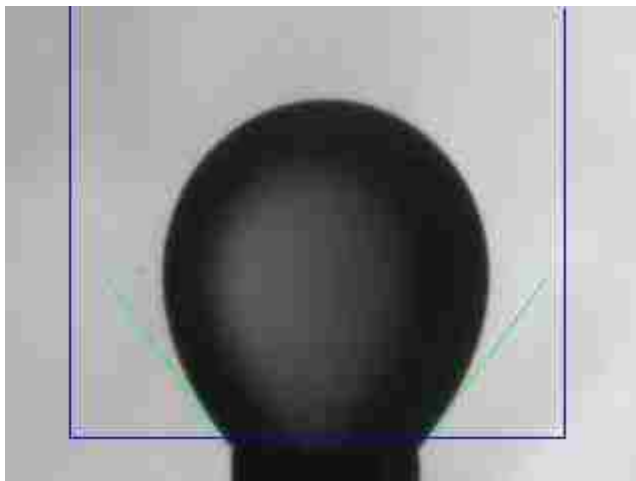
Oil drop in the medium of SW/10 x2 SO₄



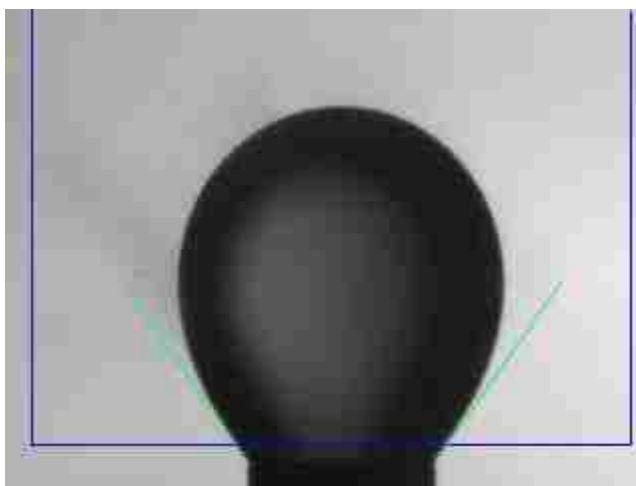
Oil drop in the medium of SW/10 x6 SO₄



Oil drop in the medium of SW/50



Oil drop in the medium of SW/50 x2 SO₄



Oil drop in the medium of SW/50 x6 SO₄

Appendix VII: Contact Angle categories at HPHT

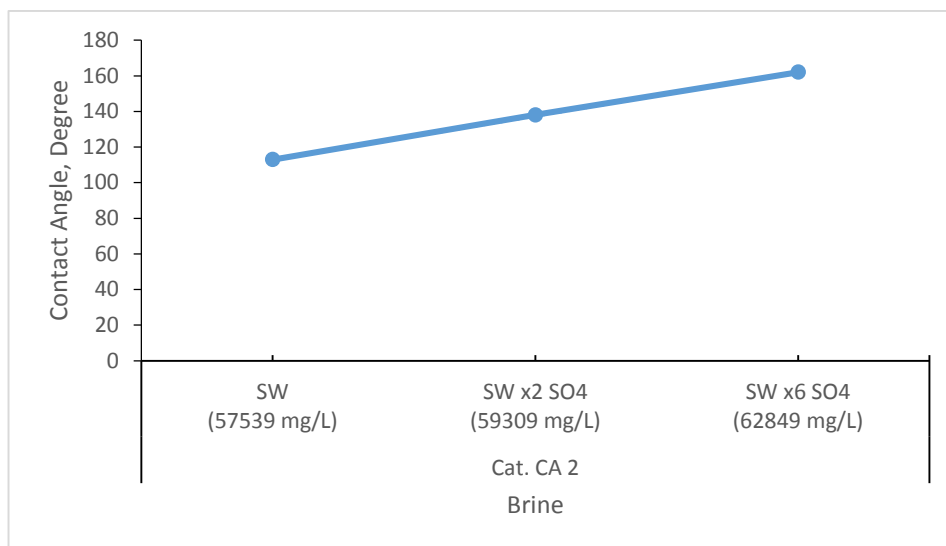


Figure VII.1: Contact angle measurements of category CA 1

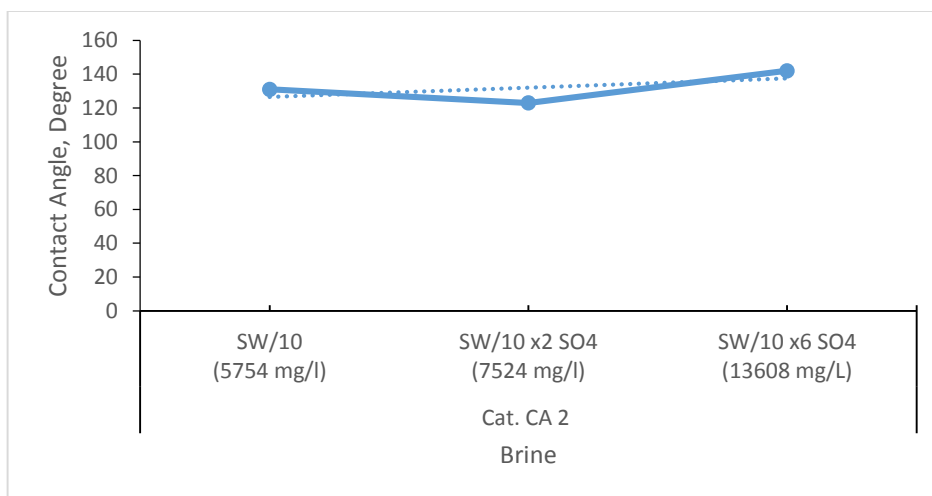


Figure VII.2: Contact angle measurements of category CA 2

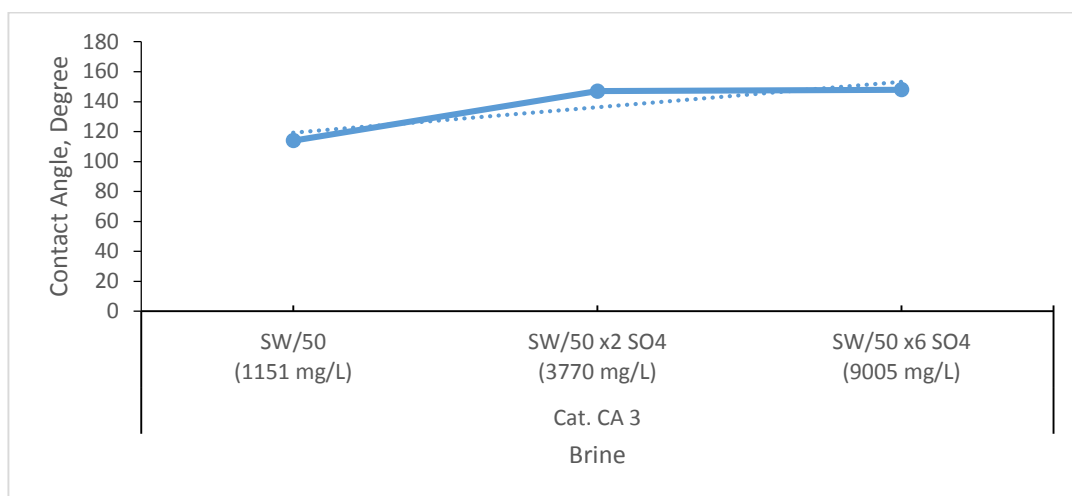


Figure VII.3: Contact angle measurements of category CA 3

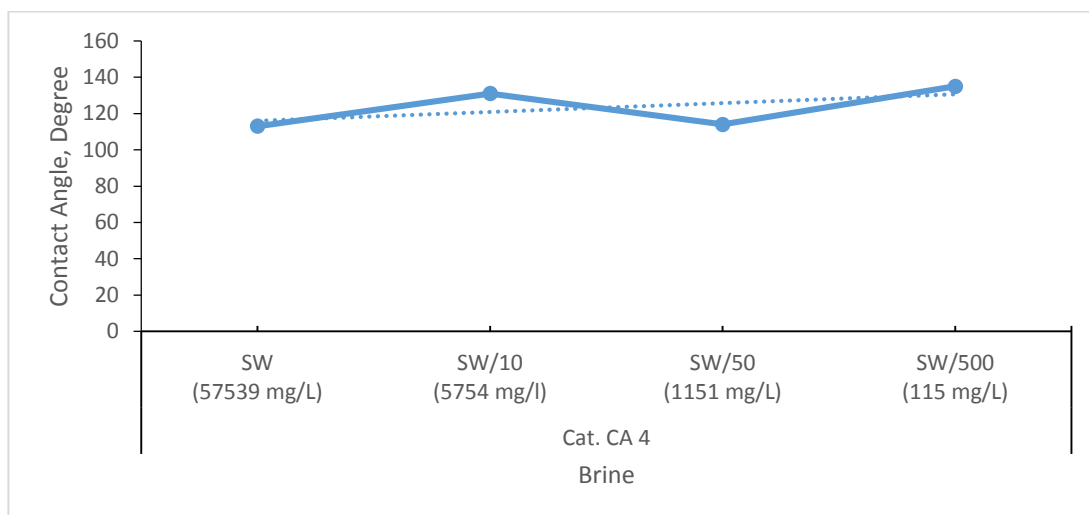


Figure VII.4: Contact angle measurements of category CA 4

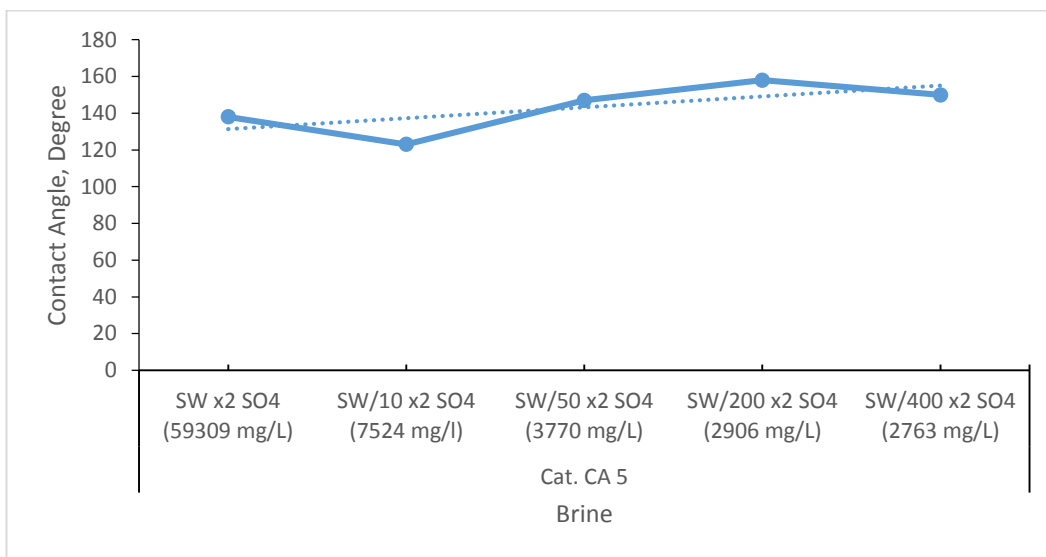


Figure VII.5: Contact angle measurements of category CA 5

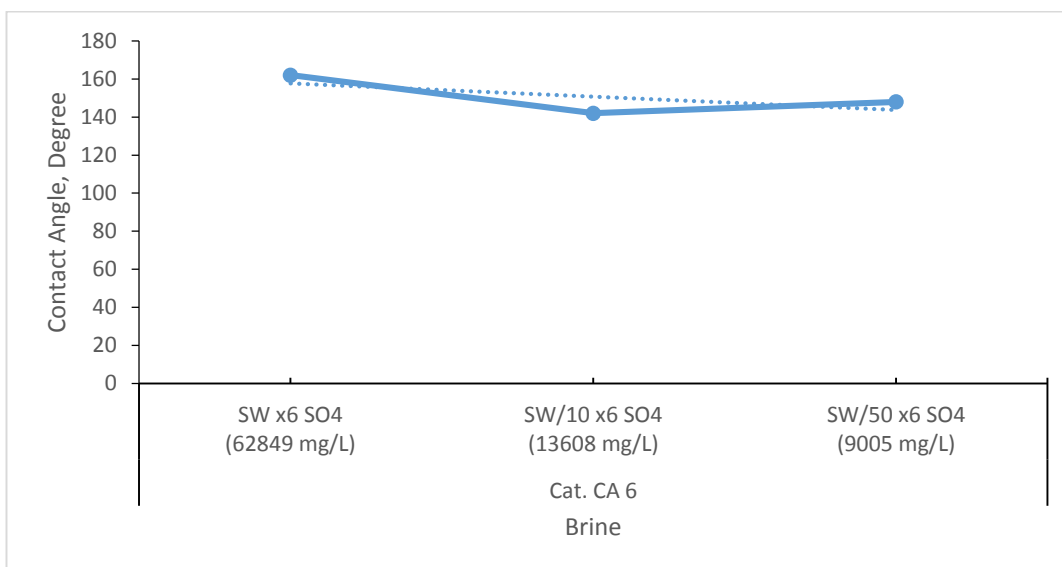
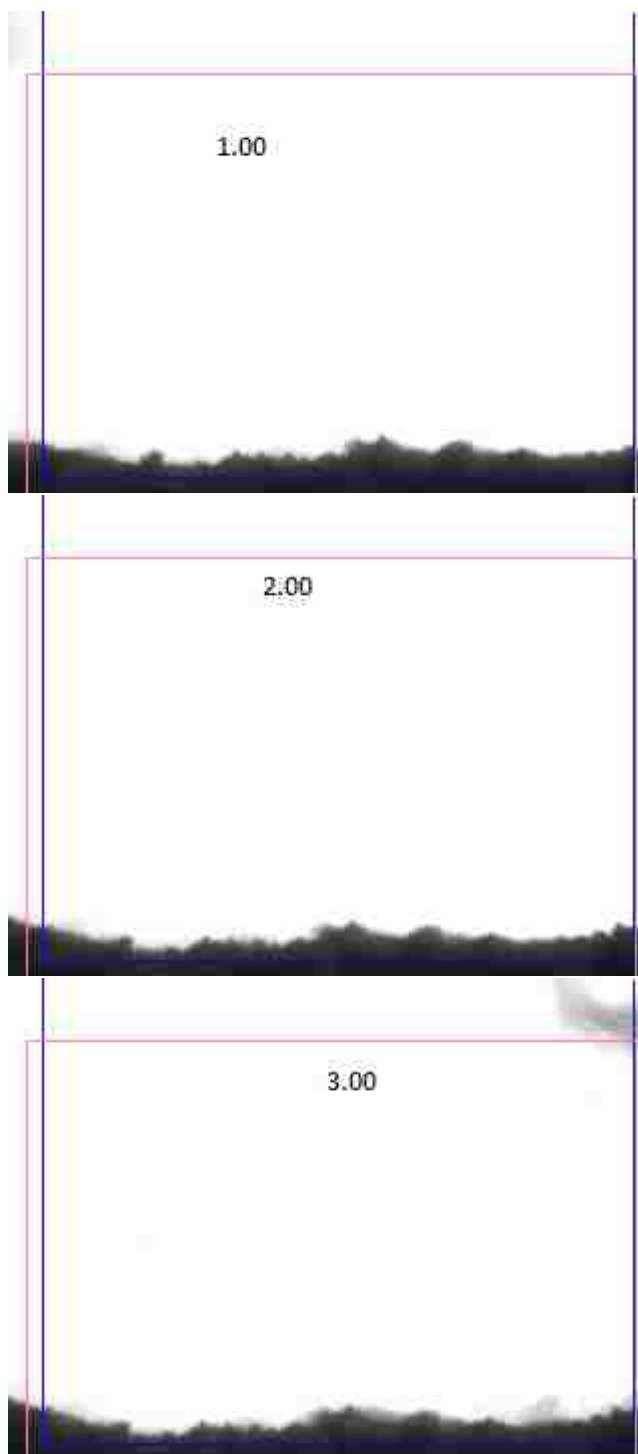


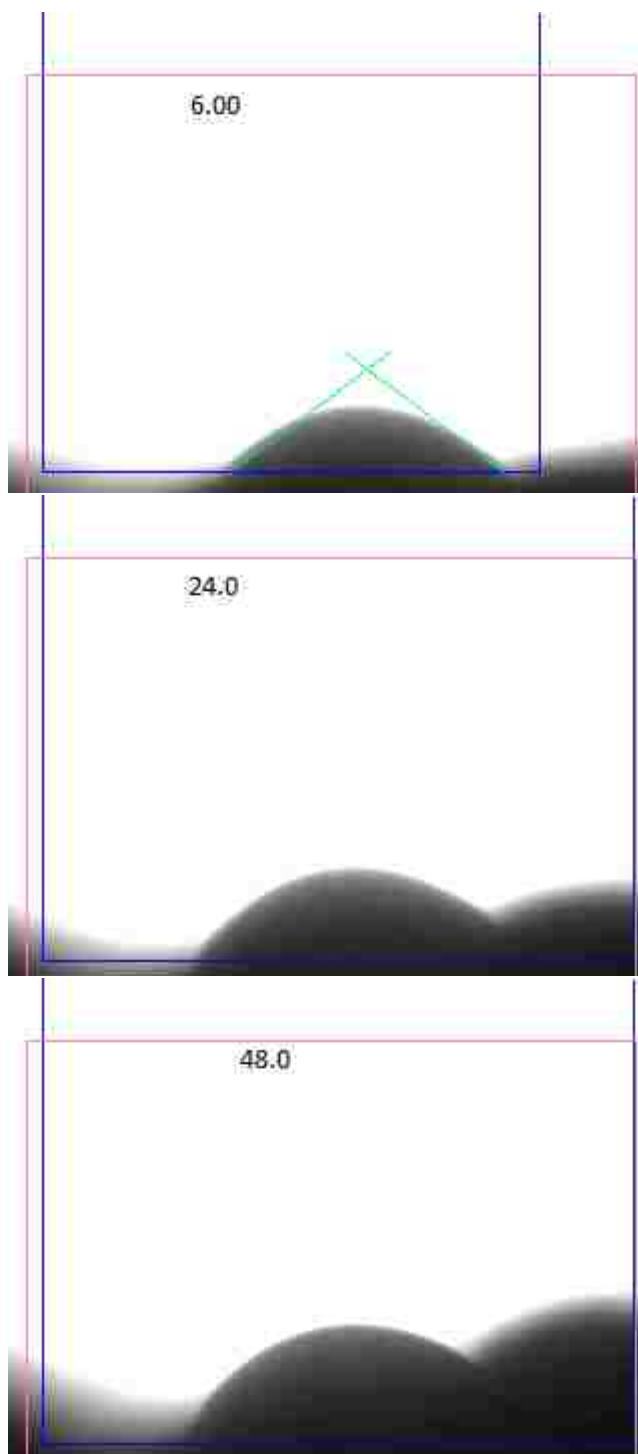
Figure VII.6: Contact angle measurements of category CA 6

Appendix VIII: Contact Angle Images at HPHT

Contact Angle Measurements of SW

NOTE: The measurement time is recorded in each picture

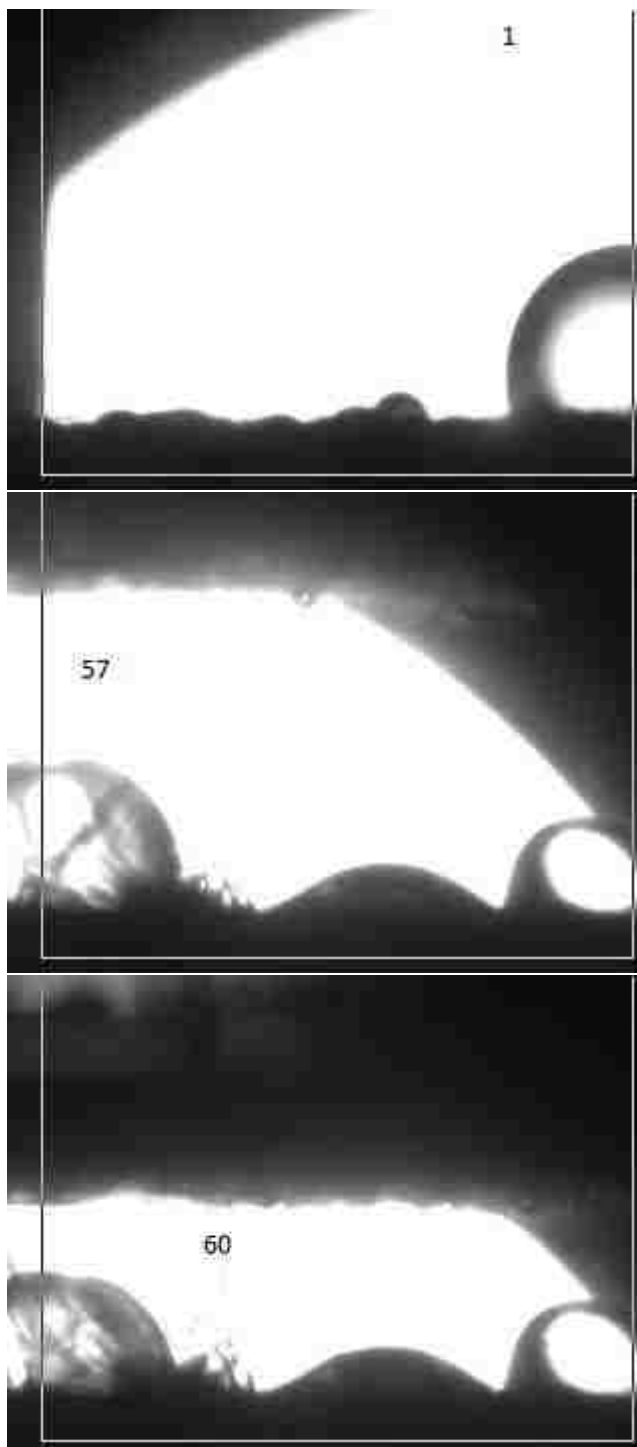






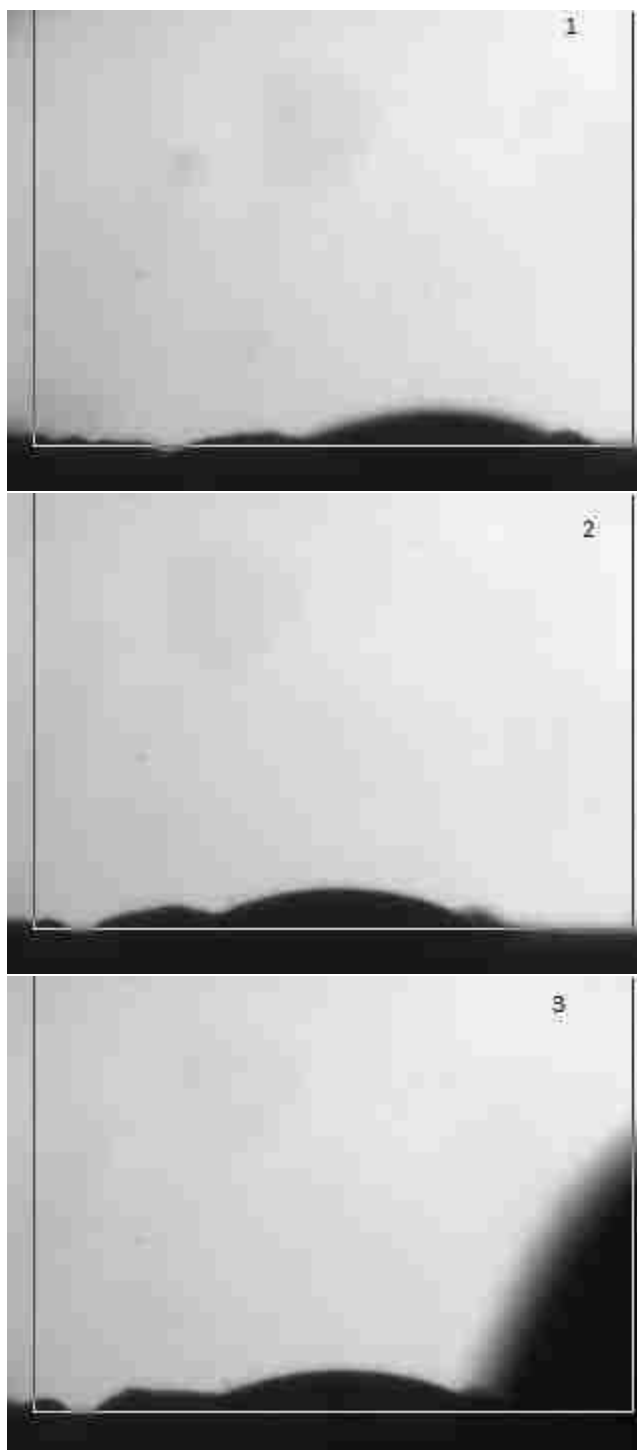
Contact Angle Measurements of SW x2 SO₄

NOTE: The measurement time is recorded in each picture



Contact Angle Measurements of SW x6 SO₄

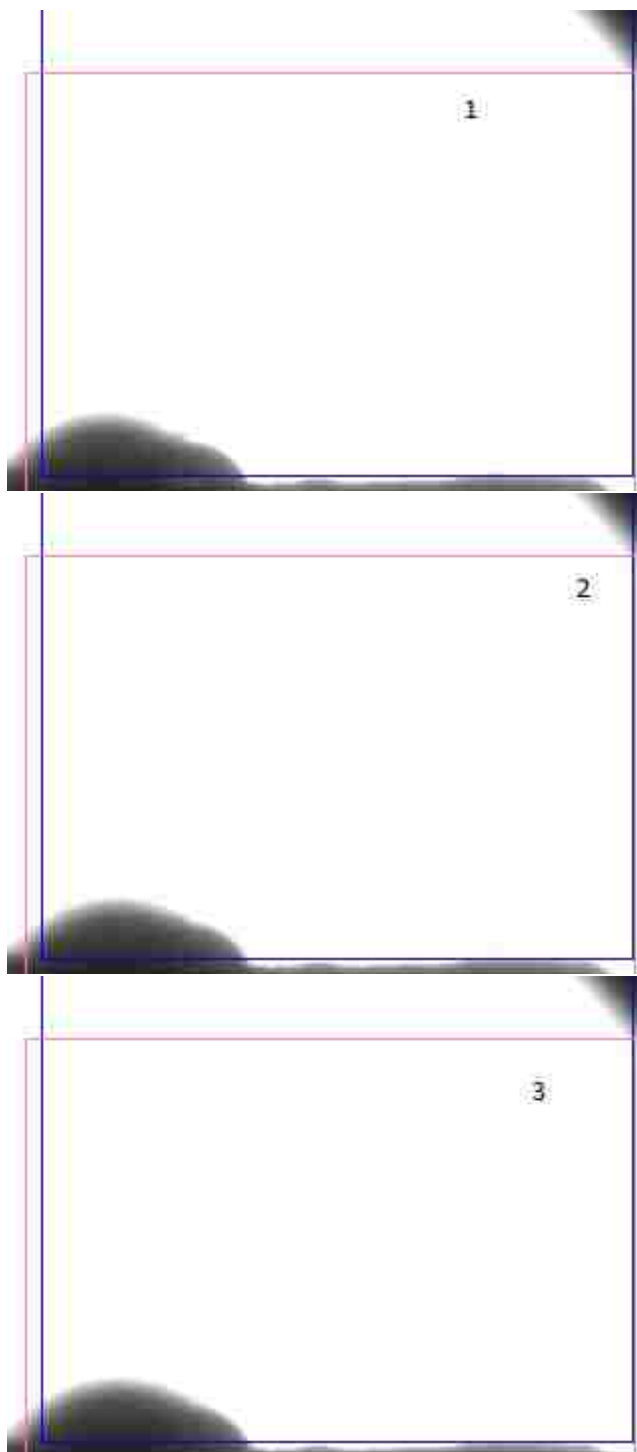
NOTE: The measurement time is recorded in each picture

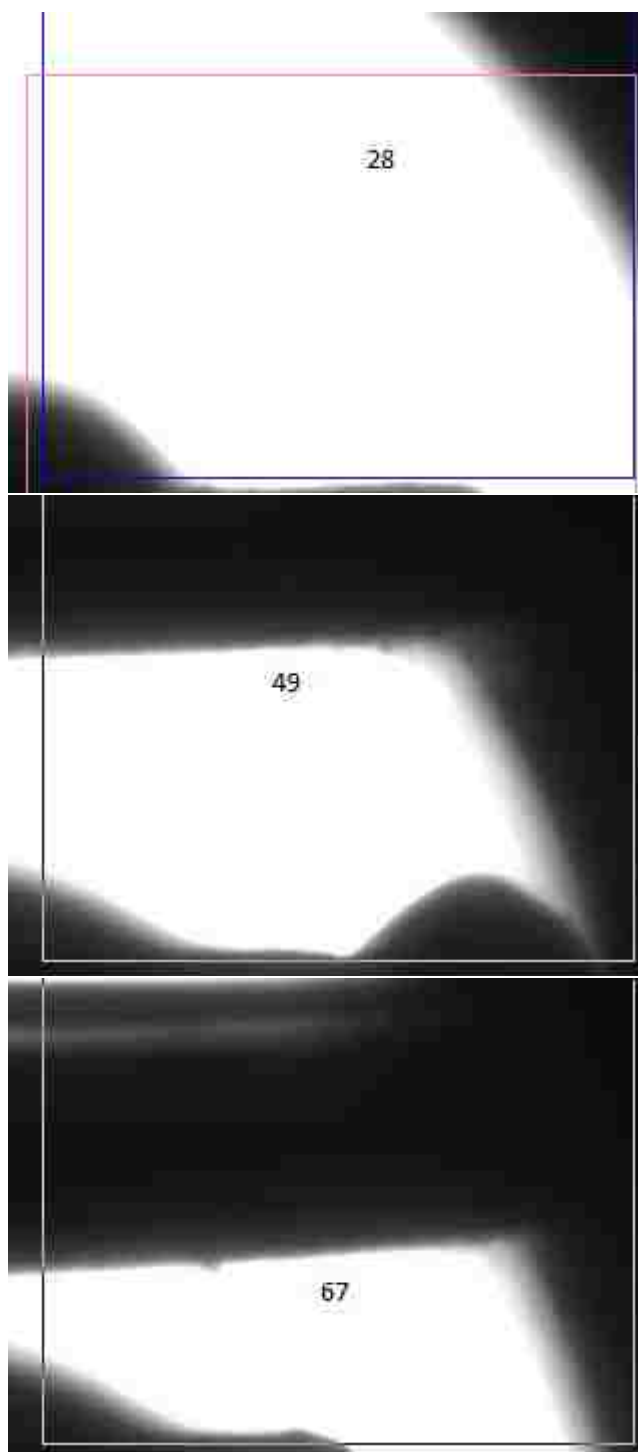




Contact Angle Measurements of SW/10

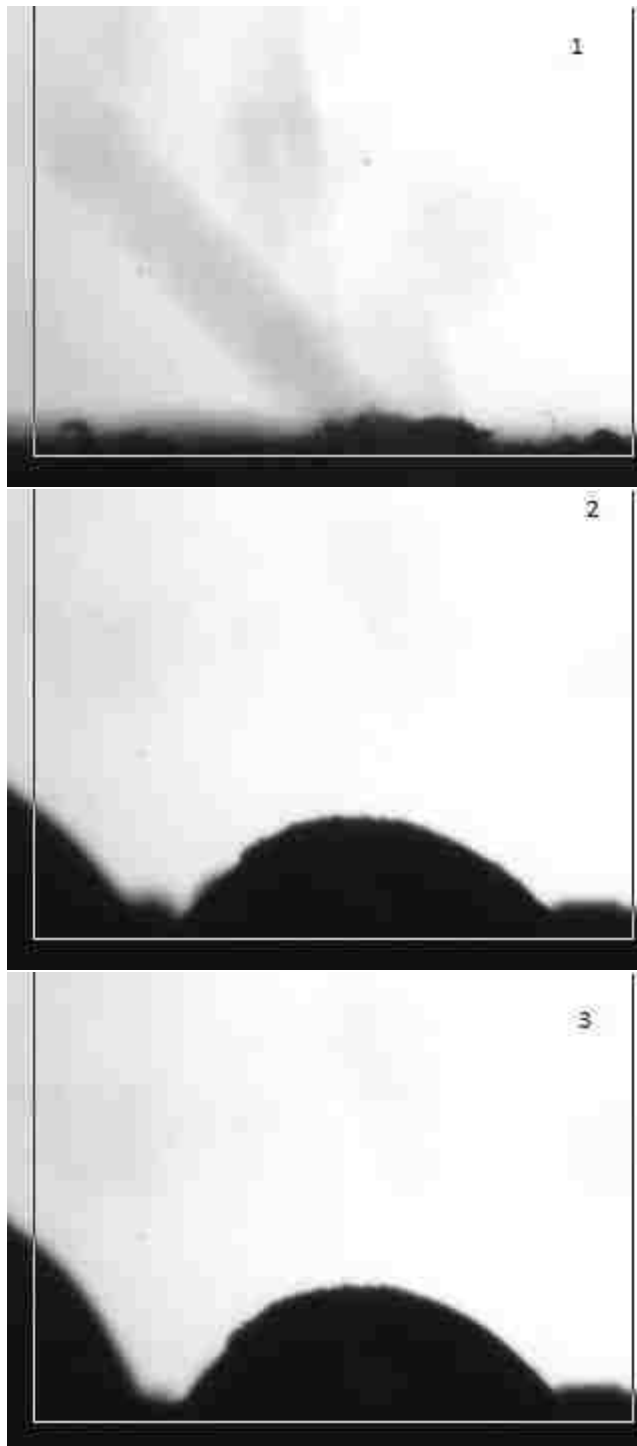
NOTE: The measurement time is recorded in each picture

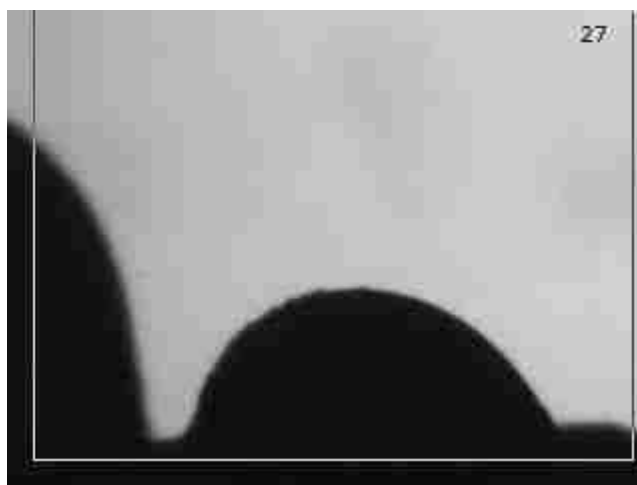




Contact Angle Measurements of SW/10 x2 SO₄

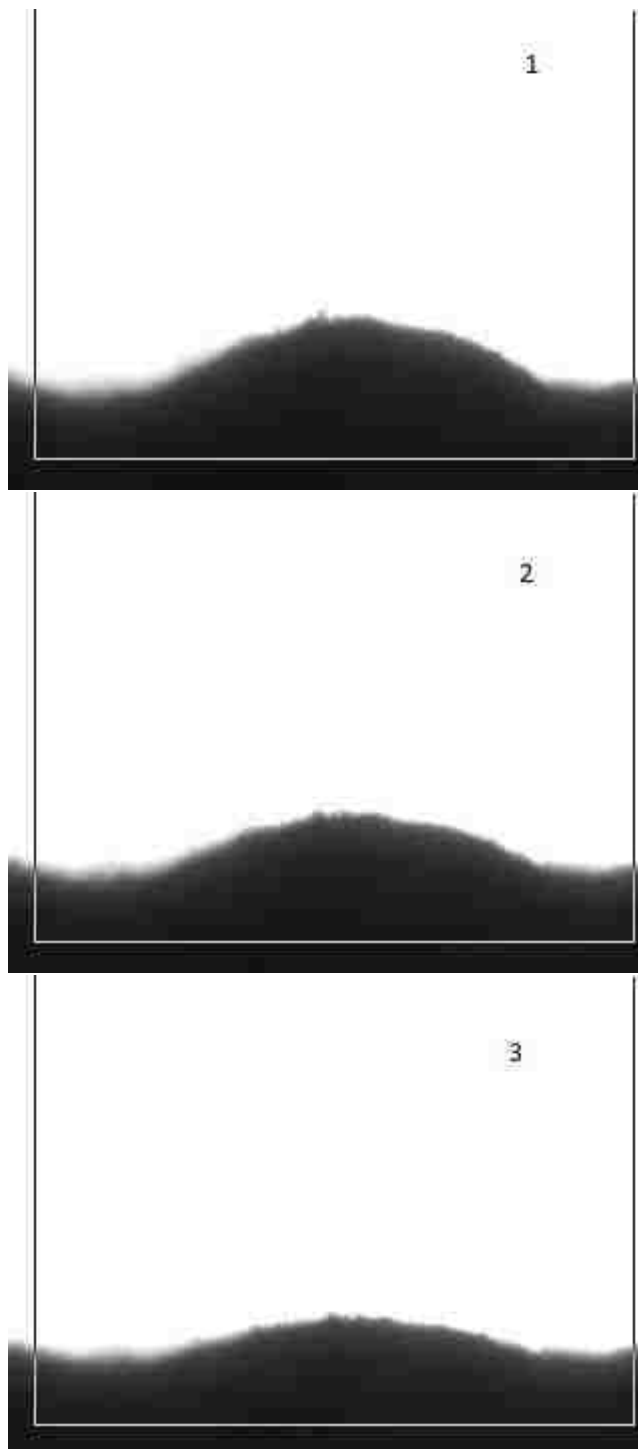
NOTE: The measurement time is recorded in each picture

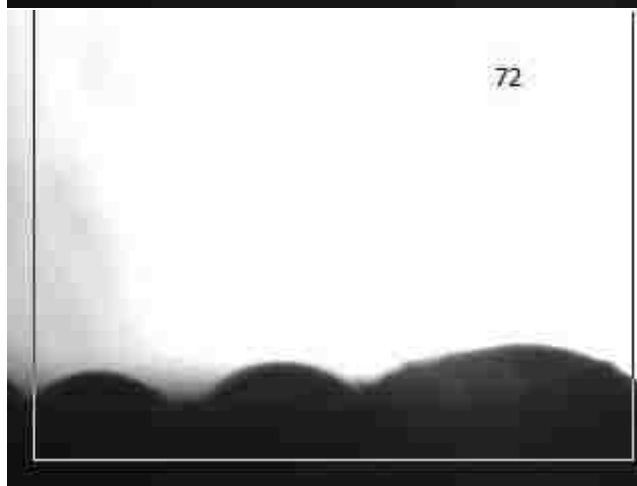
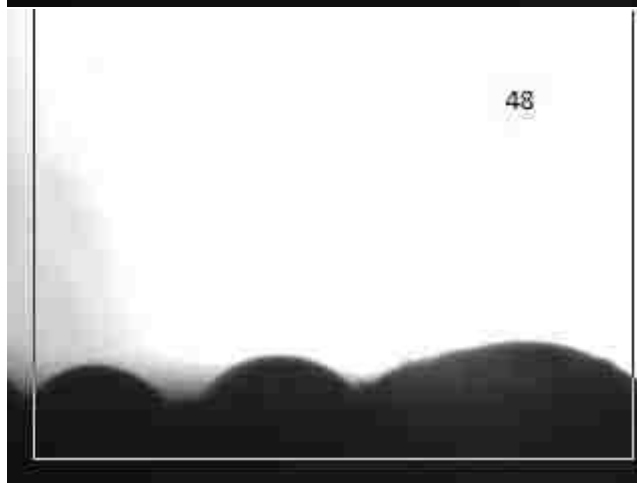




Contact Angle Measurements of SW/10 x6 SO₄

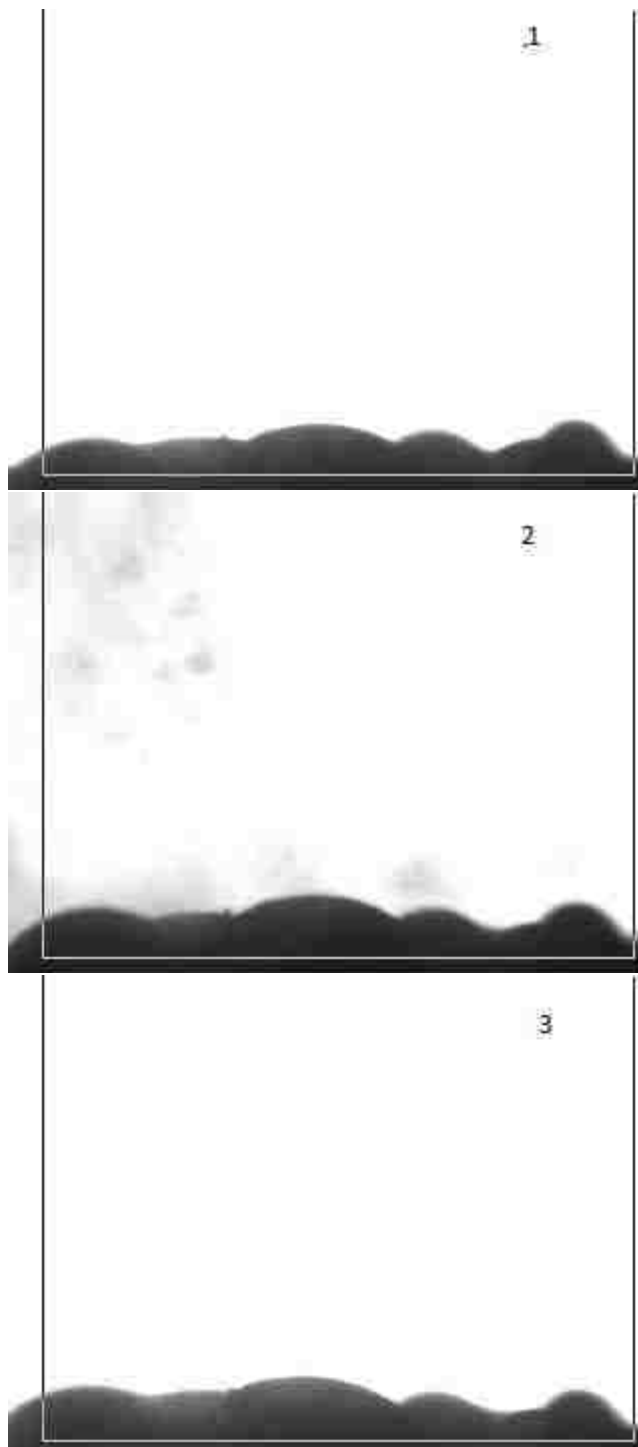
NOTE: The measurement time is recorded in each picture

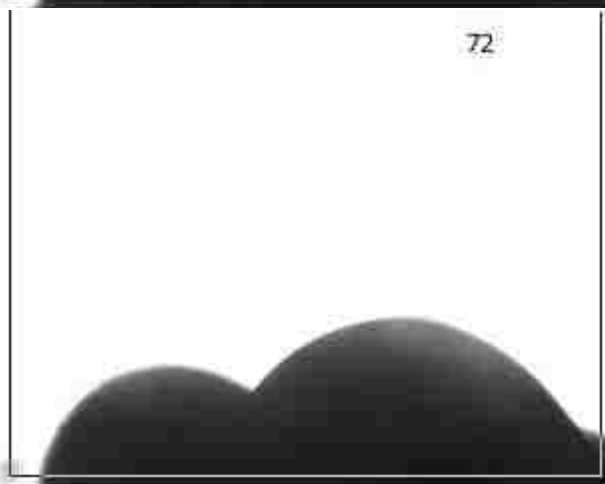
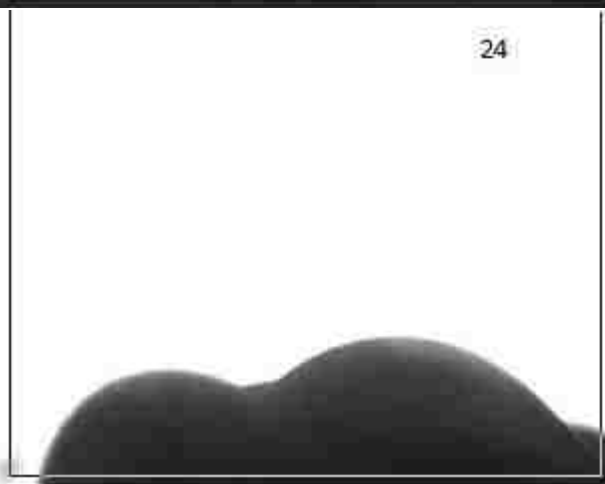




Contact Angle Measurements of SW/50

NOTE: The measurement time is recorded in each picture





Contact Angle Measurements of SW/50 x2 SO₄

NOTE: The measurement time is recorded in each picture





Contact Angle Measurements of SW/50 x6 SO₄

NOTE: The measurement time is recorded in each picture

